Revisiting Rist diagram for predicting operating conditions in blast furnaces with multiple injections

Manuel Bailera[1,2*], **Takao Nakagaki**[3], **Ryoma Kataoka**[4]

[1]**Graduate School of Creative Science and Engineering, Waseda University. 3-4-1 Okubo, Shinjuku-ku, 1698555, Tokyo, Japan**
[2]**Escuela de Ingeniería y Arquitectura, Universidad de Zaragoza. Campus Río Ebro, María de Luna 3, 50018, Zaragoza, Spain (mbailera@unizar.es)**
[3]**Department of Modern Mechanical Engineering, Waseda University. 3-4-1 Okubo, Shinjuku-ku, 1698555, Tokyo, Japan (takao.nakagaki@waseda.jp)**
[4]**Exergy Engineering Research, Nakagaki Lab, Waseda University. 3-4-1 Okubo, Shinjuku-ku, 1698555, Tokyo, Japan (ryoma.adms.1.00@suou.waseda.jp)**

*Corresponding author

Abstract

The Rist diagram is a useful methodology for predicting changes in blast furnaces when the operating conditions are modified. In this paper we revisit this methodology to provide a general model with additions and corrections. The new model is validated with three data sets corresponding to (1) an air-blown blast furnace without auxiliary injections, (2) an air-blown blast furnace with pulverized coal injection and (3) an oxygen blast furnace with top gas recycling and pulverized coal injection. The error is below 8% in all cases. The reason for revisiting the Rist diagram is to study a new concept proposal that combines oxygen blast furnaces with Power to Gas technology. The latter produces synthetic methane by using renewable electricity and CO_2 to partly replace the fossil input in the blast furnace. Carbon is thus continuously recycled in a closed loop and geological storage is avoided. Assuming a 280 t_{HM}/h oxygen blast furnace that produces 1154 kg_{CO2}/t_{HM}, we can reduce the CO_2 emissions between 6.1% and 7.4% by coupling a 150 MW Power to Gas plant. This produces 21.8 kg/t_{HM} of synthetic methane that replaces 22.8 kg/t_{HM} of coke or 30.2 kg/t_{HM} of coal. The gross energy penalization of the CO_2 avoidance is 27.1 MJ/kg_{CO2} when coke is replaced and 22.4 MJ/kg_{CO2} when coal is replaced. Considering the energy content of the saved fossil fuel, and the electricity no longer consumed in the air separation unit thanks to the O_2 coming from the electrolyzer, the net energy penalizations are 23.1 MJ/kg_{CO2} and 17.9 MJ/kg_{CO2}, respectively. The proposed integration has energy penalizations greater than conventional amine carbon capture (typically 3.7 – 4.8 MJ/kg_{CO2}), but in return it could reduce the economic costs thanks to diminishing the coke/coal consumption, reducing the electricity consumption in the air separation unit, and eliminating the requirement of geological storage.

Keywords

Blast furnace; Rist diagram; ironmaking; operating diagram; Carbon capture; Power to Gas; Oxyfuel combustion; CO_2.

Plain language summary

The steel industry is one of the most CO_2 emitting industries worldwide. In this article we study the possibility of recycling the CO_2 that is emitted in order to produce natural gas. Thus, the CO_2 emissions are converted to a useful fuel instead of released to the atmosphere. For this process, renewable electricity is used, so the natural gas produced can be considered environmentally friendly. With this natural gas we want to replace the fossil fuel that is conventionally used in the steel industry. To make this study we have used a mathematical model that was developed by a researcher named Rist between 1963 and 1967. We made some corrections and additions to this mathematical model to make it more accurate. The results of this study show that the CO_2 emissions can be reduced between 6.1% and 7.4% by using commercially available technology.

1. Introduction

The potential contribution of carbon capture and utilization to the global warming mitigation challenge has shown to be very limited when compared to geological storage or electrification [1,2]. If we talk in particular about e-fuels (e.g., hydrogen from renewables and synthetic methane), the electricity-to-useful-energy efficiencies range from roughly 10% to 35%, meaning that energy requirements are 2–14 times higher than for direct electrification [2]. However, some of the most energy- and carbon-intensive sectors worldwide face limitations when applying electrification. In some cases this is because the requirement of high-temperature heat above 400 °C (e.g., glass, cement) and others because the nature of the process itself (e.g., ironmaking, long-distance aviation and shipping) [2]. Renewable hydrogen and synthetic fuels can overcome this barriers, delivering the same service at lower costs than the other CO_2 abatement alternatives, so they should be targeted on these industries from an economic and carbon-neutrality perspective [1,2]. Furthermore, given the substantial size of the mentioned sectors, the application of e-fuels within them should be prioritized [2].

Within this framework, several authors have studied the application of Power to Gas (PtG) to ironmaking processes based

on the reduction of iron ores with coke in a blast furnace (BF). The Power to Gas concept includes all those processes that converts renewable electricity into gaseous fuel by using an electrolysis stage (among other steps) [3]. In this case, the renewable fuel is used for the replacement of coke or coal in the blast furnace. According to literature [4], the integrations involving Power to Syngas may lead to CO_2 emission reductions between 11% and 22%, with respect to conventional blast furnaces. The required electricity consumption of the overall system, per kilogram of CO_2 recycled, lies in the range 4.8 – 10.8 MJ/kg_{CO2}. Moreover, the thermal energy necessities vary from 1 to 2.5 MJ/kg_{CO2}, increasing to 7.8 MJ/kg_{CO2} if carbon capture is used. The electrolysis power capacity required in this integrations range between 100 MW to 900 MW.

Regarding the integration of ironmaking with Power to Methane, the available studies in literature are very scarce. In these studies [5][6], the CO_2 emissions reduction compared to conventional ironmaking is in the range 13% – 19%. Even for this moderate reductions, water electrolysis power capacities of about 880 MW would be required. Additionally, Bailera et al. [4] proposed a novel concept that combines Power to Methane with oxygen blast furnaces (OBF). In oxygen blast furnace, pure oxygen is used for combustion instead of air, thus obtaining a top gas with very little contain of nitrogen. In this type of blast furnaces, it is usual to separate the CO_2 from the top gas and to recycle the H_2 and CO content again to the blast furnace to act as reducing agents and as a sink of heat (because N_2 is no longer present) [7]. Since the water electrolysis of the PtG by-produces O_2, it allows diminishing the electricity consumption of the air separation unit that feeds the oxygen blast furnace. A first approach to this OBF-PtG system was studied by Perpiñán et al. [8] by using overall energy and mass balances. Assuming 430 MW electrolysis power capacity, he found CO_2 emissions reduction of 8% and specific electricity consumptions of 34 MJ/kg_{CO2}.

In order to deep in the concept of OBF-PtG integration, a more detailed analysis of the behavior of the blast furnace is required. To do so, the Rist diagram (also known as operating diagram) is a convenient methodology for predicting changes in blast furnaces when the operating conditions are modified. This methodology is based on the graphical representation of carbon, oxygen, and hydrogen balances through an operation line, restricted by the energy balance, which depicts the participation of these elements in the formation of the reducing gas and its later utilization inside the furnace [9]. The original model is thoroughly explained in a series of papers that progressively deeps into the topic [9–13]. However, some of the most important parts were not written in English, and a paper summarizing the general model is not available. As a result, relevant aspects of his work are sometimes no widely known. Such is the case that some authors claim to modify Rist diagram to include the H_2 contribution [14,15], when in fact this was already took into account by Rist. For these reasons, we decided to revisit his original work, during which we made a number of additions and corrections.

Thus, the first major novelty of this paper is presenting a general operating diagram methodology that considers multiple injectants treated separately, with all calculations given as a function of the temperature of the thermal reserve zone that exist inside the furnace. Besides, the new model calculates the sensible heats of the hot metal and slag as a function of their composition, and the heat of carburization as a function of the austenite and cementite content in iron. Furthermore, it is added a supplementary model to compute the heat of decomposition of coal, an additional energy balance in the upper zone of the blast furnace to compute the final composition of the blast furnace gas, as well as other energy balance for the calculation of the flame temperature. Regarding corrections with respect to the Rist's original model, the heat associated to the direct reduction of FeO now accounts for the moisture of the hot blast, the heat associated to the lack of chemical ideality now includes the influence of the hydrogen coming from auxiliary fuels and of the moisture of the hot blast, and lastly, the sensible heats of hot metal and slag are now correctly computed and accounted.

The second major novelty of the paper is analyzing for the first time the OBF-PtG integration under the operating diagram methodology and, therefore, by using consistent operation data sets. Besides, the operating lines of these blast furnaces are obtained, which cannot be found elsewhere in literature. The third major novelty is to provide full operation data sets for different blast furnaces, with detailed composition of all streams and their most relevant operating parameters (e.g., temperature of the thermal reserve zone, heat evacuated by the staves, and the temperature of the flame). The availability of this information in literature is very scarce, especially for oxygen blast furnaces.

The paper is divided in the following sections. First, a brief description of a blast furnace is presented to summarize the processes that will be taken into account during the elaboration of the operating diagram and in the calculation of the operating line (Section 2). Then, the construction of the operating diagram (Section 3) and the calculation methodology of the operating line (Section 4) are thoroughly described, highlighting the new contributions with respect to the original work of Rist. The model is validated with different data sets elaborated from literature data (Section 5), and then used to obtain new operating lines of oxygen blast furnaces with synthetic natural gas injection (Section 6). The paper also includes an exhaustive section of appendixes to make the proposed methodology and the obtained results fully reproducible by the reader. Moreover, it was used the same notation than Rist in order to make easier the comparison between both methodologies.

2. Blast furnace

The largest blast furnaces at present can produce 10 – 13 kt of hot metal a day. They are about 34 m in inner height (distance from the raw material entrance to the hot metal exit) and 16 m in diameter, with an internal volume in the range 5000 – 5500 m^3 [16][17]. It has a vertical cylindrical structure, externally covered with a shell of steel and internally with refractories. Between the shell and the refractories, the structure is cooled by staves [16]. Staves are cooling gadgets having one or more inside channels through which water flows. The heat removed by cooling may be about 400 – 1800 MJ/THM [10,17–20].

Iron ore and coke, which are introduced at the top, take 5 to 7 hours to descend to the bottom by gravity [21]. To reduce this burden, a reducing gas (mainly CO, but also H_2) ascends throughout the furnace in 5 to 10 seconds and reduces iron ores after going through numerous chemical reactions (**Figure 1**). The gas is produced at the lower part of the furnace by burning the coke with O_2-enriched pressurized air injected through the tuyeres (coke is the only charged material which descends to

the tuyere level in the solid state). The gases move upward due to the pressure of this hot blast and exits the furnace at the top at 2.0 – 2.5 bar. Auxiliary fuels, such as pulverized coal or natural gas can also be injected through the tuyeres to diminish the amount of coke introduced with the burden. At the bottom, the molten metal is collected [16].

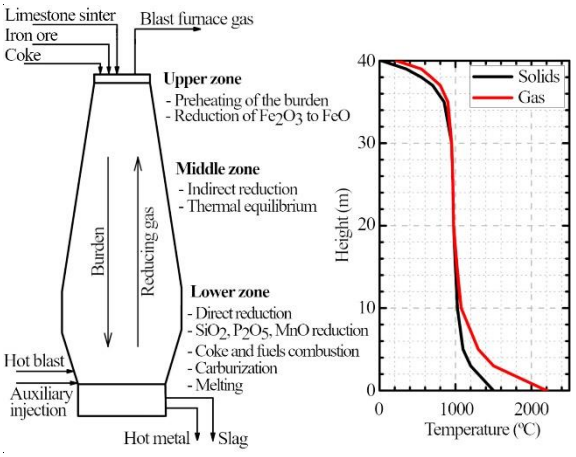

Figure 1. Schematic diagram of a blast furnace and its typical temperature profile.

2.1 Chemical reactions

Inside the blast furnace, the process is as follows (**Figure 1**). In the upper part (4 – 6 m from the top), the hematite is reduced to magnetite through irreversible reactions (Eq.(1) and Eq. (2), exothermic), and then to wüstite (Eq.(3) and Eq.(4), endothermic) [16]. To ensure the reduction, the ratios of CO/CO_2 and H_2/H_2O have to exceed their stoichiometric value. Otherwise, the reactions would not achieve equilibrium because of the short residence time of the gases in the furnace.

$$3Fe_2O_3 + CO \rightarrow 2Fe_3O_4 + CO_2 \qquad \Delta H = -52.85\ \text{kJ/mol} \qquad (1)$$
$$3Fe_2O_3 + H_2 \rightarrow 2Fe_3O_4 + H_2O \qquad \Delta H = -\ 4.86\ \text{kJ/mol} \qquad (2)$$
$$Fe_3O_4 + CO \rightarrow 3FeO + CO_2 \qquad \Delta H = +36.46\ \text{kJ/mol} \qquad (3)$$
$$Fe_3O_4 + H_2 \rightarrow 3FeO + H_2O \qquad \Delta H = +84.45\ \text{kJ/mol} \qquad (4)$$

The middle zone of the blast furnace extends about 25 m downward from the end of the upper zone. It takes 2.5 to 3 hours for the burden to traverse the zone, during which the wüstite is partially reduced following Eq.(5) and Eq.(6) (indirect reduction) [16]. This process is exothermic for CO and endothermic for H_2. In addition, the water-gas shift reaction reaches equilibrium in this zone, Eq.(7) [20].

$$FeO + CO \rightarrow Fe + CO_2 \qquad \Delta H = -17.13\ \text{kJ/mol} \qquad (5)$$
$$FeO + H_2 \rightarrow Fe + H_2O \qquad \Delta H = +30.86\ \text{kJ/mol} \qquad (6)$$
$$CO + H_2O \leftrightarrow CO_2 + H_2 \qquad \Delta H = -40.45\ \text{kJ/mol} \qquad (7)$$

In the lower zone (from 3 – 5 m above the tuyeres to the bottom), the rest of the wüstite is reduced by coke carbon through the direct reduction process (Eq.(8), endothermic) [16]. Actually, the interaction between iron and coke is limited, but at temperatures above 1000 °C the CO_2 and H_2O reacts with coke and forms CO and H_2 (Eq.(9) and Eq.(10)), which subsequently reduce the iron oxide by Eq.(5) and Eq.(6). This way, coke is consumed [16].

$$FeO + C \rightarrow Fe + CO \qquad \Delta H = +155.34\ \text{kJ/mol} \qquad (8)$$
$$CO_2 + C \rightarrow 2CO \qquad \Delta H = +172.47\ \text{kJ/mol} \qquad (9)$$
$$H_2O + C \rightarrow H_2 + CO \qquad \Delta H = +124.48\ \text{kJ/mol} \qquad (10)$$

Apart from the direct reduction, other relevant processes occur in the lower zone. The burden contains various impurities that will either dissolve in iron or will form part of the slag. For example, the Al_2O_3, CaO and MgO oxides are not reduced under the blast furnace conditions and therefore they transfer fully into the slag. In the case of SiO_2, MnO and P_2O_5, they are partially reduced and dissolved in the hot metal. It can be considered that these impurities are directly reduced by solid carbon following Eq.(11), Eq.(12) and Eq.(13). The final silicon, manganese and phosphorous contents in the hot metal are much less than the equilibrium values.

$$SiO_2 + 2C + 3Fe \rightarrow Fe_3Si + 2CO \qquad \Delta H = +622.5\ \text{kJ/mol} \qquad (11)$$
$$MnO + C \rightarrow Mn + CO \qquad \Delta H = +286.92\ \text{kJ/mol} \qquad (12)$$
$$P_2O_5 \cdot 3CaO + 5C + 6Fe \rightarrow 2Fe_3P + 3CaO + 5CO \qquad \Delta H = +1184\ \text{kJ/mol} \qquad (13)$$

Other component that will end up dissolved in the hot metal is carbon. As in the previous case, carbon never reaches saturation in pig iron [20]. At the tapping temperatures (1350 – 1450 °C) the carbon content may vary from 2.5 to 4.5% [16].

As simplification, it is assumed that the dissolved carbon forms austenite and cementite in the hot metal, according to Eq.(14) and Eq.(15), respectively [11].

$$\mathrm{C(coke)} \rightarrow \mathrm{C(austenite)} \qquad \Delta H = +34.7\ \mathrm{kJ/mol} \qquad (14)$$

$$3\mathrm{Fe} + \mathrm{C(coke)} \rightarrow \mathrm{Fe_3C} \qquad \Delta H = +6.69\ \mathrm{kJ/mol} \qquad (15)$$

Also in the lower zone, in front of the tuyeres (i.e., the raceway), coke burns with the oxygen of the hot blast, thus providing the process with heat and CO reducing gas. The total reaction of coke in the raceway can be considered as an incomplete combustion due to the shortage of oxygen (Eq.(16)) [16]. Actually, in the inner part of the flame, complete combustion also occurs but the CO_2 ends up dissociating by Eq.(9).

$$\mathrm{C} + \frac{1}{2}\mathrm{O_2} \rightarrow \mathrm{CO} \qquad \Delta H = -113.68\ \mathrm{kJ/mol} \qquad (16)$$

In case of injecting auxiliary fuels to diminish the coke consumption, the incomplete combustion is assumed to follow Eq.(17), where Z denotes the ashes in case of pulverized coal. No water is present since it rapidly dissociates by Eq.(10) as it occurred for CO_2 [16].

$$\mathrm{CH_{2a}O_{2b}N_{2c}S_{2d}Z_z} + \frac{1}{2}\mathrm{O_2} \rightarrow \mathrm{CO} + a\mathrm{H_2} + b\mathrm{O_2} + c\mathrm{N_2} + d\mathrm{S_2} + z\mathrm{Z} \qquad (17)$$

When the injected fuel contains Sulphur (e.g., pulverized coal), this will end forming part of the slag. As simplification, it can be considered that Sulphur dissolves into the hot metal by Eq.(18), and then transfers to the slag by Eq.(19) [20].

$$\mathrm{Fe} + 0.5\mathrm{S_2} \rightarrow \mathrm{FeS} \qquad (18)$$

$$\mathrm{FeS} + \mathrm{CaO} + \mathrm{C} \rightarrow \mathrm{Fe} + \mathrm{CaS} + \mathrm{CO} \qquad (19)$$

Per each mole of S that ends in the slag, one mole of CO is added to the reducing gas.

2.2 Temperature profile

The blast furnace process can be divided in three different temperatures zones (**Figure 1**). At the lower part, the flame temperature is normally between 2000 and 2300 °C (defined as the temperature reached by the raceway gas when all C and H_2O have been converted to CO and H_2) [22]. This raceway gas provides heat for the direct reduction process and for the melting of the hot metal and slag [20]. The hot metal exits at 1350 – 1450 °C and the slag at 1500 – 1550 °C [16]. The gas, which has been cooled to about 1000 °C, ascends to the middle zone.

The middle zone is a region of thermal equilibrium. In practice, a non-zero temperature difference remains between gas and solids, but it passes through a minimum value in a region of slow heat exchange. The temperature is kept almost constant around 800 – 1000 °C [10].

Lastly, in the upper zone, the gas and the burden exchanges heat rapidly. The gas is cooled down from 800 – 900 °C to 100 – 200 °C as it leaves the furnace top, and the burden is heated from ambient temperature to 800 °C while descending [16][20]. The temperature profile and the reduction zones (pre-reduction, indirect reduction, and direct reduction) more or less coincide, so these three zones can be used to study the blast furnace.

3. Generalized Rist diagram with multiple injectants

The Rist diagram is named so in reference to its author, who elaborated a model for predicting changes in blast furnaces when the operating conditions are modified [9–13]. The model is based on the graphical representation of carbon, oxygen, and hydrogen balances through an operation line that depicts the participation of these elements in the formation and utilization of the reducing gas [9]. Additionally, the diagram includes an equilibrium line to delimit the maximum oxidation state of the gas according to the Chaudron diagrams for the Fe-O-H and Fe-O-C systems [23].

The construction of the Rist diagram is introduced here with additions and corrections with respect to the original work of Rist. The model methodology is now described for the general case of multiple injectants treated separately (instead of for an overall single injection). This is especially important because it will allow to properly calculate the heat of decomposition of each auxiliary fuel, as well as to specify different inlet temperatures for each injectant. Additionally, a detailed description on how to find the equilibrium line for the diagram is included.

3.1 Formation of the reducing gas (Rist diagram in the range 0 < X < 1)

The mass balance of the formation of 1 mol of reducing gas mixture (i.e., the gas exiting the lower zone) can be written according to Eq.(20) [9].

$$x_v + 2x_e + \sum (a_j + 2b_j)x_j + x_{Si} + x_{Mn} + x_P + x_S + x_k + x_d = 1\ \text{mol of reducing gas} \qquad (20)$$

In this equation, each addend denotes the number of moles of CO and/or H_2 (per mole of the total reducing gas mixture) that are either introduced in the blast furnace or produced through a reaction. In other words, these addends are the individual

contributions (in mole fractions) to the formation of the reducing gas mixture. They are given according to the sources of hydrogen (H_2), oxygen (0.5 mole of O_2 will give 1 mole of CO) or water (1 mole of H_2O will give 1 mole of CO and 1 mole of H_2).

The term x_v denotes the CO produced when the O_2 of the hot blast react with C through Eq.(16) or Eq.(17). The term $2x_e$ accounts for the H_2 and CO produced by the moisture of the hot blast when dissociated through Eq.(10). The term $a_j x_j$ denotes the H_2 from the incomplete combustion of an auxiliary injection j (Eq.(17)), while $2b_j x_j$ is the CO produced when the oxygen of that auxiliary injection react with C according to Eq.(16). The terms x_{Si}, x_{Mn} and x_P stand for the CO produced when reducing the impurities SiO_2, MnO and P_2O_5 (Eq.(11), Eq.(12) and Eq.(13)). The addend x_S represents the CO released when transferring the dissolved Sulphur in the iron to the slag (Eq.(19)). The term x_k is the H_2 directly coming from the hydrogen content of the coke. Lastly, x_d denotes the CO released during the direct reduction of wüstite (Eq.(8)) [10].

Each of the addends of Eq.(20) can be depicted as a segment on the abscissa axis, whose total sum covers the interval 0 < X < 1 (**Figure 2**). For convenience, the notation of Eq.(21) is used for the units of the abscissas in the diagram, where the numerator is the number of moles of reducing gas related to a particular reaction or injection according to the sources of hydrogen (H_2) and oxygen (0.5 mole of O_2 giving 1 mole of CO), and the denominator is the total number of moles of reducing gas according to the sources of hydrogen (H_2) and carbon (1 mole of C giving 1 mole of CO) [12].

$$X = \frac{O + H_2}{C + H_2} \tag{21}$$

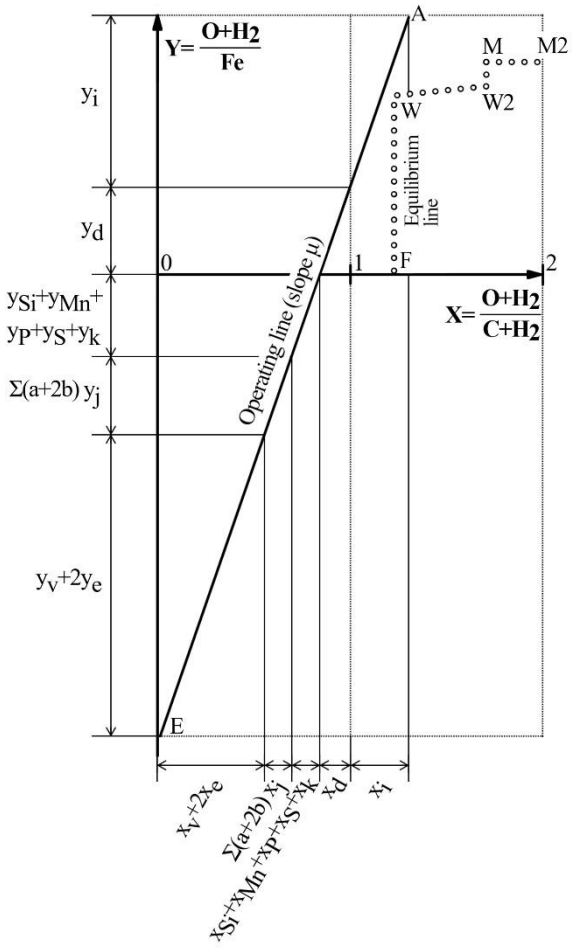

Figure 2. Rist diagram.

Alternatively, the mass balance for the production of the reducing gas mixture can also be written with reference to the production of 1 mole of Fe in the blast furnace. Under this reference, the mass balance follows Eq.(22).

$$y_v + 2y_e + \sum (a_j + 2b_j) y_j + y_{Si} + y_{Mn} + y_P + y_S + y_k + y_d = \mu \text{ moles of reducing gas/mol}_{Fe} \tag{22}$$

Here, the addends denote the moles of reducing gas (CO and H_2) that are introduced in the blast furnace or produced through a reaction, per unit of Fe obtained (the meaning of each addend is identical than in Eq.(20)) [10]. The sum of these segments represents the total moles of reducing gas per unit of Fe (denoted by μ) [9]. Each of the addends of Eq. (22) can be represented as a segment on the ordinate axis (**Figure 2**). In this case, the origin on the Y axis of the operating diagram is arbitrary. For convenience, it is chosen so that the oxygen originally combined to iron appears on the positive side (i.e., y_d), whereas other sources of oxygen and hydrogen appear on the negative side (this ordinate is denoted by Y_E for convenience,

Eq.(23)) [9].

$$Y_E = -\left(y_v + 2y_e + \sum(a_j + 2b_j)y_j + y_{Si} + y_{Mn} + y_P + y_S + y_k\right) \quad (23)$$

The units of the ordinate axis are set according to Eq.(24), given as a function of the sources of hydrogen (H_2) and oxygen (0.5 mole of O_2 giving 1 mole of CO) for the production of the reducing gas.

$$Y = \frac{O + H_2}{Fe} \quad (24)$$

The corresponding terms of Eq.(20) and Eq.(22) form sets of proportional numbers and, as such, they can be read on two rectangular axes as the projections of the same straight line. The **Figure 2** shows the straight line thus obtained, called the "operating line" [9], whose slope has the units of Eq.(25).

$$\mu = \frac{C + H_2}{Fe} \quad (25)$$

This corresponds to the total number of moles of reducing gas, per unit of Fe, according to the sources of hydrogen and carbon.

3.2 Utilization of the reducing gas (Rist diagram in the range 1 < X < 2)

Following the same principle, it is simple to depict the utilization of the reducing gas mixture (Eq.(1) – Eq.(6)) by means of a segment representing the oxygen removed from the iron oxides. The number of oxygen moles transferred from the iron oxides to the reducing gas is denoted by x_i when referred to 1 mole of reducing gas mixture, and by y_i when referred to 1 mole of Fe (same convention than before). Thus, the ratio between both variables (i.e., y_i/x_i) is the number of moles of reducing gas mixture per mole of Fe produced. Since the reduction of iron oxides does not change the total number of moles of the reducing gas, the ratio y_i/x_i is constant and equal to μ. In other words, in all equations from Eq.(1) to Eq.(6) the gas gets oxidized without increasing or decreasing the number of moles in the gas (1 mole of CO gives 1 mole of CO_2, and 1 mole of H_2 gives 1 mole of H_2O). Therefore they can also be read as projections of the same straight line of slope μ (segment in the range 1 < X < 2 of the Rist diagram, **Figure 2**) [9].

This segment in the range 1 < X < 2 is particularly useful because it provides information on the average oxidation state of the reducing gas mixture (abscissa) and of the iron oxides (ordinate) [12]. The abscissa can be interpreted as the reducing gas having an average oxidation state equal to $X - 1$ (see Eq.(26)). This means that at the abscissa $X = 1$, we find a reducing gas mixture composed by CO and H_2, while at the abscissa $X = 2$ the gas is completely oxidized to CO_2 and H_2O. On the other hand, the Y coordinates represent the oxidation state of the iron oxides according to Eq.(27). This interpretation allow identifying the point A in the Rist diagram, whose ordinate is the initial oxidation state of the burden (e.g., $Y_A = 1.5$ for Fe_2O_3) [12] and whose abscissa is the final degree of oxidation of the gas leaving the top of the furnace plus 1 [13].

$$X = 1 + \frac{CO_2 + H_2O}{CO + CO_2 + H_2 + H_2O} \quad (26)$$

$$Y = \frac{O}{Fe} \quad (27)$$

The necessary condition to understand the segment 1 < X < 2 in this way is that the total number of moles of reducing gas keeps constant and that the oxygen supplied to the gas must come only from the reduction of the iron oxides (i.e., no additional injections in the middle or upper zone, and no $CaCO_3$ introduced, which would decompose into CaO and CO_2 through calcination) [12]. Moreover, it should be noted that such a correspondence between the abscissa and the composition of the mixture does not exist in the interval 0 < X < 1, where the segments could be arranged in any order.

3.3 Equation of the operating line

According to the theory described above, the equation of the operating line can be written as Eq.(28). The slope, μ, is the number of moles of reducing gas required for the production of 1 mole of Fe. The intercept, Y_E, represents the moles of H_2 and O coming from sources other than iron oxides that contribute to the formation of the reducing gas (negative sign by convention, Eq. (23)) [12].

$$Y = \mu \cdot X + Y_E \quad (28)$$

If the operating line is characterized, relevant information can be deduced from it. The slope accounts for the total reducing agent rate required (in terms of C and H_2 per mole of Fe) so, if an auxiliary fuel is introduced, the decrease in the input rate of coke can be computed [5]. The intercept stands for the hydrogen and oxygen brought into the furnace (except for the O_2 contained in the iron ore), therefore the necessary air flow rate can be calculated by subtracting the other O_2 and H_2 sources (moisture, auxiliary fuels, coke and impurities) [5]. Also, the initial oxidation state of the iron oxides introduced in the blast furnace (Y_A) allows to know the final degree of oxidation of the gas leaving the top of the furnace ($X_A - 1$). Finally, the ratio

between direct and indirect reduction is identified by construction. The abscissa X = 1 gives the oxygen removed by direct reduction, y_d (**Figure 2**), and then the oxygen removed by indirect reduction is easily calculated as $y_i = Y_A - y_d$.

3.4 Equilibrium line

In the blast furnace, the reducing gas can never oxidize the solids. For this reason, the operating line in the segment 1 < X < 2 must necessarily remain on the left of the equilibrium line of the Fe-O-H-C system (**Figure 2**). If we were at some point at the right of the equilibrium line, the way to reach equilibrium would be displacing us upwards (i.e., providing O to the Fe) or leftwards (removing O from the gas), what in both cases means to oxidize the solids.

The contour of the equilibrium line is delimited by five points, which we will denoted by F, W, W2, M, M2. The point W is of special interest since it corresponds to the chemical equilibrium between gases and solids at the beginning of the middle zone, where pure wüstite is found if the blast furnace operates under ideal conditions. The coordinates of these points are given in **Table 1**. The ordinates of the five points are easily calculated as the ratio of the oxygen and iron atoms of the corresponding components (Eq.(27)) [24]. The abscissas (X_W Eq.(29) and X_M Eq.(30), which are equivalent to Eq.(26)) depend on the molar fraction x_h that relates the hydrogen and water content of the reducing gas mixture (Eq.(31)). This is used to combine the state of oxidation at equilibrium ω for the individual CO-CO_2 and H_2-H_2O mixtures (**Figure 3**). It should be noted that the molar fraction x_h is independent of the state of oxidation of the reducing gas (i.e., independent of the abscissa X), and can be calculated as a function of y_e, y_k, $a_j y_j$ and μ.

$$X_W = 1 + (1 - x_h)\omega_{WC} + x_h\omega_{WH} \quad (29)$$

$$X_M = 1 + (1 - x_h)\omega_{MC} + x_h\omega_{MH} \quad (30)$$

$$x_h = \frac{H_2 + H_2O}{CO + CO_2 + H_2 + H_2O} = \frac{(y_e + y_k + \sum a_j y_j)}{\mu} \quad (31)$$

Table 1. Delimiting points of the equilibrium line for the Fe-O-H-C system in a Rist diagram.

		Abscissa X	Ordinate Y
F	Iron Fe	$X_F = X_W$	$Y_F = 0$
W	Wüstite $Fe_{0.95}O$	X_W = Eq.(29)	$Y_W = 1.05$
W2	Wüstite $Fe_{0.89}O$	$X_{W2} = X_M$	$Y_{W2} = 1.12$
M	Magnetite Fe_3O_4	X_M = Eq.(30)	$Y_M = 1.33$
M2	Magnetite Fe_3O_4	$X_{M2} = 2$	$Y_{M2} = 1.33$

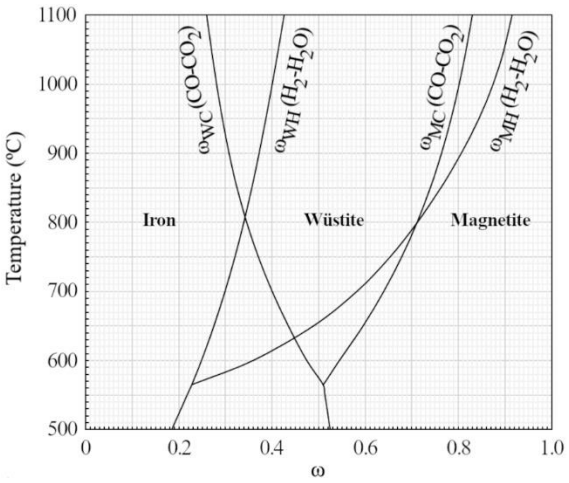

Figure 3. Equilibrium of the Fe-O-C and Fe-O-H systems. The variable ω stands for $n_{CO2}/(n_{CO}+n_{CO2})$ in the case of ω_{WC} and ω_{MC}, and for $n_{H2O}/(n_{H2}+n_{H2O})$ in the case of ω_{WH} and ω_{MH}.

For computing ω, Chaudron diagrams or tabulated data must be used [9]. In our case, we adjusted the data from [10][23] to a polynomic equation where T is given in °C (Eq.(32)).

$$\omega = a_0 + a_1 T + a_2 T^2 + a_3 T^3 + a_4 T^4 + a_5 T^5 \quad (32)$$

The coefficients are presented in **Table 2**. The temperature at which ω is calculated corresponds to the temperature of the middle zone (normally between 800 and 1000 °C), where the chemical equilibrium between the gas and the solids occurs. We denote this temperature as T_R.

Table 2. Coefficients for the calculation of the oxidation state at equilibrium in Fe-O-C and Fe-O-H systems (Eq.(32)). Valid from 500 to 1100 °C.

	T (°C)	Equilibrium	$a_0 \cdot 10$	$a_1 \cdot 10^3$	$a_2 \cdot 10^5$	$a_3 \cdot 10^8$	$a_4 \cdot 10^{11}$	$a_5 \cdot 10^{15}$
ω_{WC}	>565	Iron-Wüstite	4.0894101	3.8856440	-1.3778206	1.7924558	-1.0465659	2.3054702
	<565	Iron-Magnetite	6.3672662	-0.2230216	0	0	0	0
ω_{MC}	>565	Wüstite-Magnetite	-7.8765294	3.6286637	-0.2811151	0.0772069	0	0
	<565	Iron-Magnetite	6.3672662	-0.2230216	0	0	0	0
ω_{WH}	>565	Iron-Wüstite	-0.4957779	-0.5074581	0.4367340	-0.6744924	0.4402173	-1.0668513
	<565	Iron-Magnetite	-1.4558633	0.6611511	0	0	0	0
ω_{MH}	>565	Wüstite-Magnetite	-215.36181	115.54294	-24.611536	26.555149	-14.341369	30.845286
	<565	Iron-Magnetite	-1.4558633	0.6611511	0	0	0	0

4. Calculation of the operating line

In practice, and especially when predicting new operating conditions, the equation of the operating line cannot be directly computed by calculating μ and Y_E because the required data is missing. The operating line must be obtained through two characteristic points denoted as R (coordinates X_R, Y_R) and P (coordinates X_P, Y_P). The former represents the equilibrium between gases and solids reached in the middle zone. The latter is a fixed point imposed by the energy balance of the blast furnace. When these two points of the operating line are known, it is easy to compute the slope and the Y-intercept of the operating line (Eq.(33) and Eq.(34)):

$$\mu = \frac{Y_R - Y_P}{X_R - X_P} \tag{33}$$

$$Y_E = Y_R - X_R \left(\frac{Y_R - Y_P}{X_R - X_P}\right) \tag{34}$$

In the following subsections, it is explained how to calculate the points R and P. The additions and corrections to the original work of Rist are introduced mainly during the calculation of the energy balance (explained more in detail in the appendixes.). These are the following:

- All calculations are given as a function of the temperature of the middle zone, T_R (i.e., of the temperature of the thermal reserve zone where thermal equilibrium exists).
- Each auxiliary fuel can enter at different temperatures because they are now treated separately, rather than as an overall injection.
- The heat associated to the direct reduction of FeO is now corrected taking into account the moisture of the hot blast.
- The sensible heat of the hot metal is calculated as a function of its composition.
- The sensible heat of the slag is calculated as a function of its SiO_2, Al_2O_3, CaO and MgO content.
- The heat of carburization is calculated as a function of the austenite and cementite content in iron.
- The heat associated to the lack of thermal ideality is calculated as a function of the burden and coke composition.
- The heat associated to the lack of chemical ideality is calculated as a function of the burden in the thermal reserve zone.
- The heat associated to the lack of chemical ideality now accounts also for the hydrogen coming from auxiliary fuels and for the moisture of the hot blast.
- A supplementary model is added to compute the heat of decomposition of coal when injected as auxiliary fuel.
- An additional energy balance in the upper zone of the blast furnace is added to compute the final composition of the blast furnace gas, instead of only computing the final oxidation state.

4.1 Point W and point R: chemical and thermal reserve zones

In an ideal blast furnace, the reducing gas and the burden are in chemical equilibrium after the upper zone. This is known as the chemical reserve zone, in which wüstite is the only iron oxide present. This point is denoted by W and was already identified during the construction of the equilibrium line (**Table 1**).

In practice, a blast furnace does not operate under ideal conditions, so a zone of pure wüstite cannot be distinguished (the operating line no longer passes through the point W). For these cases, it is defined the chemical efficiency of the furnace, r, representing the oxygen actually exchanged to the oxygen theoretically exchangeable (typically, r is around 0.92) [10][5]. The coordinates of the new point R, through which the operation line passes, is calculated by Eq.(35) and Eq.(36) as a function of the point W, the chemical efficiency r, and the initial oxidation state of the burden Y_A. [10].

$$X_R = 1 + r(X_W - 1) \tag{35}$$

$$Y_R = Y_A - r(Y_A - Y_W) \tag{36}$$

Despite there is no chemical equilibrium, the temperature is still nearly constant in the middle zone (thermal reserve zone where thermal equilibrium exists), so this temperature is used for the calculations (T_R).

4.2 Point P: energy balance in the elaboration zone

The operating line, Eq.(28), depends on different parameters which are not all independent. In particular, any energy balance, whether global or partial, imposes a relationship between them. An option is to use the energy balance of the

elaboration zone (i.e., middle zone plus lower zone), which follows Eq.(37). As in the original work of Rist, we are going to work in kcal per mole of Fe [10]. Moreover, the reference temperature for the energy balance is chosen at T_R, i.e., at the temperature of the thermal reserve zone.

$$q_c y_v + q_v y_v + (q_{iw} \mathrm{Y_W} - \delta) = q_g(y_d - y_e) + q_k y_k + q_e y_e + \sum q_j y_j - \delta' + q_{\mathrm{Si}} y_{\mathrm{Si}} + q_{\mathrm{Mn}} y_{\mathrm{Mn}} + q_P y_P + q_\gamma \gamma + f + l + p + C_{\Delta T_R} \quad (37)$$

The input/production of energy was written in the left side of the equation, and the output/consumption was specified in the right side of the equation. Regarding the former, we have the term $q_c y_v$ that represents the heat released by the incomplete combustion of carbon, $q_v y_v$ for the sensible heat of the air, $q_{iw} Y_w$ as the heat released by the reduction of wüstite, and δ to account for the lack of chemical ideality in wüstite reduction. In the right side of the equation we have $q_g(y_d - y_e)$ which is the heat absorbed during direct reduction because of CO_2 dissociation, $q_k y_k$ as the heat consumed due to the hydrogen entering with the coke, $q_e y_e$ for the overall heat absorbed by the moisture of the air, $\sum q_j y_j$ to quantify the overall heat absorbed by the auxiliary injections, δ' accounting for the lack of chemical ideality in the conversion of H_2 to H_2O, $(q_{\mathrm{Si}} y_{\mathrm{Si}} + q_{\mathrm{Mn}} y_{\mathrm{Mn}} + q_P y_P)$ for the heat absorbed by the reduction of the accompanying elements SiO_2, MnO and P_2O_5, then $q_\gamma \gamma$ as the heat absorbed by the carburization of the iron, f denoting the heating and melting of the hot metal, l for the heating and melting of the slag, p for the heat removed by the staves and, lastly, $C_{\Delta T_R}$ accounting for the lack of thermal ideality (in case the temperature of the gas and the solid is not the same at the thermal reserve zone).
All the addends of Eq.(37) are thoroughly explained in the Appendix A to avoid breaking here the flow of the explanation. Besides, they are compared with the calculation method appearing in Rist's original work when appropriate to highlight the differences. The meaning and units of each variable is specified in the nomenclature list, and a table summarizing the calculation of the heats denoted by q is available in **Table 6** of Appendix A.
From the energy balance of Eq.(37), we can find a relation between y_d (number of O moles removed from iron oxides by direct reduction) and y_v (number of O moles brought by the air), under given operating conditions defined by the inlet/outlet temperatures, the chemical efficiency, the tuyeres injections, and the composition of hot metal and slag. This relation can be written as Eq.(38), where A, B and C are given by Eq.(39), Eq.(40) and Eq.(41).

$$y_d = \frac{\mathrm{A} y_v - \mathrm{C}}{\mathrm{B}} \quad (38)$$

$$\mathrm{A} = q_c + q_v - e q_e + e q_k (1 - r) + e q_g \quad (39)$$

$$\mathrm{B} = q_g \quad (40)$$

$$\mathrm{C} = -q_{iw} Y_w + \delta + q_k y_k + \sum q_j y_j - (1 - r)\left(y_k + \sum a_j y_j\right) q_k + q_{\mathrm{Si}} y_{\mathrm{Si}} + q_{\mathrm{Mn}} y_{\mathrm{Mn}} + q_P y_P + q_\gamma \gamma + f + l + p + C_{\Delta T_R} \quad (41)$$

Here, the variable e denotes the moles of H_2O per O moles in the air (i.e., $e = y_e / y_v$), which is a convenient notation to write the water injected with the air as a function of the air injected through the tuyeres (i.e., to include the term $q_e y_e$ in A). Similarly, the term δ' was decomposed according to Eq.(92) to separate the terms that depends on y_v (see Appendix A.9). It should be noted that Rist did not decomposed δ' and therefore he wrongly included a term that is actually dependent on y_v in C instead of adding it to A [10]. Moreover, Rist did not included the term $+e q_g$ that appears in A, which corrects the heat absorbed during direct reduction (part of the direct reduction takes place through Eq.(10), see Appendix A.5).
Now, we can impose the relation of Eq.(38) from the energy balance to the operating line defined by Eq.(28). To do that, we first rewrite Eq.(28) as Eq.(42), taking into account that $\mu = -\mathrm{Y_E} + y_d$ according to Eq.(22) and Eq.(23).

$$\mathrm{Y} = -\mathrm{Y_E}(\mathrm{X} - 1) + y_d \mathrm{X} \quad (42)$$

By substituting Eq.(38) in Eq.(42), and by using the convenient notation of Eq.(43) to decompose $\mathrm{Y_E}$ on two terms (one dependent of y_v and another independent), we found Eq.(44) where Δ_1 and Δ_2 are given by Eq.(45) and Eq.(46).

$$\mathrm{Y_E^*} \equiv \mathrm{Y_E} + (1 + 2e) y_v = -\sum (a_j + 2b_j) y_j - y_{Si} - y_{Mn} - y_P - y_S - y_k \quad (43)$$

$$\Delta_1 y_v + \Delta_2 = 0 \quad (44)$$

$$\Delta_1 = \left(\frac{\mathrm{A}}{\mathrm{B}} + 1 + 2\mathrm{e}\right)\mathrm{X} - (1 + 2\mathrm{e}) \quad (45)$$

$$\Delta_2 = -\mathrm{Y} - \left(\frac{\mathrm{C}}{\mathrm{B}} + \mathrm{Y_E^*}\right)\mathrm{X} + \mathrm{Y_E^*} \quad (46)$$

From this operating line in the form of Eq.(44), which accounts for the energy balance, we know that the operating line will pass through a point P of coordinates $\mathrm{X_P}$ and $\mathrm{Y_P}$ fulfilling simultaneously $\Delta_1 = 0$ and $\Delta_2 = 0$. Applying this condition, we can find from Eq.(45) and Eq.(46) the coordinates $\mathrm{X_P}$ and $\mathrm{Y_P}$ (Eq.(47) and Eq.(48)). Now, the operating line of the blast furnace is known.

$$X_P = \frac{B(1+2e)}{A+B(1+2e)} \tag{47}$$

$$Y_P = Y_E^* - \left(\frac{C}{B} + Y_E^*\right)\left(\frac{B(1+2e)}{A+B(1+2e)}\right) \tag{48}$$

It is worth to mention that both coordinates of P depend on the chemical efficiency of the furnace, r, through A and C. However, Rist only considered the dependence on the chemical efficiency through C because he did not decompose δ'. Therefore, he found that X_P was independent of r [10]. Here we have shown that is not.

4.3 Additional results derived from the operating line

The relevance of characterizing the operating line comes from the possibility of deducing operational data such as the required reducing agent rate, the air consumption, the top gas composition, the ratio between direct and indirect reduction, and the flame temperature.

4.3.1 Reducing agent rate (coke consumption)

The reducing agent rate, μ, obtained from the operating line, denotes the number of moles of C and H_2 needed inside the blast furnace as reducing gas for the production of 1 mole of Fe as hot metal. When solving the Rist diagram, we assume the auxiliary injections to be known. Therefore, we can compute the required amount of coke by subtracting the contributions of the injections to μ. The carbon that ends up dissolved in the hot metal must be also taken into account (which increases the required reducing agent rate), as well as the H_2 that is produced when the H_2O from the hot blast is dissociated (which decreases the required reducing agent rate). Thus, the mass flow of coke is calculated by Eq.(49).

$$m_K = \left(\mu + \gamma - e y_v - \sum(\tau_j + a_j) y_j\right) n_{HM,Fe} / \epsilon_{coke} \tag{49}$$

In this equation, γ is the number of moles of C dissolved in the hot metal (Eq.(50)), τ_j is equal to 1 when the auxiliary injection contains carbon and 0 when not, and ϵ_K is the ratio of C and H_2 moles in coke per kg of coke (Eq.(51)). The variables $\Omega_{j,i}$ are the mass fraction of element i in compound j.

$$\gamma = (10^6 \Omega_{HM,C}/M_C)/n_{HM,Fe} \tag{50}$$

$$\epsilon_K = 10^3\left(\frac{\Omega_{K,C}}{M_C} + \frac{\Omega_{K,H}}{M_{H2}}\right) \tag{51}$$

The term $n_{HM,Fe}$ is the number of moles of Fe in hot metal per ton of hot metal (Eq.(74)).

4.3.2 Air flow rate

The intercept of the operation line, denoted by Y_E, represents the H_2 and O brought into the furnace (except for the O contained in the iron ore) with negative sign by convention. By subtracting the O and H_2 sources other than the hot blast, the necessary O flow rate as air can be calculated (i.e., calculation of y_v, Eq.(52))

$$y_v = \frac{-\left(Y_E + \sum(a_j + 2b_j) y_j + y_{Si} + y_{Mn} + y_P + y_S + y_k\right)}{1+2e} \tag{52}$$

Once we know y_v, the mass of air (dry) per ton of hot metal is calculated by Eq.(53).

$$m_v^d = \frac{y_v\, n_{HM,Fe}}{2000}\left(M_{O2} + \frac{0.79}{0.21} M_{N2}\right) \tag{53}$$

4.3.3 Blast furnace gas composition

Once the coke and air flow rate are known, the input streams to the blast furnace become completely characterized. In order to characterize also the output streams, we have to find 15 unknown variables. These are the mass flow rate of each component in the blast furnace gas ($m_{BFG,CO}$, $m_{BFG,CO2}$, $m_{BFG,H2}$, $m_{BFG,H2O}$, $m_{BFG,N2}$), the mass flow rate of hot metal m_{HM} (the individual mass flow rate of each component in hot metal is calculated through its mass fraction, which is assumed known from the beginning), and the mass flow rate of each component in the slag ($m_{Slag,SiO2}$, $m_{Slag,Al2O3}$, $m_{Slag,CaO}$, $m_{Slag,MgO}$, $m_{Slag,MnO}$, $m_{Slag,CaS}$, $m_{Slag,P2O5}$, $m_{Slag,Fe2O3}$, $m_{Slag,FeO}$). The system of 15 equations to solve the balance comprises 11 mole balances for Fe, Si, Al, Ca, Mg, Mn, C, H, N, S, P (the O balance was already accounted in the elaboration of the operating line), two mass balances for $m_{Slag,Fe2O3}$, $m_{Slag,FeO}$ (they correspond to the Fe_2O_3 and FeO content of the coal ashes, which enter at the tuyeres and are not reduced), one equation related to the final oxidation state of the blast furnace gas (information coming from the operating line, Eq.(54)), and one energy balance of the preparation zone (i.e., of the upper zone).

$$\eta_{CO-H_2} \equiv \frac{n_{BFG,CO_2} + n_{BFG,H_2O}}{n_{BFG,CO} + n_{BFG,CO_2} + n_{BFG,H_2} + n_{BFG,H_2O}} = \frac{Y_A - Y_E}{\mu} - 1 \tag{54}$$

It should be noted that knowing the final oxidation state of the gas exiting the top of the furnace (i.e., Eq.(54)) is not sufficient to compute the final composition of the top gas because the gas is not in equilibrium at the upper part of the furnace. In other words, the water-gas shift reaction (Eq.(7)) changes the BFG composition without modifying η_{CO-H_2}, but the extent of this reaction is unknown. For this reason, the energy balance of the preparation zone is required. This energy balance is detailed in Appendix C.

Most authors use the CO utilization ratio ($\eta_{CO} \equiv n_{BFG,CO_2}/(n_{BFG,CO} + n_{BFG,CO_2})$) as the 15th equation to complete the system of equations, instead of using the energy balance in the upper zone. They assume to know this parameter, since in practice they would be able to measure it at the flue gas of a real ironmaking plant. Indeed, in those cases in which the operating line is characterized for a real operation where the η_{CO} information is reliable, to use this procedure instead of the energy balance of the upper part makes the methodology easier. However, this is not a valid procedure when analyzing new operating lines for potential blast furnace configurations. In such case, the assumption of the value of η_{CO} would be arbitrary and, almost certainly, it will lead to inconsistencies in the upper zone (energy balance not fulfilled). Inconsistencies which are not detected because of not performing the corresponding energy balance in the upper zone. For this reason, it is completely necessary to use the energy balance of the upper zone instead of η_{CO} when proposing new operating lines.

4.3.4 Amount of direct and indirect reduction

By construction, the abscissa X = 1 allows computing y_d (**Figure 2**), which is the oxygen removed from the iron oxides by direct reduction (Eq.(55)).

$$y_d = \mu + Y_E \tag{55}$$

Then, the oxygen removed by indirect reduction is easily calculated as Eq.(56).

$$y_i = Y_A - y_d \tag{56}$$

4.3.5 Flame temperature

The flame temperature is the temperature that the raceway gas reaches when all oxygen from hot blast and injections has been used for the incomplete combustion of C to CO, and all water has been dissociated to CO and H_2. It can be considered as a control parameter to check if the studied configuration of blast furnace is reasonable, since the injection of auxiliary fuels drops the flame temperature as a consequence of their lower C/H ratio compared to coke (flame temperature should be kept between 2000 and 2300 °C for a proper operation). In such cases, blast oxygen enrichment may be required to maintain a suitable flame temperature.

From a theoretical point of view, this flame temperature can be calculated from an energy balance in the raceways. We use Eq.(57), where we made a similar construction to that of Eq.(37). The term $q_c y_v$ stands for the combustion of C to CO by using the O from the hot blast, the term $q_v y_v$ represents the sensible heat that the dry hot blast is providing, while the term $q_{s,C} y_C$ is the sensible heat of the coke carbon used in combustion (which comes at T_f from the lower zone). At the right side of the equation, we have $(q_{er} + q_{es}) y_e$ which is the contribution of the moisture of the hot blast (decomposition and sensible heat), also $\sum_j (q_{jd} + q_{js} - 2b_j q_c) y_j$ for the auxiliary injections (decomposition, sensible heat and combustion of the O entering with this injections), and $q_{s,N2} y_{rg,N2} + q_{s,CO} y_{rg,CO} + q_{s,H2} y_{rg,H2}$ as the energy required to heat the reducing gas up to the temperature of the flame T_{fl}. Lastly, it is included the heating from T_R to T_{fl} of the ashes from coal injections ($\sum_j z_j q_{s,Z} y_j$).

$$q_c y_v + q_v y_v + q_{s,C} y_C = (q_{er} + q_{es}) y_e + \sum_j (q_{jd} + q_{js} - 2b_j q_c) y_j + \sum_i q_{s,i} y_{rg,i} + \sum_j z_j q_{s,Z} y_j \tag{57}$$

We can say that the flame temperature is a result indirectly derived from the operating line since for its computation we need to know the amount of air injected, the amount of coke, and the amount and composition of the reducing gas (obtained from the composition of the BFG). The variables y_v, y_C, $y_{rg,N2}$, $y_{rg,CO}$ and $y_{rg,H2}$ are calculated by Eq.(52), and Eq.(58) to Eq.(61). In the case of y_C, we can compute it as the oxygen available for combustion minus the C coming from the injections (because 1 mole of O consumes 1 mole of C), or as the C coming from coke minus the C used in reactions other than combustion. The variable τ_j is equal to 1 when the auxiliary injection contains carbon and 0 when not.

$$y_C = y_v + \sum_j (2b_j - \tau_j) y_j = \frac{10^3 \Omega_{K,C} m_K}{M_C n_{HM,Fe}} - (\gamma + y_{Si} + y_{Mn} + y_P + y_S + y_d) \tag{58}$$

$$y_{rg,N2} = n_{BFG,N_2}/n_{HM,Fe} \tag{59}$$

$$y_{rg,CO} = (n_{BFG,CO} + n_{BFG,CO_2})/n_{HM,Fe} \tag{60}$$

$$y_{rg,H2} = (n_{BFG,H_2} + n_{BFG,H_2O})/n_{HM,Fe} \tag{61}$$

The calculation of the rest of the terms were already explained in Appendix A for the energy balance of the elaboration zone. All the q terms are tabulated in **Table 6** according to the adjustment to Eq.(113) or Eq.(114). The variable T in these equations must be substituted by T_R for q_c and q_{er}, by T_v for q_v and q_{es}, by T_f for $q_{s,C}$, by T_j for q_{jd} and q_{js}, and by T_{fl} for $q_{s,i}$ and $q_{s,Z}$. Thus, the only missing variable in Eq.(57) is T_{fl}.

In practice, different authors have developed formulae for the calculation of the flame temperature as a function of different operating parameters [16]. Here we present the equation developed by Babich [25][16], which accounts for natural gas and pulverized coal injections (Eq.(62)). We will use it for comparison and validation purposes.

$$T_{fl} = \frac{44.455V_v T_v\left(c_{p,v} + 0.0012c_{p,H2O}\eta_{nat}\right) + 3146V_v\omega_{v,O_2} - 1170V_{NG}\omega_{NG,CH4} - 600m_{PC}\Omega_{PC,C} - 1.65V_v\eta}{\left(0.2387V_v + 0.24V_v\omega_{v,O_2} + 0.48V_{NG}\omega_{NG,CH4} + 6m_{PC}\Omega_{PC,H} + 0.0006V_v\eta\right)186.785c_{p,rg}} \quad (62)$$

Where V_v is the dry blast volume per ton of hot metal, T_v is the temperature of the blast, ω_{v,O_2} is the oxygen content in the blast, η_{nat} is the natural moisture in the blast, η is the total moisture in the blast, V_{NG} is the natural gas consumption, m_{PC} is the pulverized coal consumption, $\Omega_{PC,C}$ is the carbon content in pulverized coal, $\Omega_{PC,H}$ is the hydrogen content in pulverized coal, $\omega_{NG,CH4}$ is the methane content in natural gas, and $c_{p,v}$, $c_{p,H2O}$ and $c_{p,rg}$ are the specific heats of blast, moisture and reducing gas. The units are provided in the nomenclature list.

5. Model validation

In order to validate the model, we are going to use three different data sets. The first one comes from the original work of Rist [10], corresponding to a conventional air-blown blast furnace without auxiliary injections. The second one is elaborated from the work of Babich et al. [18], for an air-blown blast furnace with pulverized coal injection and O_2-enriched air. The last one is taken from the work of Sahu et al. [26] for an oxygen blast furnace with top gas recycling. When solving the operating diagram, we assume the composition of iron ore, coke, auxiliary injections and hot metal to be known. For iron ore and injections, also the total mass flow is known. For the hot blast, the moisture is fixed. Regarding energy balances, all the inlet and outlet temperatures are known. Finally, the operating conditions on chemical efficiency, heat removed by the staves, the proportion of heat evacuated between the preparation and elaboration zone, and the temperature of the thermal reserve zone are set to known values. Under this framework, the model allows to compute the mass flows of coke, hot blast, hot metal and blast furnace gas. Moreover, the composition of the blast furnace gas and slag can be calculated. Regarding operation conditions, the slope and intercept of the operating line, the amount of direct and indirect reduction, the flame temperature and the oxidation state of the BFG are obtained. The list of inputs and outputs are summarized in **Figure 4** together with a conceptual scheme of the blast furnace. Exceptionally, for those cases in which we are not introducing air in the blast furnace, we assume the mass of the host blast to be known ($m_v = 0$) and we calculate instead the mass flow of the injection that carries the main oxygen input (m_j).

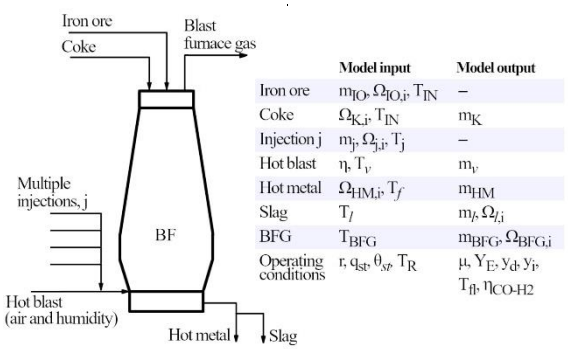

Figure 4. Conceptual diagram of a blast furnace, indicating the input and output data of the model.

5.1 Air-blown blast furnace without auxiliary injections (Rist, Data set 1)

This data set was elaborated from the original work of Rist [10], corresponding to an air-blown blast furnace without auxiliary injections. The input mass flow of iron ore and its composition was calculated through mass balances based on Rist's results, assuming typical mass fractions for those oxides other than iron. Also, it was assumed a typical mass fraction distribution for oxides in coke [27]. The outlet temperature of BFG was assumed 180 °C to estimate the gas composition.

As explained through the model description and appendixes, three potential errors were identified in the original model provided by Rist: (1) underestimation of the heat required inside the blast furnace because not accounting the heating of slag between T_R and T_f (see Appendix A.12), (2) overestimation of the heat required because of wrongly computing the term l with c_{p,SiO_2} in wrong units (see Appendix A.13) and (3) overestimation of the heat required because of considering twice the heat absorbed during direct reduction for a number of moles equals to y_e (see Appendix A.5). For the sake of comparison, we intentionally introduced the same three errors in our model (third column in **Table 3**). This way, the model reproduces the results of Rist with a discrepancy below 3.5%, thus validating the consistency of the model.

The results of the model are also presented with the three mentioned corrections included (fifth column in **Table 3**). In this case, the variation with respect to the data provided by Rist is beyond 5% in some cases, without overpassing the 6%. Fortunately for Rist, the three errors counterbalanced, and reasonable results could be achieved despite of them. Making the comparison fair, the variation between the results of our model with and without the corrections is in the range 1 – 2%. This clearly shows how well the three errors counterbalanced.

Looking for further validation, we compare the flame temperature computed through our model with the calculated by Eq.(62). The latter gives 1898 °C (see Appendix D) and we obtained 1879 °C with our model, what means we have a

discrepancy of only 1.0%. In both cases, the flame temperature is below 2000 °C, which is not suitable for blast furnaces. Nevertheless, the purpose of this data set is validation only, which can be assumed achieved. The type of configuration provided by this data set does not correspond to a state-of-the-art blast furnace, since nowadays most blast furnaces use auxiliary injections like pulverized coal and burdens of greater quality that lead to lower slag productions.
The operating line of this blast furnace is depicted in **Figure 5**, showing that 23% of the oxygen bonded to iron oxides is removed by direct reduction, and the remaining 77% through indirect reduction. The chemical efficiency was assumed 1, so the operating line passes through the point W of the equilibrium line.

5.2 Air-blown blast furnace with pulverized coal injection and O_2-enriched air (Babich, Data set 2)

This data set was elaborated from the work of Babich et al [18], corresponding to an air-blown blast furnace with pulverized coal injection and O_2-enriched air. We consider the O_2-enriched hot blast as an auxiliary injection. The proximate analysis of the coal is 74.1% Ω_{FC}, 17.2% Ω_{VM}, 7.6% Ω_Z and 1.2% Ω_M [18]. Typical mass fractions for iron ore and coke were assumed. Moreover, since the operating parameters r, T_R and θ_{st} are not provided in the work of Babich et al., typical values are chosen.
All results show a discrepancy below the 1% with respect to the data of Babich [18], except for the coke consumption, which varies a 2.1%. The flame temperature calculated by Eq.(62) gives the same result than the one provided by Babich, since he developed that formula. The error in the flame temperature calculated by our model is 1%. The operating line of this blast furnace is depicted in **Figure 5**, which no longer passes through the point W of the equilibrium line (chemical efficiency is 0.92). The direct reduction represents a 30.6% and the indirect reduction a 69.4%.

5.3 Oxygen blast furnace with pulverized coal injection and top gas recycling (Sahu, Data set 3)

In order to validate the model also under oxygen regimes, a third data set from literature is used. The availability of complete data sets in literature is limited (probably because of non-disclosure agreements) and the information gets even more scarce when it comes to oxygen blast furnaces. For this reason, we take the only full data set we found (Sahu et al. [26]), despite it has some underlying inconsistencies (which are consequently reflected in the results of our model). Nevertheless, it gives a good idea on the possibilities of the model when assessing oxygen blast furnaces. The data set corresponds to an oxygen blast furnace with pulverized coal injection and top gas recycling (**Figure 6**). The proximate analysis of the coal is 58% Ω_{FC}, 27% Ω_{VM}, 10% Ω_Z and 5% Ω_M.
The results of the model are compared to the reference data in **Table 4**. Most of the results have an error below the 8%, so it can be considered validated. The greatest discrepancy comes from the nitrogen content of the blast furnace (38% error) because the nitrogen mass balance is not correct in the data set provided by Sahu et al. The total inlet mass of nitrogen is 17.6 kg/t_{HM} (from coal and top gas injection), while the total outlet mass was reported as 26.7 kg/t_{HM} (in the blast furnace gas). Assuming that the correct content of nitrogen in the BFG should be 17.6 kg/t_{HM}, the relative error of the result of the model drops to a reasonable 6%. Other relevant inconsistencies are the incorrect mass balances of Fe, Mn and P. The former leads to an overestimation of the hot metal produced, and the latter to negative mass flows of MnO and P_2O_5 in the slag (the inlet mass flows of MnO and P_2O_5 are not enough to reach the specified Mn and P content in the hot metal). Despite of these issues, the model can reproduce the behavior of the oxygen blast furnace described by Sahu et al. [26] within reasonable discrepancy limits. Moreover, the model has turn out to be a useful tool to identify potential inconsistencies in data sets.
Regarding the flame temperature, in this case we cannot use the Eq.(62) to compute it since this formula does not account for top gas injections. By using our model, we found a flame temperature of about 1770 °C, which is a 17% lower than the one reported by Sahu et al. (2126 °C) [26]. Although they did not explain how they calculated this temperature, they probably did not account for the heating of the injected top gas, while our model does. In fact, one of the reasons of recirculating top gas is to substitute N_2 as heat sink during oxygen regimes, so probably that is why Sahu et al. had to set the inlet temperature of the oxygen to 25 °C (otherwise they would found excessive flame temperatures because of not accounting for the recycled gas). If we calculate in our model the temperature of the flame without taking into account the sensible heat of the recycled gas, we found temperatures between 2200 and 2300 °C, which are closer to the one provided by Sahu et al.
The operating line of this blast furnace is depicted in **Figure 5**. It passes through the point W of the equilibrium line because it is assumed chemical ideality. It can be seen that that the direct reduction represents only a 0.3% of the total reduction, which is unrealistic for a real operation. Therefore, for this reason and the other mentioned inconsistencies, we do not recommend to take this data set for farther analyses.

Table 3. Comparison of model results with literature data sets for air-blown blast furnaces, for validation purposes. *This column shows the results of the model when corrections are not included (see text).

	DATA SET 1					DATA SET 2		
Input streams (kg/t_{HM})	**Rist** [10]	**Model***	**Δ (%)**	**Model**	**Δ (%)**	**Babich** [18]	**Model**	**Δ (%)**
Iron ore (25 °C)	**2276.4**	**2276.4**	**-**	**2276.4**	**-**	**1558.0**	**1558.0**	**-**
# Fe_2O_3	947.4	947.4	-	947.4	-	1146.9	1146.9	-
# FeO	357.3	357.3	-	357.3	-	187.3	187.3	-
# SiO_2	327.5	327.5	-	327.5	-	69.9	69.9	-
# Al_2O_3	133.1	133.1	-	133.1	-	107.2	107.2	-
# CaO	446.0	446.0	-	446.0	-	26.9	26.9	-
# MgO	4.0	4.0	-	4.0	-	16.2	16.2	-
# MnO	19.9	19.9	-	19.9	-	3.6	3.6	-
# P_2O_5	41.2	41.2	-	41.2	-	0.0	0.0	-
Coke (25 °C)	**598.9**	**612.8**	**2.3**	**619.9**	**3.5**	**283.0**	**289.0**	**2.1**
# C	509.0	520.9	2.3	526.9	3.5	251.4	256.7	2.1

# H	3.0	3.1	2.3	3.1	3.3	-	-	-
# S	8.2	8.4	2.3	8.5	3.6	-	-	-
# Fe_2O_3	-	-	-	-	-	1.7	1.8	2.1
# SiO_2	26.5	27.1	2.3	27.4	3.5	19.7	20.1	2.1
# Al_2O_3	10.8	11.0	2.3	11.2	3.5	9.1	9.3	2.1
# CaO	36.1	37.0	2.3	37.4	3.5	0.8	0.8	2.1
# MgO	5.4	5.5	2.2	5.5	3.6	0.3	0.3	2.1
Coal (25 °C)	-	-	-	-	-	**200.0**	**200.0**	**-**
# C	-	-	-	-	-	153.6	153.6	-
# H	-	-	-	-	-	8.3	8.3	-
# O	-	-	-	-	-	10.2	10.2	-
# N	-	-	-	-	-	3.1	3.1	-
# S	-	-	-	-	-	0.9	0.9	-
# H_2O	-	-	-	-	-	2.4	2.4	-
# SiO_2	-	-	-	-	-	12.3	12.3	-
# Al_2O_3	-	-	-	-	-	8.9	8.9	-
# CaO	-	-	-	-	-	0.3	0.3	-
Hot blast (700 °C Rist / 1200 °C Babich)	**2125.6**	**2198.7**	**3.4**	**2242.5**	**5.5**	**1077.8**	**1086.6**	**0.8**
# N_2	1618.0	1673.6	3.4	1706.9	5.5	826.7	833.5	0.8
# O_2	491.0	508.2	3.5	518.3	5.6	251.1	253.1	0.8
# H_2O	16.6	16.9	2.0	17.3	4.1	0.0	0.0	-
O_2 enrichment (1200 °C)	**-**	**-**	**-**	**-**	**-**	**94.3**	**95.1**	**0.8**
Output streams (kg/t_{HM})								
Hot metal (1400 °C Rist / 1500 °C Babich)	**1000.0**	**1000.0**	**0.0**	**1000.0**	**0.0**	**1000.0**	**1000.0**	**0.0**
# Fe	937.0	937.0	0.0	937.0	0.0	947.2	947.2	0.0
# C	38.0	38.0	0.0	38.0	0.0	45.0	45.0	0.0
# Si	4.0	4.0	0.0	4.0	0.0	5.3	5.3	0.0
# Mn	3.0	3.0	0.0	3.0	0.0	2.5	2.5	0.0
# P	18.0	18.0	0.0	18.0	0.0	0.0	0.0	0.0
Slag (1450 °C Rist / 1550 °C Babich)	**1000.0**	**1002.8**	**0.3**	**1003.8**	**0.4**	**260.0**	**261.8**	**0.7**
# SiO_2	-	346.1	-	346.4	-	90.4	91.0	0.7
# Al_2O_3	-	144.1	-	144.3	-	124.6	125.4	0.7
# CaO	-	468.4	-	468.6	-	26.3	26.5	0.7
# MgO	-	9.5	-	9.5	-	16.4	16.5	0.7
# MnO	-	16.0	-	16.0	-	0.4	0.4	0.7
# CaS	-	18.8	-	19.0	-	1.9	1.9	0.7
# P_2O_5	-	0.0	-	0.0	-	-	-	-
BFG (180 °C Rist / 150 °C Babich)	**3000.0**	**3085.2**	**2.8**	**3135.1**	**4.5**	**1953.2**	**1966.9**	**0.7**
# N_2	-	1673.6	-	1706.9	-	830.0	836.6	0.8
# CO_2	-	743.1	-	735.4	-	678.8	684.4	0.8
# CO	-	653.1	-	672.0	-	414.7	416.2	0.4
# H_2O	-	11.8	-	17.7	-	23.9	23.8	-0.6
# H_2	-	3.6	-	3.0	-	5.9	5.9	0.0
Operating conditions								
Chemical efficiency, r (-)	1.000	1.000	-	1.000	-	-	0.92	-
Thermal reserve zone temperature, T_R (°C)	1000.0	1000.0	-	1000.0	-	-	800	-
Flame temperature, T_{fl} (°C)	-	1879.0	-	1881.0	-	2117.0	2138.6	1.0
Heat evacuated by the staves (MJ/THM)	418.4	418.4	-	418.4	-	701.1	701.1	-
Heat evacuated in the elaboration zone, θ_{st} (-)	0.700	0.700	-	0.700	-	-	0.800	-
Oxidation state of the BFG, η_{CO-H_2} (-)	-	0.411	-	0.410	-	0.486	0.487	0.2

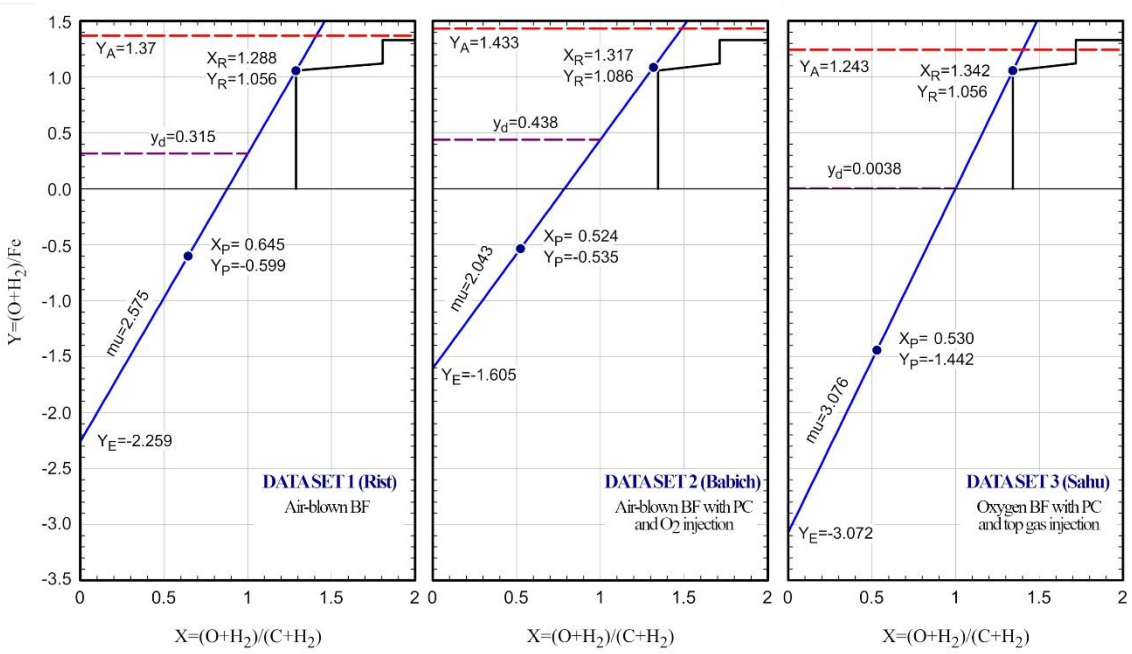

Figure 5. Operating lines obtained from the Data sets 1, 2 and 3 (**Table 3** and **Table 4**).

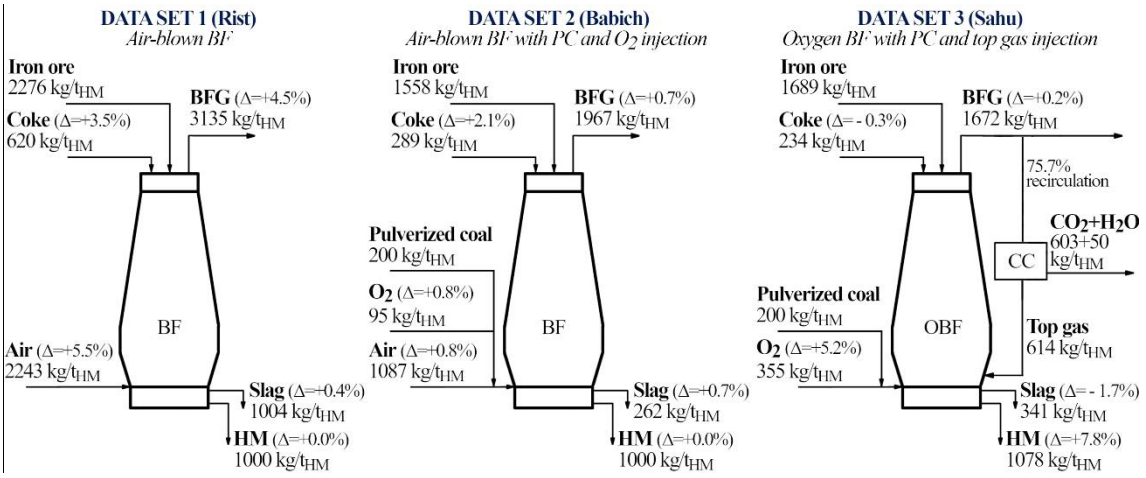

Figure 6. Conceptual schemes summarizing the mass flows and relative errors obtained during the validation of the model for Data set 1, 2 and 3 (the complete data sets are presented in **Table 3** and **Table 4**).

6. Predicting the operating line for an oxygen blast furnace integrated with Power to Gas

Once the model has been validated, we are going to analyze a potential configuration for a blast furnace operation under oxygen regime, with top gas recycling, and injections of pulverized coal and synthetic natural gas. The data set was inspired in the works of Sahu et al. [26] and Jin et al. [28], aiming to reproduce similar results than they but keeping reasonable operating conditions (e.g., flame temperature between 2000 – 2300 °C, direct reduction about 10-15%, slag production above 200 kg/t_{HM}). The proximate analysis of the coal for this data set is 70.7% Ω_{FC}, 17.2% Ω_{VM}, 10.8% Ω_{Z} and 1.2% Ω_{M}.

The proposed oxygen blast furnace would be integrated with a Power to Gas plant, which renewably produces the synthetic methane. This methane is used to reduce the consumption of coke or coal, thus substituting a fossil fuel by a renewable fuel. The conceptual scheme of the blast furnace is the one depicted in **Figure 7** (Data set 5 when coke is replaced and Data set 6 when coal is replaced). We assume a 150 MW electrolyzer and a 280 t_{HM}/h blast furnace. This means that the electrolyzer produces 11 kg/t_{HM} of hydrogen, which are converted to 21.8 kg/t_{HM} of synthetic methane by consuming 60 kg/t_{HM} of CO_2. This carbon is continuously recycled in a closed loop, and therefore the corresponding emissions are avoided. The CO_2 would come from the carbon capture stage that is used to recycle the top gas, which can benefit from the exothermal heat available from the methanation process. Furthermore, the electrolyzer by-produces 87 kg/t_{HM} of O_2 that can be used in the blast furnace, thus reducing the energy requirements in the air separation unit that enriches the hot blast. For these calculations, it was assumed an electrolysis efficiency of 68% [29].

For comparison purposes, the blast furnace was also modelled without the integration of the Power to Gas plant, and therefore without the injection of synthetic methane (Data set 4, which is considered as the base case). In all cases, the mass flow of injected top gas was kept constant at 600 kg/t_{HM} (despite its composition changes). The three data sets are presented in **Table 4**. In the base case (Data set 4), the total CO_2 that would be emitted after the combustion of the BFG is 1154 kg_{CO2}/t_{HM}, of which the 41.4% (i.e., 478 kg_{CO2}/t_{HM}) could be directly captured since they come from the carbon capture stage. When implementing Power to Gas, 60 kg/t_{HM} of CO_2 are recycled in closed loop, which allow to reduce the coke consumption by 8.7% or alternatively the coal consumption by 16.3%. In case of substituting coke, the total emissions become 1083 kg_{CO2}/t_{HM}, of which the 31.8% can be directly captured and stored (i.e., 345 kg_{CO2}/t_{HM}). Thus, in overall terms, the CO_2 is diminished by 71 kg_{CO2}/t_{HM} with respect to the base case by using 1.93 GJ/t_{HM} of electricity in the electrolyzer, so the energy penalty of the CO_2 avoidance is 27.1 MJ/kg_{CO2}. This value is line with the results of Perpiñán et al. [8] for similar Power to Gas integrations in the steel industry (he reported 34 MJ/kg_{CO2}). Actually, since we have cut the coke consumption by 22.8 kg/t_{HM}, which in terms of electricity is equivalent to a reduction of 0.24 GJ/t_{HM} (assuming a coke heating value of 27.3 MJ/kg and a subcritical power plant net efficiency of 38% [30]), and additionally we diminished the O_2 that has to be produced in the air separation unit by 77 kg_{O2}/t_{HM} (we need injecting 10 kg_{O2}/t_{HM} more than in the base but we have available 87 kg_{O2}/t_{HM} from electrolysis), which translates into a reduction of 0.05 MJ/t_{HM} of electric consumption (assuming a typical ASU specific consumption of 0.61 MJ/kg_{O2} [31]), the net energy penalization of the CO_2 avoidance becomes 23.1 MJ/kg_{CO2}. Alternatively, in the case of using the synthetic methane to replace part of the coal, the total emissions become 1068 kg_{CO2}/t_{HM}. Following the same calculations just mentioned, the gross energy penalization of CO_2 avoidance in this case would be 22.4 MJ/kg_{CO2} and the net energy penalization 17.9 MJ/kg_{CO2} (the heating value of coal is 29.4 MJ/kg, Eq.(130)). The **Table 5** summarizes these calculations.

These values of energy penalization for the avoidance of CO_2 are clearly above the typical consumptions of conventional amine carbon capture, which are usually in the range 3.7 – 4.8 MJ/kg_{CO2} [32,33]. Nevertheless, the integration of Power to Gas presents the additional benefits of diminishing the coke/coal consumption in the blast furnace, reducing the electricity consumption in the air separation unit, and suppressing the requirement of geological storage for the avoided CO_2 (it is kept in a closed carbon loop thanks to Power to Gas). Therefore, an overall economic and energy analysis of the whole integrated steel plant should be necessary to reach farther conclusions. Furthermore, there exist other potential PtG integrations that

may lead to lower energy penalizations, such as the utilization of the BFG in the methanation stage rather than the captured CO_2 (which allow producing more SNG with the same amount of H_2) or the injection of the H_2 in the blast furnace without considering a methanation stage.

Regarding the flame temperature, it is reduced about 90 °C when injecting 22 kg/t_{HM} of synthetic methane for replacing coke. This is a reduction of 4.0 °C per kg_{SNG}/t_{HM}, which is in good agreement with the value reported by Babich for natural gas (4.5 °C per kg_{NG}/t_{HM} [16]). When we replace coal by synthetic natural gas, the temperature of the flame is reduced by 3.1 °C per kg_{SNG}/t_{HM}, which also matches the value reported by Babich for this type of replacement (3.0 °C per kg_{NG}/t_{HM} [16]).

Lastly, the percentage of direct reduction is 15% for the base case and about 12% when injecting synthetic natural gas. The decrease in this value was expected since direct reduction takes place through solid carbon, and the coke/coal input is diminished when Power to Gas is integrated. The operating lines are presented in **Figure 8**.

Table 4. Data sets for oxygen blast furnaces with top gas recycling. The Data set 3 is taken from Sahu et al. [26] and compared to the results of our model. The Data sets 4, 5 and 6 were elaborated in the present paper.

Input streams (kg/t_{HM})	**DATA SET 3** **Sahu** [26]	**Model**	**Δ (%)**	**DATA SET 4** **OBF-PtG**	**DATA SET 5** **OBF-PtG with coke replacement**	**DATA SET 6** **OBF-PtG with coal replacement**
Iron ore (25 °C)	**1689.4**	**1689.4**	**-**	**1500.0**	**1500.0**	**1500.0**
# Fe_2O_3	616.4	616.4	-	954.7	954.7	954.7
# FeO	771.8	771.8	-	369.2	369.2	369.2
# SiO_2	78.8	78.8	-	58.9	58.9	58.9
# Al_2O_3	58.4	58.4	-	70.8	70.8	70.8
# CaO	129.4	129.4	-	15.7	15.7	15.7
# MgO	34.6	34.6	-	21.5	21.5	21.5
# MnO	-	-	-	9.2	9.2	9.2
Coke (25 °C)	**234.9**	**234.1**	**-0.3**	**261.3**	**238.5**	**261.3**
# C	195.7	195.0	-0.3	217.7	198.7	217.7
# S	1.2	1.2	-0.3	1.3	1.2	1.3
# SiO_2	22.8	22.7	-0.3	25.4	23.1	25.4
# Al_2O_3	13.6	13.6	-0.3	15.1	13.8	15.1
# CaO	1.1	1.1	-0.3	1.2	1.1	1.2
# MgO	0.5	0.5	-0.3	0.6	0.5	0.6
Coal (25 °C)	**200.0**	**200.0**	**-**	**185.0**	**185.0**	**154.8**
# C	147.3	147.3	-	142.1	142.1	118.9
# H	9.0	9.0	-	5.9	5.9	4.9
# O	8.9	8.9	-	9.4	9.4	7.9
# N	4.0	4.0	-	4.7	4.7	3.9
# S	1.1	1.1	-	0.8	0.8	0.7
# H_2O	10.0	10.0	-	2.2	2.2	1.9
# FeO	0.7	0.7		-	-	-
# SiO_2	11.9	11.9	-	11.4	11.4	9.5
# Al_2O_3	6.2	6.2	-	8.2	8.2	6.9
# CaO	0.5	0.5	-	0.3	0.3	0.3
# MgO	0.3	0.3	-	-	-	-
# P_2O_5	0.1	0.1	-	-	-	-
O_2 injection (25 °C Sahu / 1200 °C Bailera)	**337.6**	**355.3**	**5.2**	**334.7**	**345.4**	**340.0**
# O_2	330.7	348.1	5.3	318.1	328.2	323.0
# H_2O	6.9	7.3	4.6	7.7	8.0	7.8
# N_2	-	-	-	9.0	9.3	9.1
Recycled gas injection (900 °C Sahu / 1200 °C Bailera)	**613.6**	**613.6**	**0.0**	**600.0**	**600.0**	**600.0**
# N_2	13.6	12.5	-8.0	27.0	24.1	24.6
# CO_2	34.2	31.7	-7.1	53.1	45.0	48.7
# CO	554.4	558.2	0.7	512.5	524.7	518.7
# H_2	11.5	11.2	-2.5	7.5	6.3	8.0
Synthetic methane injection (25 °C Bailera)	**-**	**-**	**-**	**-**	**21.8**	**21.8**
# CH_4	-	-	-	-	21.1	21.1
# CO_2	-	-	-	-	0.5	0.5
# H_2O	-	-	-	-	0.1	0.1
# H_2	-	-	-	-	0.1	0.1
Output (kg/t_{HM})						
Hot metal (1425 °C Sahu / 1500 °C Bailera)	**1000.0**	**1078.1**	**7.8**	**1002.3**	**1002.3**	**1002.3**
# Fe	949.5	1023.7	7.8	951.2	951.2	951.2
# C	42.3	45.6	7.9	44.7	44.7	44.7
# Si	5.8	6.3	7.9	5.8	5.8	5.8
# Mn	0.6	0.7	8.3	0.6	0.6	0.6
# P	1.8	1.9	0.0	-	-	-
Slag (1500 °C Sahu / 1550 °C Bailera)	**347.8**	**341.3**	**-1.9**	**226.1**	**222.4**	**222.8**
# FeO	-	0.7	-	-		
# SiO_2	-	100.1	-	83.2	81.0	81.4
# Al_2O_3	-	78.1	-	94.1	92.8	92.8
# CaO	-	127.0	-	13.5	13.5	13.6
# MgO	-	35.4	-	22.1	22.0	22.1
# MnO	-	-0.8	-	8.4	8.4	8.4
# CaS	-	5.2	-	4.8	4.5	4.5
# P_2O_5	-	-4.3	-	-		

BFG (100 °C Sahu / 150 °C Bailera)	**1668.1**	**1672.0**	**0.2**	**1652.7**	**1666.0**	**1652.7**
# N_2	26.7	16.5	-38.2	40.6	38.0	37.6
# CO_2	798.7	838.1	4.9	799.8	710.7	745.0
# CO	762.2	737.0	-3.3	772.1	828.6	793.4
# H_2O	66.7	65.7	-1.5	28.9	78.8	64.5
# H_2	13.8	14.7	7.0	11.3	9.9	12.2
Operating conditions						
Chemical efficiency, r (-)	-	1.000	-	0.920	0.920	0.920
Thermal reserve zone temperature, T_R (°C)	807.6	807.6	-	950.0	950.0	950.0
Flame temperature, T_{fl} (°C)	2126.0	1768.9	-16.8	2082.9	1995.6	2014.2
Heat evacuated by the staves (MJ/THM)	500.0	500.0	-	700.0	700.0	700.0
Heat evacuated in the elaboration zone, θ_{st} (-)	-	0.770	-	0.800	0.800	0.800
Oxidation state of the BFG, η_{CO-H_2} (-)	0.391	0.403	3.2	0.374	0.373	0.374

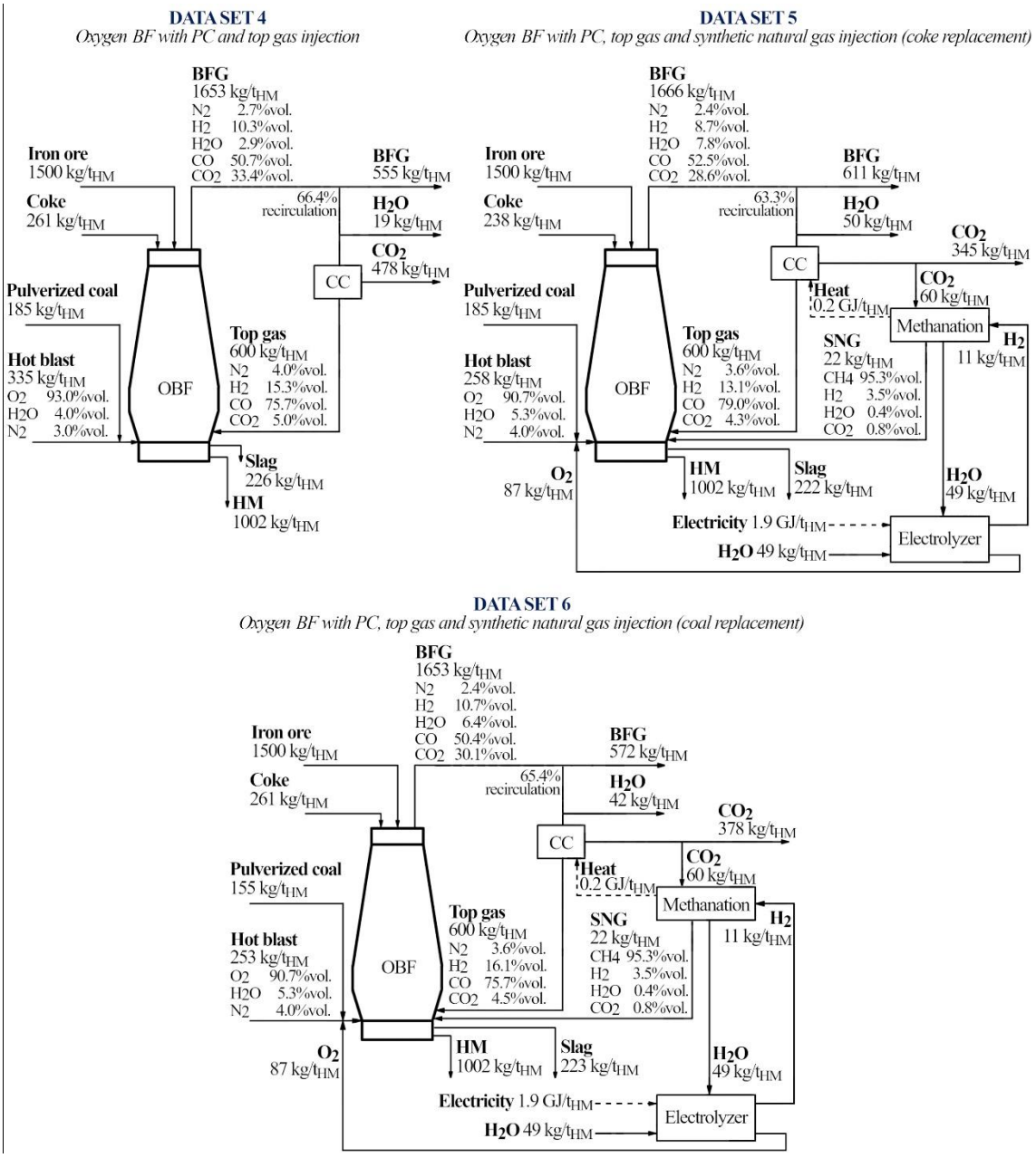

Figure 7. Conceptual schemes summarizing the mass flows obtained for Data sets 4, 5 and 6 (see **Table 4**).

Table 5. Comparison of CO_2 emissions, CO_2 avoided and energy penalization between data sets 4 (oxygen blast furnace), 5 (oxygen blast furnace with PtG integration for the replacement of coke by synthetic methane) and 6 (oxygen blast furnace with PtG integration for the replacement of coal by synthetic methane).

	OBF Base case (Data set 4)	**OBF-PtG with coke replacement (Data set 5)**	**OBF-PtG with coal replacement (Data set 6)**

Total CO_2 emissions (kg/t_{HM})	1154	1083	1068
- From BFG combustion (kg/t_{HM})	676	738	690
- From CC stage (kg/t_{HM})	478	345	378
Total CO_2 emissions avoided (kg/t_{HM})	-	71	86
Total CO_2 emissions avoidance ratio (%)	-	6.1	7.4
Electricity for PtG (GJ/t_{HM})	-	1.93	1.93
Electricity saved in the ASU (GJ/t_{HM})	-	0.05	0.05
Fossil fuel saved (kg/t_{HM})	-	22.8	30.2
- Equivalent electricity saved (GJ/t_{HM})	-	0.24	0.34
Fossil fuel replacement ratio (kg/kg_{SNG})	-	1.05	1.38
Gross CO_2 avoidance penalization (MJ/kg_{CO2})	-	27.1	22.4
Net CO_2 avoidance penalization (MJ/kg_{CO2})	-	23.1	17.9

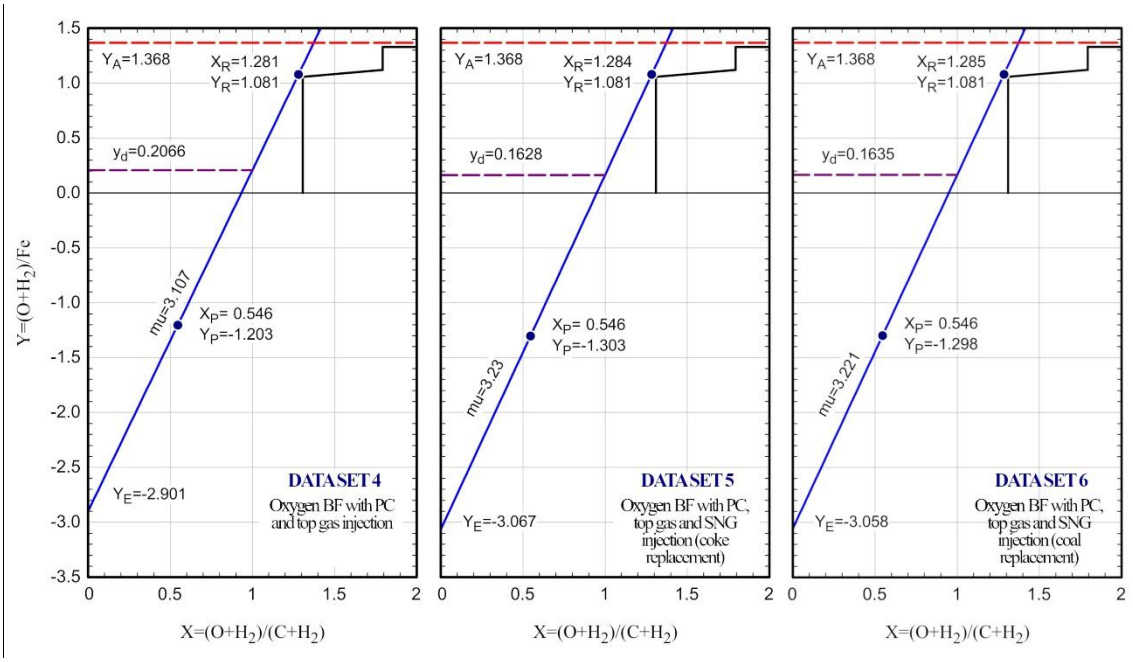

Figure 8. Operating lines of oxygen blast furnaces, obtained from Data sets 4, 5 and 6 (**Table 4**).

7. Conclusions

The operating diagram, which was originally developed by Rist in 1963, is a useful methodology for predicting the operating conditions in a blast furnace through a graphical representation which takes into account the mass and energy balances. This methodology was described in a series of papers between 1963 and 1967, of which the most relevant were published in French. In this paper we have revisited the work of Rist, summarizing his methodology and making some additions and corrections. We have presented a general model that considers multiple injectants separately, with all calculations given as a function of the temperature of the thermal reserve zone. Besides, the model now calculates the sensible heats of the hot metal and slag as a function of their composition, and the heat of carburization as a function of the austenite and cementite content in iron. Furthermore, it is added a supplementary model to compute the heat of decomposition of coal, an additional energy balance in the upper zone of the blast furnace to compute the final composition of the blast furnace gas, and other energy balance for the calculation of the flame temperature. Regarding corrections, the heat associated to the direct reduction of FeO now accounts for the moisture of the hot blast, the heat associated to the lack of chemical ideality now includes the influence of the hydrogen coming from auxiliary fuels and of the moisture of the hot blast, and lastly, the sensible heats of hot metal and slag are now correctly computed and accounted.

The model elaborated in this paper has been validated with three different operation data sets from literature. The first one corresponds to an air-blown blast furnace without auxiliary injections (error <5.6%), the second one to an air-blown blast furnace with pulverized coal injection (error <2.1%), and the third one to an oxygen blast furnace with top gas recycling and pulverized coal injection (error <8.3%). Despite it would be desirable to have a discrepancy below 5% in all cases, we consider the model validated since the slightly variation above 5% is justified. In the first case, the data set corresponds to the results of Rist, therefore they include the errors that were corrected in our model. When we deliberately include in our model the same errors than Rist, the difference between both results becomes lower than 3.5%. In the third case, the reference data set have some incorrect mass balances in origin that led to this higher error. Nevertheless, these inconsistencies were properly identified by our model, and the overall behavior of the blast furnace could be correctly described.

The objective in revisiting the operating diagram of Rist is to study a new concept for the reduction of CO_2 emissions in blast furnaces. This concept combines oxygen blast furnaces with Power to Gas technology. The latter renewably produces

synthetic methane, which is used to replace part of the coke or coal. Carbon is thus continuously recycled in a closed loop, and the corresponding emissions are avoided without requiring geological storage. Furthermore, the electrolyzer of the Power to Gas plant by-produces O_2 that can be used in the blast furnace to reduce the electricity consumption in the air separation unit that enriches the hot blast. We presented in this study the first approach to this integration concept, comparing the performance of the blast furnace when coke is replaced to the performance when coal is replaced. It was assumed a 280 t_{HM}/h oxygen blast furnace producing 1154 kg_{CO2}/t_{HM}, coupled to Power to Gas plant with 150 MW electrolysis power capacity that produces 11 kg_{H2}/t_{HM} of hydrogen (then converted to 21.8 kg_{SNG}/t_{HM} of synthetic methane by using pure CO_2 from a carbon capture stage). The model shows fuel replacement ratios of 1.05 kg/kg_{SNG} for coke and 1.38 kg/kg_{SNG} for coal, which lead to CO_2 emission reductions of 6.1% and 7.4%, respectively. As the electricity consumed in the PtG plant is 1.93 GJ/t_{HM}, the gross energy penalization of the CO_2 avoidance is 27.1 MJ/kg_{CO2} when coke is replaced and 22.4 MJ/kg_{CO2} when coal is replaced. Considering the energy content of the fossil fuel that is saved, and the electricity that is no longer consumed in the air separation unit, the net energy penalizations are 23.1 MJ/kg_{CO2} and 17.9 MJ/kg_{CO2}, respectively. These values are several times greater than the specific consumption of amine carbon capture (typically 3.7 – 4.8 MJ/kg_{CO2}). However, the integration of Power to Gas diminishes the coke/coal consumption in the blast furnace, reduces the electricity consumption in the air separation unit, and eliminates the requirement of geological storage for the avoided CO_2. Therefore, a detailed economic comparison between both methods should be necessary to reach firm conclusions. Furthermore, there exist other potential PtG integrations that may lead to lower energy penalizations, such as the utilization of the BFG in the methanation stage rather than captured CO_2, what would allow producing more SNG with the same amount of H_2.

Lastly, the present paper has provided six full data sets of different blast furnaces operations, specifying the composition of all streams, as well as the most relevant operating parameters (e.g., temperature of the thermal reserve zone, heat evacuated by the staves, and the temperature of the flame). The availability of this information in literature is very scarce, especially for oxygen blast furnaces.

Nomenclature

In this paper we used calorie as unit of energy for calculations related to operating diagram in order to facilitate comparing results with the original work of Rist. Elsewhere, SI unit is used (joule).

Symbols

a_i	calculation parameter, $1/°C^i$
a_j	number of moles of H_2 in injectant j per number of moles of injectant j, mol_{H2}/mol_j
A	calculation parameter, kcal/mol
b_j	number of moles of O_2 in injectant j per number of moles of injectant j, mol_{O2}/mol_j
B	calculation parameter, kcal/mol
c_j	number of moles of N_2 in injectant j per number of moles of injectant j, mol_{N2}/mol_j
c_p	heat capacity, kcal/(mol·K)
C	calculation parameter, kcal/mol
$C_{\Delta T_R}$	sensible heat of the burden between $T_R - \Delta T_R$ and T_R (lack of thermal ideality), $kcal/mol_{Fe}$
d_j	number of moles of S_2 in injectant j per number of moles of injectant j, mol_{S2}/mol_j
e	number of moles of H_2O per number of moles of O in the air (i.e., $e = y_e/y_v$), mol_{H2O}/mol_O
f	sensible heat of the hot metal between T_R and T_f (outlet temperature), $kcal/mol_{Fe}$
g_i	specific Gibbs free energy of compound i, $kcal/mol_i$
ΔG	Gibbs free energy change of reaction, kcal/mol
h	enthalpy, kcal/mol
Δh_f	enthalpy of fusion, kcal/mol
$\Delta_c h$	enthalpy of combustion, kcal/mol
$\Delta_f h$	enthalpy of formation, kcal/mol
K_{eq}	equilibrium constant of the water-gas shift reaction, -
l	sensible heat of the slag between T_R and T_l (outlet temperature), $kcal/mol_{Fe}$
$m_{j,i}$	mass of compound i in stream j per ton of hot metal, kg/t_{HM}
M	molar weight, kg/kmol
$n_{j,i}$	number of moles of compound i in stream j per ton of hot metal, mol/t_{HM}
p	heat removed by the staves in the elaboration zone, $kcal/mol_{Fe}$
p'	heat removed by the staves in the preparation zone, $kcal/mol_{Fe}$
q_c	heat released at T_R by the reaction C (coke) + 0.5 O_2 → CO, $kcal/mol_O$
q_e	heat required by the H_2O in hot blast due to dissociation, reverse water-gas shift and sensible heat, $kcal/mol_{H2O}$
q_{er}	heat absorbed at T_R by the reaction $C + H_2O \rightarrow CO + H_2$, $kcal/mol_{H2O}$
q_{es}	enthalpy change of water between T_v and T_R, $kcal/mol_{H2O}$
$q_{f,i}$	heat required to melt and increase the temperature of compound i from T_R to T_f, $kcal/mol_i$
$q_{Fe_{0.95}O}$	sensible heat of wüstite between $T_R - \Delta T_R$ and T_R, $kcal/mol_O$
q_{Fe_3C}	heat absorbed at T_R by the reaction $3Fe + C \rightarrow Fe_3C$, $kcal/mol_C$
$q_{Fe_3O_4}$	sensible heat of magnetite between $T_R - \Delta T_R$ and T_R, $kcal/mol_{Fe3O4}$
q_g	heat absorbed at T_R by the reaction $C + CO_2 \rightarrow 2CO$, $kcal/mol_C$
q_{im}	heat released at T_R by the reaction $1/4\ Fe_3O_4 + CO \rightarrow 3/4\ Fe + CO_2$, $kcal/mol_O$
q_{iw}	heat released at T_R by the reaction $Fe_{0.95}O + CO \rightarrow 0.95\ Fe + CO_2$, $kcal/mol_O$
q_j	thermal demand by injectant j, $CH_{2a}O_{2b}N_{2c}S_{2d}Z_z$ (or $H_{2a}O_{2b}N_{2c}$ or $O_{2b}N_{2c}$) due to dissociation, sensible heat, reverse water-gas shift of the H_2, incomplete combustion with the O_2, and transfer of S to the slag, $kcal/mol_j$
q_{jd}	heat absorbed at T_j by the dissociation reaction of injectant j, $CH_{2a}O_{2b}N_{2c}S_{2d}Z_z \rightarrow C + aH_2 + bO_2 + cN_2 + dS_2 + zZ$, $kcal/mol_j$
$q_{js,i}$	enthalpy change of element i from injectant j between T_j and T_R, $kcal/mol_i$
q_k	heat absorbed at T_R by the total H_2 in the furnace when considering that it is completely converted to H_2O through the reverse water-gas shift reaction, $kcal/mol_{H2}$

$q_{l,\mathrm{i}}$ heat required to melt and increase the temperature of compound i (SiO_2, Al_2O_3, CaO, MgO) from T_R to T_l, kcal/mol_i
q_{Mn} heat absorbed at T_R by the reaction $C + MnO \rightarrow CO + Mn$, kcal/$mol_O$
q_P heat absorbed at T_R by the reaction $1/5\ P_2O_5 \cdot 3CaO + C + 6/5\ Fe \rightarrow 2/5\ Fe_3P + 3/5\ CaO + CO$, kcal/$mol_O$
q_{rmc} heat consumed by the reaction $1.5\ Fe_2O_3 + 0.5\ CO \rightarrow Fe_3O_4 + 0.5\ CO_2$, including also the heat exchange between reactants and products at different temperatures, kcal/mol_{Fe3O4}
q_{rwc} heat consumed by the reaction $0.5\ Fe_2O_3 + 0.5\ CO \rightarrow FeO + 0.5\ CO_2$, including also the heat exchange between reactants and products at different temperatures, kcal/mol_{FeO}
$q_{R,\mathrm{i}}$ sensible heat of compound i (SiO_2, Al_2O_3, CaO, MgO, C) between $T_R - \Delta T_R$ and T_R, kcal/mol_i
q_{S} heat absorbed at T_R by the reaction $1/2\ S_2 + CaO\ + C \rightarrow CaS + CO$, kcal/$mol_S$
$q_{s,i}$ sensible heat of component i between T_{fl} and T_R, kcal/mol_i
$q_{s,nr,i}$ sensible heat of non-reacting compound i, kcal/mol_i
q_{Si} heat absorbed at T_R by the reaction $C + 1/2\ SiO_2 + 3/2\ Fe \rightarrow CO + 1/2\ Fe_3Si$, kcal/$mol_O$
q_{st} heat removed by the staves from the blast furnace per ton of hot metal, kcal/$t_{\text{hot metal}}$
q_v energy available from the sensible heat of the air between T_v and T_R, kcal/mol_O
q_γ heat absorbed at T_R by the carburization of the iron, kcal/mol_C
$q_{\gamma\mathrm{Fe}}$ heat absorbed at T_R by the reaction C(coke) → C(austenite), kcal/mol_C
q_ε heat absorbed at T_R by the reaction $H_2 + CO_2 \rightarrow H_2O + CO$, kcal/$mol_{H2}$
q'_ε heat absorbed by the reaction $H_2 + CO_2 \rightarrow H_2O + CO$ taking into account the temperature of reactants and products, kcal/$mol_{H2(reacting)}$
r chemical efficiency of the blast furnace, -
R ideal gas constant, kcal/(mol K)
s_i specific entropy of compound i, kcal/(mol_i K)
T temperature, °C (unless otherwise specified)
ΔT_R difference of temperature between the gas and the solid at the beginning of the middle zone, °C
V_j volume flow of stream j consumed in the blast furnace per ton of hot metal, Nm^3/t_{HM}
x_d number of moles of O removed from wüstite by direct reduction per total moles of reducing gas mixture, $mol_O/(mol_C+mol_{H2})$
x_e number of moles of H_2O in hot blast per total moles of reducing gas mixture, $mol_{H2O}/(mol_C+mol_{H2})$
$\mathrm{x_h}$ molar fraction of hydrogen and water in the reducing gas mixture, -
x_i number of moles of O transferred from the iron oxides to the gas by indirect reduction per total moles of reducing gas mixture, $mol_O/(mol_C+mol_{H2})$
x_j number of moles of injectant j (overall formula $CH_{2a}O_{2b}N_{2c}S_{2d}Z_z$, $H_{2a}O_{2b}N_{2c}$ or $O_{2b}N_{2c}$) per total moles of reducing gas mixture, $mol_j/(mol_C+mol_{H2})$
x_k number of moles of H_2 in the coke per total moles of reducing gas mixture, $mol_{H2}/(mol_C+mol_{H2})$
x_{Mn} number of moles of O removed by direct reduction of MnO per total moles of reducing gas mixture, $mol_O/(mol_C+mol_{H2})$
x_P number of moles of O removed by direct reduction of P_2O_5 per total moles of reducing gas mixture, $mol_O/(mol_C+mol_{H2})$
x_S number of moles of O replaced by S in the slag per total moles of reducing gas mixture, $mol_O/(mol_C+mol_{H2})$
x_{Si} number of moles of O removed by direct reduction of SiO_2 per total moles of reducing gas mixture, $mol_O/(mol_C+mol_{H2})$
x_v number of moles of O in hot blast per total moles of reducing gas mixture, $mol_O/(mol_C+mol_{H2})$
X abscissa in the Rist diagram, $(mol_O+mol_{H2})/(mol_C+mol_{H2})$
y_{C} number of moles of C (coke) that are consumed in combustion in the raceways per mol of Fe produced, mol_C/mol_{Fe}
y_d number of moles of O removed from wüstite by direct reduction per mol of Fe produced, mol_O/mol_{Fe}
y_e number of moles of H_2O in hot blast per mol of Fe produced, mol_{H2O}/mol_{Fe}
y_i number of moles of O transferred from the iron oxides to the gas by indirect reduction per mol of Fe produced, mol_O/mol_{Fe}
y_j number of moles of injectant j (overall formula $CH_{2a}O_{2b}N_{2c}S_{2d}Z_z$, $H_{2a}O_{2b}N_{2c}$ or $O_{2b}N_{2c}$) per mol of Fe produced, mol_j/mol_{Fe}
y_k number of moles of H_2 in the coke per mol of Fe produced, mol_{H2}/mol_{Fe}
y_{Mn} number of moles of O removed by direct reduction of MnO per mol of Fe produced, mol_O/mol_{Fe}
$y_{nr,i}$ number of moles of compound i that is traversing the preparation zone without reacting per mol of Fe produced, mol_i/mol_{Fe}
y_P number of moles of O removed by direct reduction of P_2O_5 per mol of Fe produced, mol_O/mol_{Fe}
$y_{\mathrm{rg,i}}$ number of moles of component i in the reducing gas at the raceways per mol of Fe produced, mol_i/mol_{Fe}
y_{rmc} number of moles of Fe_3O_4 produced in the preparation zone per mol of Fe produced, mol_{Fe3O4}/mol_{Fe}
y_{rwc} number of moles of FeO produced in the preparation zone per mol of Fe produced, mol_{FeO}/mol_{Fe}
y_S number of moles of O replaced by S in the slag per mol of Fe produced, mol_O/mol_{Fe}
y_{Si} number of moles of O removed by direct reduction of SiO_2 per mol of Fe produced, mol_O/mol_{Fe}
y_v number of moles of O in hot blast per mol of Fe produced, mol_O/mol_{Fe}
y_{wgs} number of moles of H_2 reacting in the preparation zone, mol_{H2}/mol_{Fe}
Y ordinate in the Rist diagram, $(mol_O+mol_{H2})/mol_{Fe}$
$\mathrm{Y_E}$ intercept of the operating line representing the moles of H_2 and O coming from sources other than iron oxides that contribute to the formation of the reducing gas per mol of Fe produced (negative sign by convention), $(mol_O+mol_{H2})/mol_{Fe}$
$\mathrm{Y_E^*}$ terms of $\mathrm{Y_E}$ that are independent of y_v, $(mol_O+mol_{H2})/mol_{Fe}$
Y_M^* number of moles of O per mole of Fe_3O_4 (i.e., $Y_M^* = 4$), mol_O/mol_{Fe3O4}
$\mathrm{z_j}$ number of moles of ashes in injectant j per number of moles of injectant j, mol_{ash}/mol_j

Greek symbols

γ number of moles of C dissolved in the hot metal, mol_C/mol_{Fe}
$\gamma_{\mathrm{Fe_3C}}$ number of moles of C dissolved in the hot metal as cementite, mol_C/mol_{Fe}
$\gamma_{\gamma\mathrm{Fe}}$ number of moles of C dissolved in the hot metal as austenite, mol_C/mol_{Fe}
δ decrease in the available heat due to the presence of magnetite in the elaboration zone, kcal/mol_{Fe}
δ' decrease in the heat absorbed by the reverse water-gas shift reaction because of the lack of chemical ideality, kcal/mol_{Fe}
Δ_1 calculation parameter, -
Δ_2 calculation parameter, $(mol_O+mol_{H2})/mol_{Fe}$
ϵ_{K} number of moles of C and H_2 in coke per kg of coke, $(mol_C+mol_{H2})/mol_K$
η humidity in the air, (g/Nm^3)
$\eta_{\mathrm{CO-H_2}}$ oxidation state of the blast furnace gas leaving the top, -
θ_{st} fraction of the total heat removed by the staves that is coming from the elaboration zone (i.e., from the control volume of the energy balance), -

μ	slope of the Rist diagram, i.e., number of moles of reducing gas per mol of Fe produced, $(mol_C+mol_{H2})/mol_{Fe}$
τ_j	calculation parameter that is 1 when the auxiliary injection j contains carbon and 0 when not, -
Φ	percentage of H_2 consumed in the preparation zone, -
ω	molar fraction, -
$\Omega_{j,i}$	mass fraction of compound i in stream j, -

Subscripts and superscripts

A	initial oxidation state of the iron oxides at the inlet of the blast furnace
BFG	blast furnace gas
C	related to carbon or C-CO_2 mixtures
d	dry basis (superscript), decomposition (subscript)
e	moisture in hot blast
f	hot metal (at the outlet)
FC	fixed carbon
Fe_3C	referred to the number of moles of C in hot metal dissolved as cementite
fl	flame
H	related to hydrogen or H_2-H_2O mixtures
HM	hot metal
IN	inlet of solids at the top of the furnace
IO	iron ore
j	injectant (overall formula $CH_{2a_j}O_{2b_j}N_{2c_j}S_{2d_j}Z_{z_j}$) or stream
K	coke
l	slag (at the outlet)
M	magnetite or moisture
nat	natural moisture in blast
NG	natural gas
nr	non-reacting in the preparation zone
P	characteristic point of the operating line referring to the energy balance of the blast furnace
PM	primary volatile matter
R	characteristic point of the operating line referring to the thermal reserve zone
SM	secondary volatile matter
v	hot blast / air
VM	volatile matter
W	referring to wüstite or to the characteristic point of the equilibrium line in which pure wüstite is in equilibrium with the gas
Z	ashes
γFe	referred to the number of moles of C in hot metal that are dissolved as austenite

Competing interests
No competing interests were disclosed.

Grant information
This project has received funding from the European Union's Horizon 2020 research and innovation programme under the Marie Sklodowska-Curie grant agreement No 887077.

Appendix A – Terms of the energy balance in the elaboration zone
This appendix presents the calculation methodology for the energy balance of Eq.(37). The **Table 6** gathers the equations for the calculation of the different q as a function of the temperature of the corresponding stream j (T_j) and the temperature of the thermal reserve zone (T_R). In his original work, Rist only provided data for $T_R = 1000$ °C and fixed values of T_j. Furthermore, we work in kcal per mole of Fe, as Rist did in his original work, to facilitate comparison [10].
The calculation of the y variables is given as a function of the mass flows of the corresponding stream, m_j, and the mass fraction of each compound i in that stream, $\Omega_{j,i}$. When solving the Rist diagram, we assume that the mass and composition of Iron ore, Pulverized coal, Injectants and Hot metal are known (**Figure 4**). The moisture in the air is also fixed.
It must be noted that to obtain the coordinates X_P and Y_P we actually need to compute Eq.(39), Eq.(40), Eq.(41) and Eq.(43), instead of Eq.(37). For this reason, the terms y_v and y_d are not computed. These two variables are results from the model, not inputs.

A.1 Term $q_c y_v$: heat released by the incomplete combustion of carbon
The heat released by the incomplete combustion of carbon with the air at the tuyeres (per mol of Fe in the hot metal) is denoted by $q_c y_v$. The term is given as a function of the moles of O entering with the air, so it may account for any carbon independently of the source (coke or injectants). The fact that it can account for the carbon of different sources does not imply that it accounts for the incomplete combustion of all of the carbon. Some part of the carbon will be partially combusted by using the O from the injectants itself (e.g., O contained in pulverized coal) instead of with O from air. That part is accounted in the corresponding term $q_j y_j$ of each injectant.
The variable q_c is the heat released through the reaction of Eq.(16). Thermodynamic data for carbon is usually provided for graphite. However, we have part of the carbon coming from coke. Therefore, the enthalpy change in the graphitization of coke carbon must be taken into account Eq.(63) [11]. Since we do not know how much carbon comes from coke and how much from the decomposition of the injectants (and it will be different for each configuration), we make the calculations

considering all carbon as coke carbon (Eq.(64)). Therefore, we will have to consider that injectants decompose into coke carbon, instead of graphite, when computing $q_j y_j$.

$$\mathrm{C\ (coke)} \rightarrow \mathrm{C\ (graphite)} \qquad \Delta H = -5.02\ \mathrm{kJ/mol} \qquad (63)$$

$$\mathrm{C\ (coke)} + 0.5\ \mathrm{O_2} \rightarrow \mathrm{CO} \qquad \Delta H = -118.7\ \mathrm{kJ/mol} \qquad (64)$$

The heat released by the incomplete combustion of coke carbon (Eq.(65)) was tabulated using data from NIST and Aspen Plus data bases as a function of temperature. These data were adjusted to a polynomial of degree 5 (Eq.(113), **Table 6**). The temperature at which q_c must be calculated is T_R, i.e., the temperature of the thermal reserve zone.

$$q_c = h_{\mathrm{C(coke)}} + 0.5\ h_{\mathrm{O2}} - h_{\mathrm{CO}} \qquad (65)$$

The variable y_v is unknown and is calculated as a result from the operating line (computed from the intercept $\mathrm{Y_E}$).

A.2 Term $q_v y_v$: sensible heat of the air

The air is injected in the blast furnace at temperatures higher than T_R. Since we select T_R as the reference temperature for the energy balance, it means that the air will provide its sensible heat between T_v and T_R as available heat (left side of Eq. (37)). The term $q_v y_v$ denotes this energy. For its calculation, we tabulated data of $c_{p,air}$ and adjusted it to a polynomial of degree 3. Then, we integrated that equation (Eq.(66)), thus obtaining Eq.(114). To change the units from $\mathrm{kcal/mol_{air}}$ (tabulated data) to $\mathrm{kcal/mol_O}$, (our model units) the factor 0.42 $\mathrm{mol_O/mol_{air}}$ is used.

$$q_v = \int_{T_R}^{T} c_{p,air}\, dT \qquad (66)$$

The variable y_v is unknown and is calculated as a result from the operating line (computed from the intercept $\mathrm{Y_E}$).

A.3 Term $q_{iw}\mathrm{Y_w}$: heat released by the reduction of wüstite

The term $q_{iw}\mathrm{Y_w}$ denotes the heat released by the reduction of wüstite to iron, per mol of Fe produced in the blast furnace. Three assumptions are taken for this term:

- Only wüstite is entering the middle zone (i.e., ideal operation, with operating line passing through point W). This assumption is corrected later with the term δ.
- The reduction of wüstite takes place only through indirect reduction. This is corrected with the heat absorbed during direct reduction (term $q_g y_d$).
- All the reduction is carried out by CO (Eq.(5)). This is corrected through q_k, which appears in different terms referring to hydrogen. The term q_k accounts for the energy absorbed during the reverse water-gas shift reaction. In other words, the reverse of Eq.(7) plus Eq.(5) is equal to Eq.(6).

The variable $\mathrm{Y_w}$ is known (see **Table 1**), denoting the number of moles of O per mol of Fe in wüstite. The variable q_{iw} is tabulated as a function of temperature with data from NIST and Aspen Plus data bases (Eq.(67)). It must be mentioned that the computed values differ between the two databases. The data from Aspen was chosen for the data fit of Eq.(113) (**Table 6**).

$$q_{iw} = h_{\mathrm{Fe_{0.95}O}} + h_{\mathrm{CO}} - 0.95\ h_{\mathrm{Fe}} - h_{\mathrm{CO2}} \qquad (67)$$

In the energy balance, q_{iw} must be calculated at T_R.

A.4 Term δ: lack of chemical ideality in wüstite reduction

The term δ is used to correct $q_{iw}\mathrm{Y_w}$, since it assumed that only wüstite is entering the middle zone (which is not the case under non-ideal conditions). The presence of magnetite in the elaboration zone makes the available heat to decrease because the reduction of magnetite to wüstite is endothermic (Eq.(3)). Assuming a mixture of wüstite and magnetite characterized by $\mathrm{Y_R}$, the term δ is given by Eq.(68). This equation is a simplification for $\mathrm{Fe_{0.95}O\text{-}Fe_3O_4}$ mixtures derived from a triangular diagram for $\mathrm{Fe\text{-}Fe_{0.95}O\text{-}Fe_3O_4}$ mixtures (see annexes of [11]).

$$\delta = (\mathrm{Y_R} - 1.05) \cdot (3.75 \cdot q_{iw} - 4.75 \cdot q_{im}) \qquad (68)$$

The term q_{im} is the heat released by the overall reaction Eq.(69) (for the energy balance, q_{im} must be calculated at T_R). To compute it in $\mathrm{kcal/mol_O}$, it is used Eq.(70). It must be mentioned that the computed values for q_{im} differ between different databases (Aspen Plus and NIST). The data from Aspen was chosen for the data fit of Eq.(113) (**Table 6**).

$$\mathrm{Fe_3O_4} + 4\ \mathrm{CO} \rightarrow 3\ \mathrm{Fe} + 4\ \mathrm{CO_2} \qquad (69)$$

$$q_{im} = 0.25\ h_{\mathrm{Fe_3O_4}} + h_{\mathrm{CO}} - 0.75\ h_{\mathrm{Fe}} - h_{\mathrm{CO2}} \qquad (70)$$

As occurred for $q_{iw}Y_w$, the variable δ assumes that reduction takes place only by CO. The energy that would be consumed by the H_2 during the reduction is accounted in those terms including q_k.

A.5 Term $q_g(y_d - y_e)$: heat absorbed during direct reduction

The direct reduction of wüstite it is actually the combination of CO_2 (or H_2O) dissociation and the indirect reduction of FeO by CO (or H_2). In the term $q_{iw}Y_w$ it was already accounted the heat released by the indirect reduction, including the comprised during the overall process of direct reduction (because it was computed for all the O atoms in wüstite, i.e., Y_w). It means that here, in the term $q_g(y_d - y_e)$, we have to take into consideration only the heat absorbed because of the CO_2 dissociation. Moreover, not all the O atoms that are reduced from FeO through direct reduction are due to CO_2 dissociation. Some of them will be removed because of the H_2O dissociation. The latter are accounted in the term $q_e y_e$. For this reason, we subtract the moles of O removed because of water dissociation (y_e) to the total moles of O removed during direct reduction (y_d). Thus, the term $q_g(y_d - y_e)$ accounts only for the heat absorbed during the direct reduction of wüstite when it occurs through Eq.(9).

It must be noted that this correction was not made by Rist in his original work. He considered that all the O atoms removed by direct reduction were because of the CO_2 dissociation and, in addition, he accounted for the H_2O dissociation of the hot blast. Therefore, he overestimates the absorbed heat by direct reduction, because he accounted the absorbed heat twice for a number of moles equals to y_e (once through CO_2 dissociation and again through H_2O dissociation).

To know the term $q_g(y_d - y_e)$ we would have to compute the variables q_g, y_d, and y_e. Nevertheless, when calculating X_P and Y_P, which is what we want, there is no need to compute y_d. Actually, the variable y_d will be a result from the operating line (Eq.(55)). Regarding y_e, it is written as $y_e = e y_v$ during the construction of Eq.(38), where e is the moisture of the hot blast in mol_{H2O}/mol_O, calculated by Eq.(71) as a function of air humidity, η (assumed known, in g/Nm^3) . Again, we do not need y_v, which will be a result from the operating line (Eq.(52)).

$$e = \eta/(18.75 M_{H2O}) \tag{71}$$

Lastly, the variable q_g is the heat absorbed by the CO_2 dissociation, calculated as Eq.(72) at T_R and tabulated in **Table 6**.

$$q_g = 2h_{CO} - h_{C(coke)} - h_{CO_2} \tag{72}$$

It must be noted that per 1 mol of O reduced from iron by Eq.(8), only 1 mol of C is consumed in Eq.(9). For this reason, there is no problem in mixing the units $kcal/mol_C$ of q_g and the units mol_O/mol_{Fe} of y_d in the term $q_g y_d$, since mol_C and mol_O are equivalent in this case. The same occurs with the dissociation of H_2O and the units of y_e.

A.6 Term $q_k y_k$: heat consumed due to the hydrogen entering with the coke

The term $q_k y_k$ is the heat consumed by the hydrogen entering with the coke because of the reverse water-gas shift reaction. The variable y_k is the number of moles of H_2 in the coke per mole of Fe produced (Eq. (73)). This is written as a function of the coke mass flow rate and its H mass fraction, which are assumed known. The number of moles of Fe produced are calculated by Eq.(74) as a function of the Fe mass fraction in the hot metal (also assumed known).

$$y_k = 10^3 \Omega_{K,H} m_K/(M_{H2} n_{HM,Fe}) \tag{73}$$
$$n_{HM,Fe} = \Omega_{HM,Fe} 10^6/M_{Fe} \tag{74}$$

Regarding q_k, it stands for the heat consumed per mole of H_2 in the reducing gas (whether the mole react or not, $kcal/mol_{H2}$). In order to write this heat, it is used the Eq.(75). It comprises ω_{WH} and q_ε. The former is the number of H_2 moles that has reacted (by the moment the gas reaches the thermal reserve zone) per moles of H_2 that were in the reducing gas at the beginning, i.e., ω_{WH} (Eq.(32), **Table 2**, calculated at T_R). In other words, it must be understood as the fraction of H_2 that reacts inside the control volume ($mol_{H2(reacting)}/mol_{H2}$). The other variable, q_ε, is the heat absorbed by the reverse water-gas shift, calculated through Eq.(76), whose units are $kcal/mol_{H2(reacting)}$ (tabulated in **Table 6**).

$$q_k = \omega_{WH} q_\varepsilon \tag{75}$$
$$q_\varepsilon = h_{H_2O} + h_{CO} - h_{H_2} - h_{CO_2} \tag{76}$$

The term q_k will appear also in all other terms related to hydrogen. Thanks to this, other terms like $(q_{iw}Y_w - \delta)$ can be written as a function of CO only, because the endothermic behavior of H_2 has been considered in advance in q_k. In other words, Eq.(6) is equivalent to Eq.(5) plus the reverse of Eq.(7) for example.

A.7 Term $q_e y_e$: overall heat absorbed by the moisture of the air

The term $q_e y_e$ represents the overall heat that is absorbed because of the presence of moisture in the air. The variable q_e (Eq.(77)) has three contributions that comprise the dissociation of H_2O during the direct reduction of wüstite (q_{er}), the endothermic behavior during indirect reduction (q_k), and the sensible heat (q_{es}).

$$q_e = q_{er} + q_k + q_{es} \tag{77}$$

The meaning of variable q_k was explained in detail in Appendix A.6 (Eq.(75)) and it is used to correct the assumption taken in $q_{iw}\mathrm{Y_w}$ (Appendix A.3) for which all the reduction of wüstite occurred by CO (which is not true). The variable q_{es} is the sensible heat of the water in the air between its inlet temperature T_v and the temperature of the thermal reserve zone T_R. Since it appears in the right side of Eq.(37) as a sink of heat, instead of as a contribution, it was calculated by Eq.(78) (tabulated in **Table 6** in the form of Eq.(114) with $T = T_v$).

$$q_{es} = -\int_{T_R}^{T} c_{p,\mathrm{H_2O}}\, dT \tag{78}$$

Lastly, the variable q_{er} standing for the heat absorbed during H_2O dissociation (which takes place at the tuyeres and it forms part of the overall direct reduction process) is calculated by Eq.(79) (also tabulated in **Table 6**).

$$q_{er} = h_{\mathrm{CO}} + h_{\mathrm{H2}} - h_{\mathrm{C(coke)}} - h_{\mathrm{H_2O}} \tag{79}$$

The variable y_e denotes the number of moles of H_2O in hot blast. This is written as $y_e = e y_v$, where e is given by Eq.(71) as a function of air humidity (assumed known) and y_v is computed by Eq.(52) as a result from the operating line (not needed for the calculation of point P).

A.8 Term $\sum q_j y_j$: overall heat absorbed by the injection of auxiliary fuels

The summation $\sum q_j y_j$ stands for all the injections in the tuyeres (except for the hot blast). Each addend $q_j y_j$ corresponds to one single injection, which might be an auxiliary reducing agent (pulverized coal, natural gas, hydrogen, etc.) or an injection of oxygen to enrich the blast. Thus, we may have injections with an overall chemical formula $\mathrm{CH_{2a}O_{2b}N_{2c}S_{2d}Z_z}$, $\mathrm{H_{2a}O_{2b}N_{2c}}$ or even $\mathrm{O_{2b}N_{2c}}$. The term y_j is the number of moles injected ($\mathrm{mol_{CH_{2a}O_{2b}N_{2c}S_{2d}Z_z}}$, $\mathrm{mol_{H_{2a}O_{2b}N_{2c}}}$ or $\mathrm{mol_{O_{2b}N_{2c}}}$) per mole of Fe in the hot metal, calculated by Eq.(80) (the mass m_j is assumed known). The molar weight is calculated using Eq.(81), and the parameters a, b, c, d, z by using Eq.(82) to Eq.(86) (for the gas injections, we only consider CO, CO_2, H_2, H_2O, CH_4, O_2 and N_2 as potential constituents of the gas; their molar fractions in the gas injected are assumed known $\omega_{j,\mathrm{i}}$). The notation z_i refers to each of the components of the ashes in coal (see Appendix B for more detail).

$$y_j = 10^3\ \mathrm{m}_j/(\mathrm{M_j} n_{\mathrm{HM,Fe}}) \tag{80}$$

$$M_j = \begin{cases} M_C + aM_{H_2} + bM_{O_2} + cM_{N_2} + dM_{S_2} + \sum_i z_i M_{Z_i} & \text{for } \mathrm{CH_{2a}O_{2b}N_{2c}S_{2d}Z_z} \\ aM_{H_2} + bM_{O_2} + cM_{N_2} & \text{for } \mathrm{H_{2a}O_{2b}N_{2c}}\ or\ \mathrm{O_{2b}N_{2c}} \end{cases} \tag{81}$$

$$a = \begin{cases} \dfrac{\left(\Omega^d_{\mathrm{j,H}}(1-\Omega_{\mathrm{j,M}}) + \Omega_{\mathrm{j,M}}\dfrac{\mathrm{M_{H_2}}}{\mathrm{M_{H_2O}}}\right)/\mathrm{M_{H_2}}}{\Omega^d_{\mathrm{j,C}}(1-\Omega_{\mathrm{j,M}})/\mathrm{M_C}} & \text{for coal or biomass } (\mathrm{CH_{2a}O_{2b}N_{2c}S_{2d}Z_z}) \\ \dfrac{2\omega_{j,\mathrm{CH4}} + \omega_{j,\mathrm{H2}} + \omega_{j,\mathrm{H2O}}}{\omega_{j,\mathrm{CH4}} + \omega_{j,\mathrm{CO}} + \omega_{j,\mathrm{CO2}}} & \text{for gas } (\mathrm{CH_{2a}O_{2b}N_{2c}S_{2d}Z_z}) \\ \dfrac{\omega_{j,\mathrm{H2}} + \omega_{j,\mathrm{H2O}}}{\omega_{j,\mathrm{O2}} + 0.5\omega_{j,\mathrm{H2O}}} & \text{for gas } (\mathrm{H_{2a}O_{2b}N_{2c}}) \\ 0 & \text{for gas } (\mathrm{O_{2b}N_{2c}}) \end{cases} \tag{82}$$

$$b = \begin{cases} \dfrac{\left(\Omega^d_{\mathrm{j,O}}(1-\Omega_{\mathrm{j,M}}) + \Omega_{\mathrm{j,M}}\dfrac{\mathrm{M_O}}{\mathrm{M_{H_2O}}}\right)/\mathrm{M_{O_2}}}{\Omega^d_{\mathrm{j,C}}(1-\Omega_{\mathrm{j,M}})/\mathrm{M_C}} & \text{for coal or biomass } (\mathrm{CH_{2a}O_{2b}N_{2c}S_{2d}Z_z}) \\ \dfrac{0.5\omega_{j,\mathrm{CO}} + \omega_{j,\mathrm{CO2}} + 0.5\omega_{j,\mathrm{H2O}} + \omega_{j,\mathrm{O2}}}{\omega_{j,\mathrm{CH4}} + \omega_{j,\mathrm{CO}} + \omega_{j,\mathrm{CO2}}} & \text{for gas } (\mathrm{CH_{2a}O_{2b}N_{2c}S_{2d}Z_z}) \\ 1 & \text{for gas } (\mathrm{H_{2a}O_{2b}N_{2c}}) \\ 1 & \text{for gas } (\mathrm{O_{2b}N_{2c}}) \end{cases} \tag{83}$$

$$c = \begin{cases} \dfrac{\Omega^d_{\mathrm{j,N}}/\mathrm{M_{N_2}}}{\Omega^d_{\mathrm{j,C}}/\mathrm{M_C}} & \text{for coal or biomass } (\mathrm{CH_{2a}O_{2b}N_{2c}S_{2d}Z_z}) \\ \dfrac{\omega_{j,\mathrm{N2}}}{\omega_{j,\mathrm{CH4}} + \omega_{j,\mathrm{CO}} + \omega_{j,\mathrm{CO2}}} & \text{for gas } (\mathrm{CH_{2a}O_{2b}N_{2c}S_{2d}Z_z}) \\ \dfrac{\omega_{j,\mathrm{N2}}}{\omega_{j,\mathrm{O2}} + 0.5\omega_{j,\mathrm{H2O}}} & \text{for gas } (\mathrm{H_{2a}O_{2b}N_{2c}}) \\ \dfrac{\omega_{j,\mathrm{N2}}}{\omega_{j,\mathrm{O2}}} & \text{for gas } (\mathrm{O_{2b}N_{2c}}) \end{cases} \tag{84}$$

$$d = \frac{\Omega^d_{\mathrm{j,S}}/\mathrm{M_{S_2}}}{\Omega^d_{\mathrm{j,C}}/\mathrm{M_C}} \tag{85}$$

$$z_i = \frac{\Omega^d_{\mathrm{j,Z_i}}/\mathrm{M_{Z_i}}}{\Omega^d_{\mathrm{j,C}}/\mathrm{M_C}} \tag{86}$$

Then, the thermal demand q_j (Eq.(87)) covers the dissociation of the injection (q_{jd}), its sensible heat (q_{js}), the endothermal behavior of H_2 during indirect reduction ($a\ q_k$), the utilization of the O_2 for combustion ($-2b\ q_c$), and the transfer of S to the slag ($-2d\ q_S$).

$$q_j = q_{jd} + q_{js} + a\ q_k - 2b\ q_c - 2d \cdot q_S \tag{87}$$

The heat of decomposition of the injectant, q_{jd}, must be calculated for each particular case. In the case of gas mixtures of CO, CO_2, H_2, H_2O, CH_4, O_2 and N_2, the heat of decomposition can be conventionally calculated as the enthalpy difference between the products and the reactants in the reaction given by Eq.(88), at T_j. We use the Eq.(89) for this calculation, which is a pondered summation of the components that will decompose (the heats of decomposition of CO, CO_2, CH_4 and H_2O are tabulated in **Table 6**). However, in the case of coal or biomass, the enthalpy is usually unknown because the molecular structure of the solid fuel is unknown. For these cases, a more complex methodology must be followed (please see the Appendix B for the calculation of q_{jd} in the case of coal and biomass).

$$\mathrm{CH_{2a}O_{2b}N_{2c}} \rightarrow \mathrm{C} + \mathrm{aH_2} + \mathrm{bO_2} + \mathrm{cN_2} \tag{88}$$

$$q_{jd} = \begin{cases} \dfrac{\omega_{j,\mathrm{CO}} q_{\mathrm{CO},d} + \omega_{j,\mathrm{CO2}} q_{\mathrm{CO2},d} + \omega_{j,\mathrm{CH4}} q_{\mathrm{CH4},d} + \omega_{j,\mathrm{H2O}} q_{\mathrm{H2O},d}}{\omega_{j,\mathrm{CO}} + \omega_{j,\mathrm{CO2}} + \omega_{j,\mathrm{CH4}}} & \text{for gas } (\mathrm{CH_{2a}O_{2b}N_{2c}S_{2d}Z_z}) \\ \dfrac{\omega_{j,\mathrm{H2O}} q_{\mathrm{H2O},d}}{\omega_{j,\mathrm{O2}} + 0.5\omega_{j,\mathrm{H2O}}} & \text{for gas } (\mathrm{H_{2a}O_{2b}N_{2c}}) \\ 0 & \text{for gas } (\mathrm{O_{2b}N_{2c}}) \end{cases} \tag{89}$$

The sensible heat q_{js} accounts for the heating from T_j to T_R of the products of the decomposition. It is calculated by Eq.(90), where $q_{js,i}$ is the sensible heat of element i (**Table 6**). For the case of coal or biomass, an overall sensible heat of ashes can be used as simplification ($q_{js,\mathrm{Z}}$, given in **Table 6**) with $M_Z = \Omega^d_{\mathrm{j,Z}}(1 - \Omega_{\mathrm{j,M}})M_j/z$ given in $\mathrm{g_Z/mol_Z}$, and $z = \sum z_i$.

$$q_{js} = \begin{cases} q_{js,\mathrm{C}} + aq_{js,\mathrm{H2}} + bq_{js,\mathrm{O2}} + cq_{js,\mathrm{N2}} + dq_{js,\mathrm{S2}} + \mathrm{z}q_{js,\mathrm{Z}} & \text{for } \mathrm{CH_{2a}O_{2b}N_{2c}S_{2d}Z_z} \\ aq_{js,\mathrm{H2}} + bq_{js,\mathrm{O2}} + cq_{js,\mathrm{N2}} & \text{for } \mathrm{H_{2a}O_{2b}N_{2c}} \text{ or } \mathrm{O_{2b}N_{2c}} \end{cases} \tag{90}$$

The two following addends in Eq.(87) (i.e., $+a\ q_k$ and $-2b\ q_c$) are easily calculated with Eq.(82) and Eq.(83) for a and b, with Eq.(75) for q_k, and with **Table 6** for q_c. The last term, $-2d \cdot q_S$, uses the heat released during the transfer of S to the slag (Eq.(18) plus Eq.(19)), calculated by Eq.(91) and tabulated in **Table 6**.

$$q_S = h_{\mathrm{C(coke)}} + h_{\mathrm{CaO}} + 0.5h_{\mathrm{S2}} - h_{\mathrm{CO}} - h_{\mathrm{CaS}} \tag{91}$$

A.9 Term δ': lack of chemical ideality in the conversion of H_2 to H_2O

The variable q_k, which takes account for the H_2 that is converted to H_2O (see Appendix A.6, Eq.(75)), assumed that the reacted amount corresponds to the equilibrium of the H-O-Fe system at T_R (i.e., the fraction of H_2 that reacted is given by ω_{WH}). However, this would be the case only under an ideal situation in which all the exchangeable oxygen is exchanged (i.e., chemical efficiency $r = 1$), which in practice will not be the case. To take into account that less H_2 has been converted to H_2O than would correspond to an ideal case (i.e., we are at point R instead of W), the heat absorbed by the reverse water-gas shift reaction is corrected in all terms where q_k appears. The correction is written as Eq.(92), thus diminishing the contribution of q_k in Eq.(37) by a fraction $(1 - r)$.

$$\delta' = (1 - r)\left(y_k + y_e + \sum a_j y_j\right) q_k \tag{92}$$

The chemical efficiency r is assumed known, and the calculation of the other involved variables has been explained in other appendixes (Appendix A.5 for y_e, Appendix A.6 for y_k, q_k, and Appendix A.8 for $a_j y_j$).

A.10 Terms $q_{\mathrm{Si}}y_{\mathrm{Si}}$, $q_{\mathrm{Mn}}y_{\mathrm{Mn}}$ and $q_P y_P$: heat absorbed by the reduction of the accompanying elements

The heat consumed during the reduction of the accompanying elements is accounted by the terms $q_{\mathrm{Si}}y_{\mathrm{Si}}$, $q_{\mathrm{Mn}}y_{\mathrm{Mn}}$ and $q_{\mathrm{P}}y_{\mathrm{P}}$. The variables q_{Si}, q_{Mn} and q_{P} correspond to the heat of reactions of Eq.(11), Eq.(12) and Eq.(13), respectively, but calculated in $\mathrm{kcal/mol_{CO}}$ (equivalent to $\mathrm{kcal/mol_O}$, because 1 mole of O gives 1 mole of CO). Thus, they are computed by Eq.(93), Eq.(94) and Eq.(95), and tabulated in **Table 6**. For the energy balance of the operating line, these must be calculated

at T_R.

$$q_{\mathrm{Si}} = h_{\mathrm{CO}} + 0.5h_{\mathrm{Fe_3Si}} - h_{\mathrm{C(coke)}} - 0.5h_{\mathrm{SiO_2}} - 1.5h_{\mathrm{Fe}} \quad (93)$$
$$q_{\mathrm{Mn}} = h_{\mathrm{CO}} + h_{\mathrm{Mn}} - h_{\mathrm{C(coke)}} - h_{\mathrm{MnO}} \quad (94)$$
$$q_{\mathrm{P}} = h_{\mathrm{CO}} + 0.6h_{\mathrm{CaO}} + 0.4h_{\mathrm{Fe_3P}} - h_{\mathrm{C(coke)}} - 0.2h_{\mathrm{P_2O_5 \cdot 3CaO}} - 1.2h_{\mathrm{Fe}} \quad (95)$$

The variables y_{Si}, y_{Mn} and y_{P} are the number of moles of O removed from the accompanying element during its reduction (i.e., the moles of CO generated because of their reduction), per mole of Fe produced in hot metal. They are calculated by Eq.(96), Eq.(97) and Eq.(98) as a function of the mass fractions of Si, Mn and P (assumed known), and the variable $n_{\mathrm{HM,Fe}}$ (Eq.(74), also known). The calculation can be understood as the product of the number of CO moles generated per mole of Si/Mn/P ending up in the hot metal ($\mathrm{mol_{CO}/mol_i}$) by the moles of Si/Mn/P in the hot metal per ton of hot metal ($\mathrm{mol_i/t_{HM}}$), and divided by the moles of Fe in hot metal per ton of hot metal ($\mathrm{mol_{Fe}/t_{HM}}$). Thus, the three of them have the units $\mathrm{mol_{CO}/mol_{Fe}}$.

$$y_{\mathrm{Si}} = 2(10^6\Omega_{\mathrm{HM,Si}}/\mathrm{M_{Si}})/n_{\mathrm{HM,Fe}} \quad (96)$$
$$y_{\mathrm{Mn}} = (10^6\Omega_{\mathrm{HM,Mn}}/\mathrm{M_{Mn}})/n_{\mathrm{HM,Fe}} \quad (97)$$
$$y_{\mathrm{P}} = 2.5(10^6\Omega_{\mathrm{HM,P}}/\mathrm{M_P})/n_{\mathrm{HM,Fe}} \quad (98)$$

A.11 Term $q_\gamma\gamma$: heat absorbed by the carburization of the iron

The term $q_\gamma\gamma$ is the heat consumed during reactions of Eq.(14) and Eq.(15), i.e., during the carburization of iron. Rist used a fixed value for q_γ (4.2 $\mathrm{kcal/mol_C}$) in his calculations [10]. Here we provide Eq.(99), where $\gamma_{\gamma\mathrm{Fe}}$ and $\gamma_{\mathrm{Fe_3C}}$ are the number of moles of carbon dissolved in the hot metal as austenite and cementite ($\mathrm{mol_C/mol_{Fe}}$) (Eq.(100) and Eq.(101)). As simplification, we can assume that there is 1.5% (in weight) of carbon as austenite in the hot metal ($\Omega_{\mathrm{HM},\gamma\mathrm{Fe}} = 0.015$), and the rest of carbon is cementite ($\Omega_{\mathrm{HM,Fe_3C}} = \Omega_{\mathrm{HM,C}} - \Omega_{\mathrm{HM},\gamma\mathrm{Fe}}$) [11].

$$q_\gamma\gamma = q_{\gamma\mathrm{Fe}} \cdot \gamma_{\gamma\mathrm{Fe}} + q_{\mathrm{Fe_3C}} \cdot \gamma_{\mathrm{Fe_3C}} \quad (99)$$
$$\gamma_{\gamma\mathrm{Fe}} = (10^6\Omega_{\mathrm{HM},\gamma\mathrm{Fe}}/\mathrm{M_C})/n_{\mathrm{HM,Fe}} \quad (100)$$
$$\gamma_{\mathrm{Fe_3C}} = (10^6\ \Omega_{\mathrm{HM,Fe_3C}}/\mathrm{M_C})/n_{\mathrm{HM,Fe}} \quad (101)$$

The terms $q_{\gamma\mathrm{Fe}}$ and $q_{\mathrm{Fe_3C}}$ are the heat absorbed by the corresponding reactions in $\mathrm{kcal/mol_C}$ (Eq.(102) and Eq.(103)). The value of $q_{\gamma\mathrm{Fe}}$ is taken from [10].

$$q_{\gamma\mathrm{Fe}} = 8.3\ \mathrm{kcal/mol_C} \quad (102)$$
$$q_{\mathrm{Fe_3C}} = h_{\mathrm{Fe_3C}} - 3h_{\mathrm{Fe}} - h_{\mathrm{C}} \quad (103)$$

The terms $q_{\gamma\mathrm{Fe}}$ and $q_{\mathrm{Fe_3C}}$ are tabulated in **Table 6** according to Eq.(113). It is worth to mention that the value of $q_{\mathrm{Fe_3C}}$ provided here for 1000 °C (3.8 $\mathrm{kcal/mol_C}$) differs from the value provided by Rist (1.6 $\mathrm{kcal/mol_C}$). We use the Aspen Plus database for this kind of calculation.

A.12 Term f: sensible heat of the hot metal

The sensible heat of the hot metal can be written as summation of the sensible heat of its constituents pondered by their molar fraction [34]. Therefore, we write the term f as Eq.(104), in $\mathrm{kcal/mol_{Fe}}$, where $q_{f,i}$ includes the sensible heat of element i between T_f and T_R, plus its heat of fusion. The variables $\Omega_{\mathrm{HM},\gamma\mathrm{Fe}}$ and $\Omega_{\mathrm{HM,Fe_3C}}$ are the mass fractions of C in hot metal when dissolved as austenite and cementite respectively, with $\Omega_{\mathrm{HM,C}} = \Omega_{\mathrm{HM},\gamma\mathrm{Fe}} + \Omega_{\mathrm{HM,Fe_3C}}$.

$$f = \sum_i \frac{\left(\frac{\Omega_{\mathrm{HM,i}}}{\mathrm{M_i}} q_{f,i}\right)}{\left(\frac{\Omega_{\mathrm{HM,Fe}}}{\mathrm{M_{Fe}}}\right)} = q_{f,\mathrm{Fe}} + \frac{\mathrm{M_{Fe}}}{\Omega_{\mathrm{HM,Fe}}}\left(\frac{\Omega_{\mathrm{HM,Si}}}{\mathrm{M_{Si}}} q_{f,\mathrm{Si}} + \frac{\Omega_{\mathrm{HM,Mn}}}{\mathrm{M_{Mn}}} q_{f,\mathrm{Mn}} + \frac{\Omega_{\mathrm{HM,P}}}{\mathrm{M_P}} q_{f,\mathrm{P}} + \frac{\Omega_{\mathrm{HM},\gamma\mathrm{Fe}}}{\mathrm{M_C}} q_{f,\gamma\mathrm{Fe}} + \frac{\Omega_{\mathrm{HM,Fe_3C}}}{\mathrm{M_C}} q_{f,\mathrm{Fe_3C}}\right) \quad (104)$$

The variables $q_{f,i}$ (Eq.(105)) are adjusted to Eq.(114) using data from Aspen Plus data base and NIST data base (**Table 6**). By direct comparison of Eq.(105) and Eq.(114), it can be seen that the heat of fusion coincides with the term a_0 in that equation, while the integration of c_p between T_f and T_R is calculated by the rest of the terms of Eq.(114).

$$q_{f,i} = \Delta h_{f,i} + \int_{T_R}^{T_f} c_{p,i}\, dT \quad (105)$$

The heat of fusion of carbon, when forming part of austenite and cementite, is calculated using data taken from [35]. The heat of fusion of pure austenite is 59.29 cal/g, which corresponds to 53.69 $\mathrm{kcal/mol_{Fe16C}}$ (the Fe atoms of austenite forming

a face centered cubic crystal structure, and one C atom in the middle of an edge). The contribution of C to this heat of fusion is 1/17, thus obtaining 3.16 kcal/$mol_{C(austenite)}$. The same reasoning is follow for cementite, whose heat of fusion is 64.93 cal/g, corresponding to 11.66 kcal/mol_{Fe3C}. The contribution of C to this heat of fusion is 1/4, i.e., 2.91 kcal/$mol_{C(cementite)}$. Rist, in his original work, only provided a simple overall formula as a function of the exit temperature of the hot metal (Eq.(106)) [11]. This formula is only valid for $T_R = 1000$ °C and the hot metal composition he used in his studies ($\Omega_{HM,Fe} = 0.937$, $\Omega_{HM,Si} = 0.004$, $\Omega_{HM,Mn} = 0.003$, $\Omega_{HM,P} = 0.018$, $\Omega_{HM,\gamma Fe} = 0.015$ and $\Omega_{HM,Fe_3C} = 0.023$). If we compare results of Eq.(104) for this particular case to the results of Eq.(106), we found they match well with an error below 5% (**Figure 9**). Therefore, we can consider that the general formula we provided is validated.

$$f_{(\text{Rist})} = 9.8349 \cdot 10^{-3}\, T_f - 5.6625 \tag{106}$$

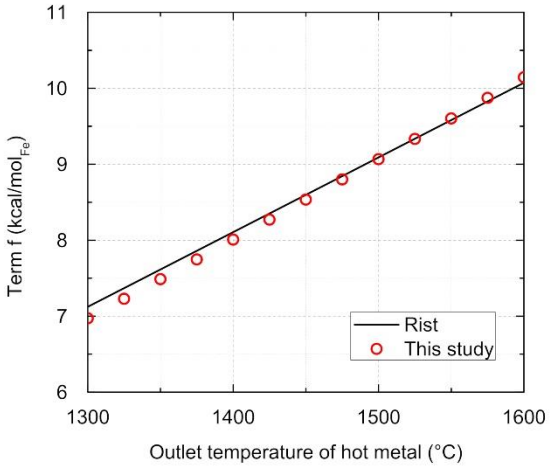

Figure 9. Comparison of term f (kcal/mol_{Fe}) vs. the exit temperature of the hot metal, calculated through the general formula elaborated in this study and through the overall formula provided by Rist, for a particular hot metal composition ($\Omega_{HM,Fe} = 0.937$, $\Omega_{HM,Si} = 0.004$, $\Omega_{HM,Mn} = 0.003$, $\Omega_{HM,P} = 0.018$, $\Omega_{HM,\gamma Fe} = 0.015$ and $\Omega_{HM,Fe_3C} = 0.023$) and $T_R = 1000\,°C$.

We have shown here that the term f does not account in any way for the sensible heat of the slag of for its heat of fusion. It is important to notice this because Rist assumed that Eq.(106) do account for the slag, when it is clearly not the case. Therefore, he remarkably underestimated the necessary heat inside the furnace and, as a consequence, the required amount of coke. Fortunately for Rist, this error was partially counterbalanced by the overestimation he made of the heat absorbed by direct reduction (explained in Appendix A.5). Even so, the final coke amount calculated by Rist is still lower than it should be because his underestimation of the energy for slag heating and melting (about 40% less heat than actually required) is bigger than the overestimation of the heat consumed by direct reduction (34% greater than actually consumed).

A.13 Term l: sensible heat of the slag

The sensible heat of the slag is the summation of the sensible heat of its constituents [34]. Since in this case we do not know the final composition of the slag, we have to calculate this value as a function of the inlets. We write the term l as Eq.(107), in kcal/mol_{Fe}, where the term $\left(10^3 \Omega_{j,i} m_j\right)/\left(M_i\, n_{HM,Fe}\right)$ is the number of moles of element i (SiO_2, Al_2O_3, CaO, MgO) coming from the iron source j (iron ore, coke, coal) per mole of Fe in hot metal (with $n_{HM,Fe}$ given by (74)). The term $q_{l,i}$ is the sensible heat of compound i between T_l and T_R plus its heat of fusion (Eq.(108), which is adjusted to Eq.(114) and tabulated in **Table 6**). Additionally, the contribution of SiO_2 has to be diminished according to the moles of Si that end up dissolved in the hot metal (term $0.5\, q_{l,SiO_2} y_{Si}$, with y_{Si} given by Eq.(96)). It should be noted that we neglect minor components in the slag as simplification, so the index of summation i only covers SiO_2, Al_2O_3, CaO and MgO.

$$l = \sum_j \sum_i \left(\frac{10^3 \Omega_{j,i} m_j}{M_i\, n_{HM,Fe}}\, q_{l,i} \right) - 0.5\, q_{l,SiO_2} y_{Si} \tag{107}$$

$$q_{l,i} = \Delta h_{f,i} + \int_{T_R}^{T_l} c_{p,i}\, dT \tag{108}$$

While computing the operating line, we assume known all the variables in Eq. (107) except for the mass of coke entering the blast furnace (m_K). In case of solving the entire Rist diagram through an equation solver software, there is no problem because the mass of coke will be given by Eq.(49) when the entire system of equations is solved at once. In case of solving one equation at a time, then we would have to assume a given amount of coke at first (e.g., 300-400 kg), solve the operating line (Eq.(33) and Eq.(34)), compute y_v (Eq.(52)), calculate the actual mass of coke (Eq.(49)), and repeat the calculations

with this new value in an iterative process until the assumed value and the calculated value are the same.
Rist, in his original work, only provided a very simplified equation for the calculation of this term (Eq.(109)) [11]. Moreover, his equation is only valid to compute the sensible heat between the outlet temperature of the slag and the outlet temperature of the hot metal, providing that the latter is 1400 °C. He presented the equation in this way because he assumed that f already accounted for the sensible heat of the slag between T_f and T_R, which is actually not the case, as we have shown during the construction of the detailed equation for f (see Appendix A.12).

$$l_{(\text{Rist})} = 2.98034 \cdot 10^{-2}\, T_l - 31.8889 \tag{109}$$

When comparing Eq.(109) to our Eq.(107) (computing in our case the integral of $q_{l,i}$ between T_l and T_f for a fair comparison), we found an additional error in the equation provided by Rist. It seems that Eq.(109) was elaborated using the heat capacity of SiO_2 in kJ/mol instead of kcal/mol, as it can be seen in **Figure 10**. This figure compares the results of Eq.(109), with the results of Eq.(107) when c_{p,SiO_2} is deliberately taken with the wrong units kJ/mol, and with the results of Eq.(107) with the proper units.

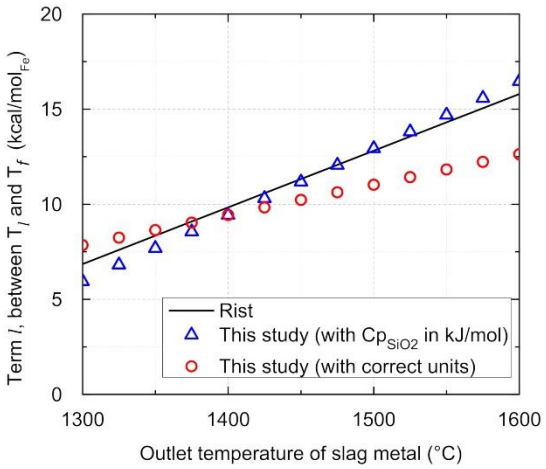

Figure 10. Comparison of term l (kcal/mol_{Fe}) vs. the exit temperature of the slag, calculated through the general formula elaborated in this study and through the overall formula provided by Rist, for the case of **Table 3**. For proper comparison, the term l was calculated between T_l and T_f, with $T_f = 1400\ °C$ (instead of between T_l and T_R).

In summary, Rist underestimate the heat required inside the blast furnace because not accounting the heating of slag between T_R and T_f (explained in Appendix A.12), but at the same time he overestimated the heat required because of wrongly computing the term l with c_{p,SiO_2} in wrong units, and also because of considering twice the heat absorbed during direct reduction for a number of moles equals to y_e (explained in Appendix A.5). Thus, these three errors counterbalanced more or less, and Rist was able to reach reasonable results.

A.14 Term p: heat removed by the staves

The term p denotes the heat removed by the staves in the elaboration zone (i.e., in the middle and lower zone). It is calculated by Eq.(110) as a fraction of the total heat removed.

$$p = \theta_{st} \cdot q_{st} / n_{\text{HM,Fe}} \tag{110}$$

The total heat removed is denoted by q_{st}, which is typically between 10^5 and $4.2 \cdot 10^5$ kcal/t_{HM} [10,17–19]. The fraction of this heat that is removed in the elaboration zone, θ_{st}, is usually between 70 – 80%. Both parameters are assumed known during the calculations. It is worth to mention that θ_{st} remarkably affects to the energy balance in the upper zone (Appendix C) and therefore to the final blast furnace gas composition.

A.15 Term $C_{\Delta T_R}$: lack of thermal ideality

In practice, in the thermal reserve zone, where thermal equilibrium is assumed, a non-zero temperature difference may exist between gas and solids. In this case, T_R is assumed to be the temperature of the gas, which is ΔT_R degrees above the temperature of the solids (i.e., solids are at $T_R - \Delta T_R$) [10]. The temperature difference ΔT_R is assumed known.
Under this situation, the energy balance of Eq.(37) is corrected by the term $C_{\Delta T_R}$, which accounts for the sensible heat of solids between T_R and $T_R - \Delta T_R$ (this effect is also taken into account in the energy balance of the upper zone, Appendix C). The term $C_{\Delta T_R}$ is calculated by Eq.(111), where the first addend accounts for the sensible heat of wüstite, the second for the magnetite (assuming that at point R the excess of O/Fe corresponds to magnetite), and the third addend accounts for the

accompanying elements and carbon entering at the top of the blast furnace. In this case, the index of summation j goes through iron ore and coke (coal is not present at this point since it enters at the tuyeres in the bottom), while the index of summation i must include SiO_2, Al_2O_3, CaO, MgO and also C (which has not been yet consumed in the thermal reserve zone). As it happened with the sensible heat of slag, l, the amount of coke will be unknown until the Rist diagram is solved, so either an equation solver is used or an iterative process must be followed.

$$C_{\Delta T_R} = Y_W \cdot q_{\mathrm{Fe_{0.95}O}} + (Y_R - Y_W) \cdot \frac{q_{\mathrm{Fe_3O_4}}}{Y_M^*} + \sum_j \sum_i \left(\frac{10^3 \Omega_{\mathrm{j,i}} \mathrm{m_j}}{\mathrm{M_i}\, n_{\mathrm{HM,Fe}}}\, q_{R,\mathrm{i}} \right) \tag{111}$$

The terms $q_{\mathrm{Fe_{0.95}O}}$, $q_{\mathrm{Fe_3O_4}}$ and $q_{R,\mathrm{i}}$ are the sensible heat of the corresponding element, calculated by Eq.(112) and tabulated in **Table 6** (due to the construction of Eq.(114), we must substitute T by $T_R - \Delta T_R$, and therefore the parameters of $q_{R,i}$ and $q_{l,i}$ have different sign in **Table 6**). The difference with $q_{l,i}$ is that in this case we do not include the heat of fusion. As in the case of l, we neglect the components MnO and P_2O_5 since their contribution in the energy balance is minor.

$$q_{R,i} = \int_{T_R - \Delta T_R}^{T_R} c_{p,i}\, dT \tag{112}$$

It is worth to mention that it seems that Rist had minor errors in the calculation of $C_{\Delta T_R}$ in his original work [10], which lead him to the conclusion that its effect is near to negligible, when its effect is actually one order of magnitude greater than the effect of δ' and δ when $\Delta T_R > 30$ °C.

A.16 List of q as function of T and T_R

The heats denoted by q in Eq.(37) are adjusted either by Eq.(113) or Eq.(114), and they represent a heat of reaction, a heat of fusion, a sensible heat, or a combination of them. They were calculated using data mainly from Aspen Plus database and from NIST. Specific data from other sources is cited when necessary along the appendixes. The parameters a_i of these equations are tabulated in **Table 6**. For the specific case of the heat of decomposition of coal, $q_{\mathrm{CH_{2a}O_{2b}N_{2c}S_{2d}Z_{z,d}}}$, please see Appendix B.

$$q = a_0 + a_1 T + a_2 T^2 + a_3 T^3 + a_4 T^4 + a_5 T^5 \tag{113}$$

$$q = a_0 + a_1 (T - T_R) + a_2 (T^2 - T_R^2) + a_3 (T^3 - T_R^3) + a_4 (T^4 - T_R^4) + a_5 (T^5 - T_R^5) \tag{114}$$

Table 6. Parameters of Eq.(113) and Eq.(114) for the calculation of heats denoted by q (heat of reaction, sensible heat, heat of fusion, or a combination of them). The parameters in this table are already given with the proper sign according to their position in the energy balance of Eq.(37). Data were adjusted in a wide range of temperatures to cover the operating conditions of blast furnace and the typical temperatures of injection in the tuyeres. See units in the nomenclature list.

Term	Eq.	a_0	$a_1 \cdot 10^3$	$a_2 \cdot 10^6$	$a_3 \cdot 10^9$	$a_4 \cdot 10^{13}$	$a_5 \cdot 10^{16}$
q_c	(113)	27.6277930	-1.41815549	4.12842928	-2.75130169	8.96569650	-1.11904405
q_v	(114)	0	15.6189049	2.84890885	-0.71432438	0.74256946	0
q_{iw}	(113)	2.59548525	2.81753858	-0.99606163	0.086920157	0	0
q_{im}	(113)	0.859445565	-0.851066970	17.18252955	-24.10333630	126.5591818	-23.40551798
q_ε	(113)	10.09226426	-2.622646073	0.207399547	0.018499206	0	0
q_g	(113)	39.94798938	2.612463578	-6.717602910	4.175812336	-13.08493402	1.596921902
q_{er}	(113)	30.09777648	3.812836330	-4.376962349	2.238032117	-6.670590754	0.811140814
q_{es}	(114)	0	-7.811260227	-1.211331943	-0.290874925	1.152621724	0
$q_{js,\mathrm{C}}$	(114)	0	-1.892676053	-4.302515390	2.533624229	-7.781074457	0.945154899
$q_{js,\mathrm{H_2}}$	(114)	0	-7.186451796	0.703157212	-0.990666896	3.831348892	-0.526720187
$q_{js,\mathrm{O_2}}$	(114)	0	-6.918539590	-1.270122896	0.209624517	1.081052901	-0.391217761
$q_{js,\mathrm{N_2}}$	(114)	0	-6.940261215	-0.027976126	-1.017332498	0.062883870	-1.213422894
$q_{js,\mathrm{S_2}}$	(114)	0	-7.765487359	-1.916979150	1.795874077	-8.500453347	1.534226748
$q_{js,\mathrm{Z}}/\mathrm{MW_Z}$	(114)	0	-0.180125344	-0.0699977	0	0	0
q_S	(113)	3.120295853	-1.659566914	4.651898976	-2.732009370	5.882711159	0
$q_{\mathrm{CH4},d}$	(113)	18.75059048	8.630351668	-5.523977040	0.986086895	1.092848019	-0.429883603
$q_{\mathrm{CO2},d}$	(113)	95.20223495	-0.163909537	1.261058571	-0.888254503	2.048695604	-0.018479841
$q_{\mathrm{CO},d}$	(113)	27.63605349	-1.574462606	4.715185141	-3.561402315	13.63334936	-2.073317965
$q_{\mathrm{H2O},d}$	(113)	57.71443993	2.525892875	-0.684828686	0	0	0
q_{Si}	(113)	69.27049820	0.926011273	-9.106679548	6.211945102	-24.51444450	3.691837294
q_{Mn}	(113)	64.39221737	0.899351591	-4.241268160	4.984768433	-25.97307076	5.095307673
q_{P}	(113)	62.25489996	-3.534696289	-1.549594462	0.203580420	0	0
$q_{\gamma\mathrm{Fe}}$	(113)	8.3	0	0	0	0	0
$q_{\mathrm{Fe_3C}}$	(113)	4.739686419	3.895790717	-5.384478435	0.585353566	0	0

$q_{f,\mathrm{Fe}}$	(114)	3.29846	6.272019761	0.999375557	0	0	0
$q_{f,\mathrm{Si}}$	(114)	11.992	5.410629044	0.587816263	0	0	0
$q_{f,\mathrm{Mn}}$	(114)	3.8934	7.486148803	1.310221357	0	0	0
$q_{f,\mathrm{P}}$	(114)	0.1574	6.292069790	0	0	0	0
$q_{f,\gamma\mathrm{Fe}}$	(114)	3.1583	2.581965355	2.386317417	-0.585341267	0	0
$q_{f,\mathrm{Fe_3C}}$	(114)	2.9146	2.581965355	2.386317417	-0.585341267	0	0
$q_{l,\mathrm{SiO_2}}$	(114)	1.83887	15.73272597	0.714132724	0	0	0
$q_{l,\mathrm{Al_2O_3}}$	(114)	25.5565	25.56135703	2.478548686	0	0	0
$q_{l,\mathrm{CaO}}$	(114)	12.4916	11.58470766	0.772858739	0	0	0
$q_{l,\mathrm{MgO}}$	(114)	13.7695	10.89566202	0.762574946	0	0	0
$q_{\mathrm{Fe_{0.95}O}}$	(114)	0	-12.89824855	-1.404696556	-3.264582911	0	0
$q_{\mathrm{Fe_3O_4}}$	(114)	0	-51.12090518	-0.203226315	0.648765211	0	0
$q_{R,\mathrm{SiO_2}}$	(114)	0	-15.73272597	-0.714132724	0	0	0
$q_{R,\mathrm{Al_2O_3}}$	(114)	0	-25.56135703	-2.478548686	0	0	0
$q_{R,\mathrm{CaO}}$	(114)	0	-11.58470766	-0.772858739	0	0	0
$q_{R,\mathrm{MgO}}$	(114)	0	-10.89566202	-0.762574946	0	0	0
$q_{R,\mathrm{C}}$	(114)	0	-1.892676053	-4.302515390	2.533624229	-7.781074457	0.945154899
$q_{s,\mathrm{C}}$	(114)	0	1.892676053	4.302515390	-2.533624229	7.781074457	-0.945154899
$q_{s,\mathrm{N_2}}$	(114)	0	6.889861828	0.375357941	0.421099425	-2.467676481	0.388118345
$q_{s,\mathrm{CO}}$	(114)	0	6.892443	0.351944	0.760803	-5.532971	1.161065
$q_{s,\mathrm{H_2}}$	(114)	0	7.186451796	-0.703157212	0.990666896	-3.831348892	0.526720187
$q_{s,\mathrm{Z}}/\mathrm{MW_Z}$	(114)	0	0.180125344	0.0699977	0	0	0

Appendix B – Heat of decomposition of coal (dry basis)

The decomposition of coal occurs according to Eq.(115). The coefficients a, b, c, d and z can be calculated from the ultimate analysis of the coal in a dry basis and its moisture content (Eq.(116) to (120)).

$$\mathrm{CH_{2a}O_{2b}N_{2c}S_{2d}Z_z} \rightarrow \mathrm{C} + \mathrm{aH_2} + \mathrm{bO_2} + \mathrm{cN_2} + \mathrm{dS_2} + \mathrm{zZ} \tag{115}$$

$$\mathrm{a} = \frac{\left(\Omega_{\mathrm{H}}^{d}(1-\Omega_{\mathrm{M}}) + \Omega_{\mathrm{M}}\frac{\mathrm{M_{H_2}}}{\mathrm{M_{H_2O}}}\right)/\mathrm{M_{H_2}}}{\Omega_{\mathrm{C}}^{d}(1-\Omega_{\mathrm{M}})/\mathrm{M_C}} \tag{116}$$

$$\mathrm{b} = \frac{\left(\Omega_{\mathrm{O}}^{d}(1-\Omega_{\mathrm{M}}) + \Omega_{\mathrm{M}}\frac{\mathrm{M_O}}{\mathrm{M_{H_2O}}}\right)/\mathrm{M_{O_2}}}{\Omega_{\mathrm{C}}^{d}(1-\Omega_{\mathrm{M}})/\mathrm{M_C}} \tag{117}$$

$$\mathrm{c} = \frac{\Omega_{\mathrm{N}}^{d}/\mathrm{M_{N_2}}}{\Omega_{\mathrm{C}}^{d}/\mathrm{M_C}} \tag{118}$$

$$\mathrm{d} = \frac{\Omega_{\mathrm{S}}^{d}/\mathrm{M_{S_2}}}{\Omega_{\mathrm{C}}^{d}/\mathrm{M_C}} \tag{119}$$

$$\mathrm{z} = \frac{\Omega_{\mathrm{Z}}^{d}/\mathrm{M_Z}}{\Omega_{\mathrm{C}}^{d}/\mathrm{M_C}} \tag{120}$$

To calculate the endothermal heat of this decomposition by Eq.(121), $q_{\mathrm{CH_{2a}O_{2b}N_{2c}S_{2d}Z_z},d}$, it is required to know the enthalpy of the products and reactants. The enthalpy of the products (kcal/mol), as function of temperature in °C, is given by Eq.(122) to (126). It is not necessary to calculate the term zh_Z because it will appear again in $h_{\mathrm{CH_{2a}O_{2b}N_{2c}S_{2d}Z_z}}$ and therefore vanishes (ashes are inert).

$$q_{\mathrm{CH_{2a}O_{2b}N_{2c}S_{2d}Z_z},d} = h_{\mathrm{C}} + \mathrm{a}h_{\mathrm{H_2}} + \mathrm{b}h_{\mathrm{O}} + ch_{\mathrm{N_2}} + \mathrm{d}h_{\mathrm{S_2}} + \mathrm{z}h_Z - h_{\mathrm{CH_{2a}O_{2b}N_{2c}S_{2d}Z_z}} \tag{121}$$

$$h_{\mathrm{C}} = -0.105 + 2.58\cdot10^{-3}\,T + 2.37\cdot10^{-6}\,T^2 - 5.8\cdot10^{-10}\,T^3 \tag{122}$$

$$h_{\mathrm{H_2}} = -0.142 + 6.7\cdot10^{-3}\,T + 3.97\cdot10^{-7}\,T^2 \tag{123}$$

$$h_{\mathrm{O_2}} = -0.527 + 8.38\cdot10^{-3}\,T \tag{124}$$

$$h_{\mathrm{N_2}} = -0.198 + 6.95\cdot10^{-3}\,T + 5.43\cdot10^{-7}\,T^2 \tag{125}$$

$$h_{\mathrm{S_2}} = 30.35 + 8.79\cdot10^{-3}\,T \tag{126}$$

The enthalpy of coal is computed from its enthalpy of formation and heat capacity by Eq.(127).

$$h_{\mathrm{CH_{2a}O_{2b}N_{2c}S_{2d}Z_z}} = \Delta_{\mathrm{f}}h^{T_{ref}}_{\mathrm{CH_{2a}O_{2b}N_{2c}S_{2d}Z_z}} + \int_{T_{ref}}^{T} c_{p,\mathrm{CH_{2a}O_{2b}N_{2c}S_{2d}Z_z}}\,dT \tag{127}$$

The calculation of both the enthalpy of formation and heat capacity should be performed experimentally. Here we provide empirical equations from literature for its calculation.
The heat of formation of coal is normally calculated from its heat of combustion and the heats of formation of the combustion products (Eq.(128)). Substituting the values for the heats of formation (water as liquid, $T_{ref} = 25$ °C), Eq.(128) results in Eq.(129) (in kcal/mol).

$$\Delta_f h^{T_{ref}}_{CH_{2a}O_{2b}N_{2c}S_{2d}Z_z} = \Delta_c h^{T_{ref}}_{CH_{2a}O_{2b}N_{2c}S_{2d}Z_z} + \Delta_f h^{T_{ref}}_{CO_2} + a\Delta_f h^{T_{ref}}_{H_2O} + 2c\Delta_f h^{T_{ref}}_{NO_2} + 2d\Delta_f h^{T_{ref}}_{SO_2} + z\Delta_f h^{T_{ref}}_{Z} \quad (128)$$

$$\Delta_f h^{T_{ref}}_{CH_{2a}O_{2b}N_{2c}S_{2d}Z_z} = \Delta_c h^{T_{ref}}_{CH_{2a}O_{2b}N_{2c}S_{2d}Z_z} - 94.05 - 68.31a + 15.87c - 141.89d + z\Delta_f h^{T_{ref}}_{Z} \quad (129)$$

The heat of combustion can be measured experimentally or calculated from empirical correlations. Here we provide the revised IGT correlation for the heat of combustion of coal, as a function of the ultimate analysis, in a dry basis (Eq.(130)) [36], in kcal/g. In the case of biomass fuel, the Eq.(131) is preferred [37] (the rest of the methodology would be the same).

$$\Delta_c h^{d,T_{ref}}_{coal} = 8.1488\Omega^d_C + 31.62\Omega^d_H - 2.8647(\Omega^d_O + \Omega^d_N) + 1.6344\Omega^d_S - 0.3658\Omega^d_A \quad (130)$$

$$\Delta_c h^{d,T_{ref}}_{biomass} = 8.34\Omega^d_C + 28.15\Omega^d_H - 2.470\Omega^d_O - 0.3607\Omega^d_N + 2.401\Omega^d_S - 0.504\Omega^d_A \quad (131)$$

In order to convert this value to wet basis and kcal/mol$_{CH_{2a}O_{2b}N_{2c}S_{2d}Z_z}$ (Eq.(132)), it is necessary to know the molar weight of $CH_{2a}O_{2b}N_{2c}S_{2d}Z_z$, and therefore the composition of the ashes.

$$\Delta_c h^{T_{ref}}_{CH_{2a}O_{2b}N_{2c}S_{2d}Z_z} = \Delta_c h^{d,T_{ref}}_{coal}(1 - \Omega_M)M_{CH_{2a}O_{2b}N_{2c}S_{2d}Z_z} \quad (132)$$

Ashes are usually a mixture of SiO_2, Al_2O_3, Fe_2O_3, CaO, MgO, MnO and P_2O_5 (Eq.(133)). The values of z_i can be calculated as in Eq.(120), from the weight fraction in a dry basis (Eq.(134)). The molar weight is thus calculated by Eq.(135).

$$Z_z \equiv (SiO_2)_{z_1}(Al_2O_3)_{z_2}(Fe_2O_3)_{z_3}(CaO)_{z_4}(MgO)_{z_5}(MnO)_{z_6}(P_2O_5)_{z_7} \quad (133)$$

$$z_i = \frac{\Omega^d_{Zi}/M_{Zi}}{\Omega^d_C/M_C} \quad (134)$$

$$M_{CH_{2a}O_{2b}N_{2c}S_{2d}Z_z} = M_C + aM_{H_2} + bM_{O_2} + cM_{N_2} + dM_{S_2} + \sum_i z_i M_{Z_i} \quad (135)$$

Regarding the heat capacity, it can be calculated as a weighted sum by mass fractions of the following components: moisture, fixed carbon, primary volatile, secondary volatile and ash. Assumed that the volatile matter in a dry, ash-free basis exceeding 10% should be considered as the primary, and up to 10% as the secondary volatile matter (Eq.(136), in kcal/g-K). If the volatile matter content in a dry, ash-free basis is less than 10%, there are only secondary volatiles [38], and therefore Eq.(137) should be used instead. To change units to kcal/mol-K, Eq.(138) is used.

$$c_{p,coal} = \left[\Omega_M c_{p_M} + (1 - \Omega_M)\left(\Omega^d_{FC} c_{p_{FC}} + \left(\Omega^d_{VM} - 0.1(1 - \Omega^d_Z)\right)c_{p_{PV}} + 0.1(1 - \Omega^d_Z)c_{p_{SV}} + \Omega^d_Z c_{p_Z}\right)\right] \quad (136)$$

$$c_{p,coal} = \left[\Omega_M c_{p_M} + (1 - \Omega_M)\left(\Omega^d_{FC} c_{p_{FC}} + \Omega^d_{VM} c_{p_{SV}} + \Omega^d_Z c_{p_Z}\right)\right] \quad (137)$$

$$c_{p,CH_{2a}O_{2b}N_{2c}S_{2d}Z_z} = c_{p,coal} M_{CH_{2a}O_{2b}N_{2c}S_{2d}Z_z} \quad (138)$$

The second term of the right side of Eq.(127) can be written as Eq.(139) showing the separate contribution of each component.

$$\begin{aligned}\int_{T_{ref}}^{T} c_{p,CH_{2a}O_{2b}N_{2c}S_{2d}Z_z}\, dT \\ = M_{CH_{2a}O_{2b}N_{2c}S_{2d}Z_z}\Omega_M \int c_{p_M} dT + M_{CH_{2a}O_{2b}N_{2c}S_{2d}Z_z}\Omega^d_{FC}(1 - \Omega_M)\int c_{p_{FC}} dT \\ + M_{CH_{2a}O_{2b}N_{2c}S_{2d}Z_z}(\Omega^d_{VM} + 0.1\Omega^d_Z - 0.1)(1 - \Omega_M)\int c_{p_{PV}} dT \\ + M_{CH_{2a}O_{2b}N_{2c}S_{2d}Z_z}(0.1 - 0.1\Omega^d_Z)(1 - \Omega_M)\int c_{p_{SV}} dT + M_{CH_{2a}O_{2b}N_{2c}S_{2d}Z_z}\Omega^d_Z(1 - \Omega_M)\int c_{p_Z} dT\end{aligned} \quad (139)$$

The last addend of this equation, together with the last one of Eq.(129), are equal to the term zh_Z appearing in Eq.(121), and therefore these terms vanishes when computing $q_{CH_{2a}O_{2b}N_{2c}S_{2d}Z_z,d}$.
The integrals of the heat capacities are given by Eq.(140) to Eq.(144) in kcal/g, and T given in °C [38]. In the case of ashes, a more accurate value could be computed as weighted sum of the contributions of the components of the ashes, because the

composition of the ashes is known (it was used to calculate the molar weight of the coal). Nevertheless, the error of Eq.(144) is minor for ashes with high weight fractions of SiO_2 and Al_2O_3, as it is usually the case. Moreover, it is not necessary to compute it because it vanishes.

$$\int_{25°C}^{T} c_{p_{\mathrm{M}}} dT = -0.025 + 10^{-3} \cdot T \tag{140}$$

$$\int_{25°C}^{T} c_{p_{\mathrm{FC}}} dT = -4.3331 \cdot 10^{-3} + 1.6491 \cdot 10^{-4} \cdot T + 3.4009 \cdot 10^{-7} \cdot T^2 - 1.3999 \cdot 10^{-10} \cdot T^3 \tag{141}$$

$$\int_{25°C}^{T} c_{p_{\mathrm{PV}}} dT = -1.0130 \cdot 10^{-2} + 3.9508 \cdot 10^{-4} \cdot T + 4.0505 \cdot 10^{-7} \cdot T^2 \tag{142}$$

$$\int_{25°C}^{T} c_{p_{\mathrm{SV}}} dT = -1.7930 \cdot 10^{-2} + 7.0959 \cdot 10^{-4} \cdot T + 3.0508 \cdot 10^{-7} \cdot T^2 \tag{143}$$

$$\int_{25°C}^{T} c_{p_{\mathrm{Z}}} dT = -4.5469 \cdot 10^{-3} + 1.8013 \cdot 10^{-4} \cdot T + 6.9998 \cdot 10^{-8} \cdot T^2 \tag{144}$$

Through this methodology, the heat of decomposition of any coal can be calculated. As example, the calculation for the coal in **Table 7** is presented in **Table 8**. The temperature at which $q_{\mathrm{CH_{2a}O_{2b}N_{2c}S_{2d}Z_z},d}$ is calculated corresponds to the temperature at which the coal is injected in the blast furnace. For this example, we assume 50 °C.

Table 7. Example of a coal analysis.

Proximate analysis			**Ultimate analysis**		
Moisture (Ω_{M})	8.5	wt.% (wet basis)	C (Ω_{C}^{d})	54.57	wt.% (dry basis)
Fixed carbon (Ω_{FC}^{d})	25.83	wt.% (dry basis)	H (Ω_{H}^{d})	3.21	wt.% (dry basis)
Volatile matter (Ω_{VM}^{d})	53.00	wt.% (dry basis)	O (Ω_{O}^{d})	15.59	wt.% (dry basis)
Ash (Ω_{Z}^{d})	21.17	wt.% (dry basis)	N (Ω_{N}^{d})	1.07	wt.% (dry basis)
			S (Ω_{S}^{d})	4.39	wt.% (dry basis)
			Z (Ω_{Z}^{d})	21.17	wt.% (dry basis)

Ash composition (wt.% dry basis)					
SiO_2 ($\Omega_{\mathrm{Z,SiO_2}}^{d}$)	Al_2O_3 ($\Omega_{\mathrm{Z,Al_2O_3}}^{d}$)	Fe_2O_3 ($\Omega_{\mathrm{Z,Fe_2O_3}}^{d}$)	CaO ($\Omega_{\mathrm{Z,CaO}}^{d}$)	MgO ($\Omega_{\mathrm{Z,MgO}}^{d}$)	MnO ($\Omega_{\mathrm{Z,MnO}}^{d}$)
12.58	6.48	1.32	0.55	0.22	0.02

Table 8. Steps for the calculation of the heat of decomposition of coal at $T_{coal} = 50\ °C$.

Term	Equation	Value	Units
a	(116)	0.4632	$mol_{H2}/mol_{CH2aO2bN2cS2dZz}$
b	(117)	0.1640	$mol_{O2}/mol_{CH2aO2bN2cS2dZz}$
c	(118)	0.0084	$mol_{N2}/mol_{CH2aO2bN2cS2dZz}$
d	(119)	0.0151	$mol_{S2}/mol_{CH2aO2bN2cS2dZz}$
z_{SiO2}	(134)	0.0461	$mol_{SiO2}/mol_{CH2aO2bN2cS2dZz}$
z_{Al2O3}	(134)	0.0140	$mol_{Al2O3}/mol_{CH2aO2bN2cS2dZz}$
z_{Fe2O3}	(134)	0.0018	$mol_{Fe2O3}/mol_{CH2aO2bN2cS2dZz}$
z_{CaO}	(134)	0.0022	$mol_{CaO}/mol_{CH2aO2bN2cS2dZz}$
z_{MgO}	(134)	0.0012	$mol_{MgO}/mol_{CH2aO2bN2cS2dZz}$
z_{MnO}	(134)	0.0001	$mol_{MnO}/mol_{CH2aO2bN2cS2dZz}$
z_{P2O5}	(134)	0.0000	$mol_{P2O5}/mol_{CH2aO2bN2cS2dZz}$
$\mathrm{M}_{\mathrm{CH_{2a}O_{2b}N_{2c}S_{2d}Z_z}}$	(135)	24.05	$g_{CH2aO2bN2cS2dZz}/mol_{CH2aO2bN2cS2dZz}$
$\Delta_c h_{\mathrm{coal}}^{d,T_{ref}}$	(130)	4.979	$kcal/g_{dry\ coal}$
$\Delta_c h_{\mathrm{CH_{2a}O_bN_{2c}S_{2d}Z_z}}^{T_{ref}}$	(132)	109.6	$kcal/mol_{CH2aO2bN2cS2dZz}$
$\Delta_f h_{\mathrm{CH_{2a}O_bN_{2c}S_{2d}Z_z}}^{T_{ref}} - z\Delta_f h_{Z}^{T_{ref}}$	(129)	-18.12	$kcal/mol_{CH2aO2bN2cS2dZz}$
$\int_{25°C}^{T} c_{p_{\mathrm{M}}} dT$	(140)	0.0250	$kcal/kg_{M}$
$\int_{25°C}^{T} c_{p_{\mathrm{FC}}} dT$	(141)	0.0086	$kcal/kg_{FC}$
$\int_{25°C}^{T} c_{p_{\mathrm{PV}}} dT$	(142)	0.0106	$kcal/kg_{PV}$
$\int_{25°C}^{T} c_{p_{\mathrm{SV}}} dT$	(143)	0.0252	$kcal/kg_{SV}$
$\int_{T_{ref}}^{T} c_{p,\mathrm{CH_{2a}O_bN_{2c}S_{2d}Z_z}}\, dT - \mathrm{M}_{\mathrm{CH_{2a}O_bN_{2c}S_{2d}Z_z}} \Omega_{\mathrm{Z}}^{d} (1 - \Omega_{\mathrm{M}}) \int c_{p_{\mathrm{Z}}} dT$	(139)	0.2543	$kcal/mol_{CH2aO2bN2cS2dZz}$

$h_{CH_{2a}O_bN_{2c}S_{2d}Z_z} - zh_z$	(127)	-17.86	kcal/mol$_{CH2aO2bN2cS2dZz}$
h_C	(122)	0.0298	kcal/mol$_C$
h_{H_2}	(123)	0.1940	kcal/mol$_{H2}$
h_{O_2}	(124)	-0.1081	kcal/mol$_{O2}$
h_{N_2}	(125)	0.1509	kcal/mol$_{N2}$
h_{S_2}	(126)	30.79	kcal/mol$_{S2}$
$q_{CH_{2a}O_{2b}N_{2c}S_{2d}Z_{z,d}}$	(121)	18.43	kcal/mol$_{CH2aO2bN2cS2dZz}$

Appendix C – Energy balance in the preparation zone

This sections presents the energy balance in the preparation zone (upper part of the blast furnace). In order to keep consistency with the rest of the methodology, we work with kcal/mol$_{Fe}$ units (which are the units used by Rist in his original work). The energy balance follows Eq.(145), where p' is the heat removed by the staves, the term $q_{rwc}y_{rwc}$ is the heat consumed during the reduction of hematite to wüstite, the term $q_{rmc}y_{rmc}$ is the heat released by the reduction of hematite to magnetite, the term $q'_\varepsilon y_{wgs}$ is the heat consumed by the reverse water-gas shift reaction, and the term $\sum q_{s,nr,i}y_{nr,i}$ stands for the sensible heat of the compounds that do not react.

$$0 = p' + q_{rwc}y_{rwc} + q_{rmc}y_{rmc} + q'_\varepsilon y_{wgs} + \sum q_{s,nr,i}y_{nr,i} \quad (145)$$

The term p' is calculated in a similar way that p, but in this case the fraction of heat removed is $(1-\theta_{st})$ instead of θ_{st} (Eq.(146)). A typical value for θ_{st} is around 0.7 [11], and the variable $n_{\mathrm{HM,Fe}}$ is computed by Eq.(74).

$$p' = (1-\theta_{st}) \cdot q_{st}/n_{\mathrm{HM,Fe}} \quad (146)$$

The term $q_{rwc}y_{rwc}$ is calculated by Eq.(147) and Eq.(148). The former is the heat consumed by the reduction of hematite to wüstite by carbon monoxide (Eq.(1) plus Eq.(3)), including also the heat exchange between reactants that gives the final temperature of the products. This is given as a function of the temperature of the iron ore entering the blast furnace (h_{Fe2O3} calculated at T_{IN}), the temperature of the reactant CO coming from the middle zone (h_{CO} calculated at T_R), the final temperature of the CO_2 exiting the top of the furnace (h_{CO2} calculated at T_{BFG}) and the temperature of the wüstite descending to the elaboration zone (h_{FeO} calculated at $T_R - \Delta T_R$) (Eq.(147)). Regarding y_{rwc}, it represents the number of moles of FeO produced through this process. This is calculated as the difference between the moles of FeO in the thermal reserve zone and the moles of FeO that were already present in the burden since the beginning (Eq.(148)).

$$q_{rwc} = 0.5h_{\mathrm{Fe2O3}} + 0.5h_{\mathrm{CO}} - h_{\mathrm{FeO}} - 0.5h_{\mathrm{CO2}} \quad (147)$$
$$y_{rwc} = \left(n_{\mathrm{R,FeO}} - \left(n_{\mathrm{IO,FeO}} + n_{\mathrm{K,FeO}}\right)\right)/n_{\mathrm{HM,Fe}} \quad (148)$$

The term $q_{rmc}y_{rmc}$ is calculated by Eq.(149) and Eq.(150). The former is the heat released by the reduction of hematite to magnetite by carbon monoxide (Eq. (1)), including also the heat exchange between reactants and products at different temperature. This is given as a function of the temperature of the iron ore entering the blast furnace (h_{Fe2O3} calculated at T_{IN}), the temperature of the reactant CO coming from the middle zone (h_{CO} calculated at T_R), the final temperature of the CO_2 exiting the top of the furnace (h_{CO2} calculated at T_{BFG}) and the temperature of the magnetite descending to the elaboration zone (h_{Fe3O4} calculated at $T_R - \Delta T_R$) (Eq.(149)). The term y_{rmc} is the number of moles of Fe_3O_4 produced through this process. This corresponds to the number of moles of Fe_3O_4 existing in the thermal reserve zone (point R), since no magnetite is originally in the burden.

$$q_{rmc} = 1.5h_{\mathrm{Fe2O3}} + 0.5h_{\mathrm{CO}} - h_{\mathrm{Fe3O4}} - 0.5h_{\mathrm{CO2}} \quad (149)$$
$$y_{rmc} = n_{\mathrm{R,Fe3O4}}/n_{\mathrm{HM,Fe}} \quad (150)$$

The term $q'_\varepsilon y_{wgs}$ is the heat consumed by the reverse water-gas shift reaction in the preparation zone. As occurred in the energy balance of the elaboration zone, the term related to this reaction is used to correct the calculation of the energy involved in the reduction of iron oxides, since it was assumed at first that it took place only by CO. Thanks to this term we consider that some part of the reduction takes place by hydrogen. In other words, Eq.(1) plus the reverse of Eq.(7) is equal to Eq.(2) for the reduction to magnetite, and the same occurs for the reduction to wüstite. Additionally, this term takes into account the H_2 converted to H_2O because of the water-gas shift reaction itself trying to reach equilibrium (i.e., iron oxide reduction is not the only responsible of the consumption of H_2). The variable q'_ε is calculated as Eq.(151), where the different temperature of reactants and products is taken into account (h_{CO2} and h_{H2} calculated at T_R, and h_{CO} and h_{H2O} calculated at T_{BFG}). The variable y_{wgs} is the number of moles of H_2 reacting in the preparation zone. This is unknown because the water-gas shift reaction does not achieve equilibrium in this zone. We write it as a fraction of the H_2 available at point R. The percentage of H_2 consumed will be such that the energy balance is fulfilled, since p' is known.

$$q'_\varepsilon = h_{\mathrm{CO2}} + h_{\mathrm{H2}} - h_{\mathrm{CO}} - h_{\mathrm{H2O}} \quad (151)$$
$$y_{wgs} = \Phi n_{\mathrm{R,H2}}/n_{\mathrm{HM,Fe}} \quad (152)$$

The summation $\sum q_{s,nr,i}y_{nr,i}$ stands for the sensible heat of the compounds that do not react. In the solid phase we are going to consider SiO_2, Al_2O_3, CaO, MgO, C, and the FeO entering with the burden at the beginning (we neglect other minor components). In the gas phase we have the N_2 and H_2O originally coming from the point R, and the non-consumed fractions of CO, CO_2 and H_2. The variables $y_{nr,i}$ are computed by Eq.(153) to Eq.(163).

$$y_{nr,\mathrm{SiO2}} = \left(n_{\mathrm{IO,SiO2}} + n_{\mathrm{K,SiO2}}\right)/n_{\mathrm{HM,Fe}} \quad (153)$$
$$y_{nr,\mathrm{Al2O3}} = \left(n_{\mathrm{IO,Al2O3}} + n_{\mathrm{K,Al2O3}}\right)/n_{\mathrm{HM,Fe}} \quad (154)$$
$$y_{nr,\mathrm{CaO}} = \left(n_{\mathrm{IO,CaO}} + n_{\mathrm{K,CaO}}\right)/n_{\mathrm{HM,Fe}} \quad (155)$$
$$y_{nr,\mathrm{MgO}} = \left(n_{\mathrm{IO,MgO}} + n_{\mathrm{K,MgO}}\right)/n_{\mathrm{HM,Fe}} \quad (156)$$
$$y_{nr,\mathrm{C}} = \left(n_{\mathrm{IO,C}} + n_{\mathrm{K,C}}\right)/n_{\mathrm{HM,Fe}} \quad (157)$$
$$y_{nr,\mathrm{FeO}} = \left(n_{\mathrm{IO,FeO}} + n_{\mathrm{K,FeO}}\right)/n_{\mathrm{HM,Fe}} \quad (158)$$
$$y_{nr,\mathrm{N2}} = n_{\mathrm{R,N2}}/n_{\mathrm{HM,Fe}} \quad (159)$$
$$y_{nr,\mathrm{CO2}} = n_{\mathrm{R,CO2}}/n_{\mathrm{HM,Fe}} - y_{wgs} \quad (160)$$
$$y_{nr,\mathrm{CO}} = n_{\mathrm{R,CO}}/n_{\mathrm{HM,Fe}} - 0.5y_{rwc} - 0.5y_{rmc} \quad (161)$$
$$y_{nr,\mathrm{H2O}} = n_{\mathrm{R,H2O}}/n_{\mathrm{HM,Fe}} \quad (162)$$
$$y_{nr,\mathrm{H2}} = n_{\mathrm{R,H2}}/n_{\mathrm{HM,Fe}} - y_{wgs} \quad (163)$$

The variables $q_{s,nr,i}$ are adjusted to Eq.(164) (T given in °C) and tabulated in **Table 9**. For solid phase, T_1 is T_{IN} and T_2 is $T_R - \Delta T_R$, while for gas phase T_1 is T_R and T_2 is T_{BFG}. Moreover, the enthalpies appearing in the different q terms of Eq.(147), Eq.(149) and Eq.(151) are adjusted to Eq.(165) (T given in °C), and the parameters are given in **Table 9**.

$$q_{s,nr,i} = a_0 + a_1(T_1 - T_2) + a_2(T_1^2 - T_2^2) + a_3(T_1^3 - T_2^3) + a_4(T_1^4 - T_2^4) + a_5(T_1^5 - T_2^5) \quad (164)$$
$$h = a_0 + a_1T + a_2T^2 + a_3T^3 + a_4T^4 + a_5T^5 \quad (165)$$

Table 9. Parameters of Eq.(164) and Eq.(165) for the calculation of sensible heats, enthalpies and entropies. See units in the nomenclature list.

Term	Eq.	a_0	$a_1 \cdot 10^3$	$a_2 \cdot 10^6$	$a_3 \cdot 10^9$	$a_4 \cdot 10^{13}$	$a_5 \cdot 10^{16}$
h_{CO}	(165)	-26.590776	6.892443	0.351944	0.760803	-5.532971	1.161065
h_{CO2}	(165)	-94.287539	8.891736	4.603344	-2.216655	6.571122	-0.900405
h_{FeO}	(165)	-65.318709	11.893590	1.896629	-0.129837	-2.104974	0.630635
h_{Fe2O3}	(165)	-197.685233	22.975743	27.962301	-25.909694	103.346475	-14.858752
h_{Fe3O4}	(165)	-267.705411	22.248252	92.414124	-113.039791	581.139433	-107.281713
h_{H2}	(165)	-0.177166	7.013815	-0.220743	0.416396	-0.735801	-0.091152
h_{H2O}	(165)	-58.019687	8.056125	0.593617	1.015110	-4.968145	0.737172
h_{N2}	(165)	-0.173848	6.926795	0.077295	0.984240	-6.296343	1.254892
$q_{s,nr,\mathrm{SiO2}}$	(164)	0	15.732726	0.714133	0	0	0
$q_{s,nr,\mathrm{Al2O3}}$	(164)	0	25.561357	2.478549	0	0	0
$q_{s,nr,\mathrm{CaO}}$	(164)	0	11.584708	0.772859	0	0	0
$q_{s,nr,\mathrm{MgO}}$	(164)	0	10.895662	0.762575	0	0	0
$q_{s,nr,\mathrm{C}}$	(164)	0	1.892676	4.302515	-2.533624	7.781074	-0.945155
$q_{s,nr,\mathrm{FeO}}$	(164)	0	11.893590	1.896629	-0.129837	-2.104974	0.630635
$q_{s,nr,\mathrm{N2}}$	(164)	0	6.926795	0.077295	0.984240	-6.296343	1.254892
$q_{s,nr,\mathrm{CO2}}$	(164)	0	8.891736	4.603344	-2.216655	6.571122	-0.900405
$q_{s,nr,\mathrm{CO}}$	(164)	0	6.892443	0.351944	0.760803	-5.532971	1.161065
$q_{s,nr,\mathrm{H2O}}$	(164)	0	8.056125	0.593617	1.015110	-4.968145	0.737172
$q_{s,nr,\mathrm{H2}}$	(164)	0	7.013815	-0.220743	0.416396	-0.735801	-0.091152
s_{CO}	(165)	0.021170	0.018098	0.009241	0.002166	0	0
s_{CO2}	(165)	0.000277	0.026154	0.011729	0.002557	0	0
s_{H2}	(165)	-0.000143	0.017941	0.009841	0.002405	0	0
s_{H2O}	(165)	-0.010844	0.021117	0.010258	0.002450	0	0

When trying to solve this energy balance, we found 8 additional unknown variables related to the mole streams at point R (solids streams $n_{\mathrm{R,FeO}}$, $n_{\mathrm{R,Fe3O4}}$, gas streams $n_{\mathrm{R,N2}}$, $n_{\mathrm{R,CO2}}$, $n_{\mathrm{R,CO}}$, $n_{\mathrm{R,H2O}}$, $n_{\mathrm{R,H2}}$, and the fraction of H_2 consumed, Φ). The solid streams of FeO and Fe_3O_4 at point R can be found through a balance of Fe in the upper zone (Eq.(166)) and the ordinate Y_R of the operating line (Eq.(167)). The gas streams are calculated through the mass balances of Eq.(168) to Eq.(172) (it must be noted that the variables n_{BFG} do not add additional unknown variables, since they appear in the mole balances of the individual elements mentioned in the section 4.3.3 Blast furnace gas composition). The last equation is the relation between CO, CO_2, H_2, and H_2O in the thermal reserve zone (at point R), where the water-gas shift reaction is at equilibrium (Eq.(173)).

$$0.947\left(n_{\mathrm{IO,FeO}} + n_{\mathrm{K,FeO}}\right) + 2\left(n_{\mathrm{IO,Fe2O3}} + n_{\mathrm{K,Fe2O3}}\right) = 0.947n_{\mathrm{R,FeO}} + 3n_{\mathrm{R,Fe3O4}} \quad (166)$$

$$Y_R = \left(4n_{R,Fe3O4} + n_{R,FeO}\right)/\left(3n_{R,Fe3O4} + 0.947n_{R,FeO}\right) \quad (167)$$

$$n_{BFG,N2} = n_{R,N2} \quad (168)$$

$$n_{BFG,CO2} = n_{R,CO2} + 0.5\left(n_{R,FeO} - \left(n_{IO,FeO} + n_{K,FeO}\right)\right) + 0.5n_{R,Fe3O4} - \Phi n_{R,H2} \quad (169)$$

$$n_{BFG,CO} = n_{R,CO} - 0.5\left(n_{R,FeO} - \left(n_{IO,FeO} + n_{K,FeO}\right)\right) - 0.5n_{R,Fe3O4} + \Phi n_{R,H2} \quad (170)$$

$$n_{BFG,H2O} = n_{R,H2O} + \Phi n_{R,H2} \quad (171)$$

$$n_{BFG,H2} = n_{R,H2}(1 - \Phi) \quad (172)$$

$$K_{eq} = \left(n_{R,CO2}n_{R,H2}\right)/\left(n_{R,CO}n_{R,H2O}\right) \quad (173)$$

In order to calculate the equilibrium constant K_{eq}, the Eq.(174) to Eq.(176) are used, with the temperature in K. The ideal gas constant is $R = 0.001987207$ kcal/(mol K). The equilibrium constant K_{eq} has to be calculated at T_R.

$$K_{eq} = \exp\left(-\frac{\Delta G}{RT}\right) \quad (174)$$

$$\Delta G = g_{CO2} + g_{H2} - g_{CO} - g_{H2O} \quad (175)$$

$$g_i = h_i - Ts_i \quad (176)$$

The enthalpies and entropies are adjusted to Eq. (165) and tabulated in **Table 9**.

Appendix D – Calculation of the flame temperature through Eq.(62)

This sections presents the data used for the calculation of the temperature of the flame when using Eq.(62). The data is presented in **Table 10** for data sets of **Table 3**.

Table 10. Calculation of flame temperature through Eq.(62).

Term	**Rist** [10]	**Babich** [18]
V_v (Nm^3/t_{HM})	1729	903
T_v (°C)	700	1200
ω_{v,O_2} (-)	0.21	0.2678
η_{nat} (g/Nm^3)	0	0
η (g/Nm^3)	10	0
V_{NG} (Nm^3/t_{HM})	0	0
m_{PC} (kg/t_{HM})	0	200
$\Omega_{PC,C}$ (-)	0	0.806
$\Omega_{PC,H}$ (-)	0	0.0435
$\omega_{NG,CH4}$ (-)	0	0
$c_{p,v}$ (kcal/mol K)	0.00789	0.00839
$c_{p,H2O}$ (kcal/mol K)	0.00981	0
$c_{p,rg}$ (kcal/mol K)	0.00850	0.00829
T_{fl} (°C)	1898	2117

References

[1] N. Mac Dowell, P.S. Fennell, N. Shah, G.C. Maitland, The role of CO2 capture and utilization in mitigating climate change, Nat. Clim. Chang. 7 (2017) 243–249. https://doi.org/10.1038/nclimate3231.

[2] F. Ueckerdt, C. Bauer, A. Dirnaichner, J. Everall, R. Sacchi, G. Luderer, Potential and risks of hydrogen-based e-fuels in climate change mitigation, Nat. Clim. Chang. 11 (2021) 384–393. https://doi.org/10.1038/s41558-021-01032-7.

[3] M. Bailera, P. Lisbona, L.M. Romeo, S. Espatolero, Power to Gas projects review: Lab, pilot and demo plants for storing renewable energy and CO2, Renew. Sustain. Energy Rev. 69 (2017). https://doi.org/10.1016/j.rser.2016.11.130.

[4] M. Bailera, P. Lisbona, B. Peña, L.M. Romeo, A review on CO2 mitigation in the Iron and Steel industry through Power to X processes, J. CO2 Util. 46 (2021) 101456. https://doi.org/10.1016/j.jcou.2021.101456.

[5] S. Hisashige, T. Nakagaki, T. Yamamoto, CO2 emission reduction and exergy analysis of smart steelmaking system adaptive for flexible operating conditions, ISIJ Int. 59 (2019) 598–606. https://doi.org/10.2355/isijinternational.ISIJINT-2018-355.

[6] D.C. Rosenfeld, H. Böhm, J. Lindorfer, M. Lehner, Scenario analysis of implementing a power-to-gas and biomass gasification system in an integrated steel plant: A techno-economic and environmental study, Renew. Energy. 147 (2020) 1511–1524. https://doi.org/10.1016/j.renene.2019.09.053.

[7] Pasquale Cavaliere, Clean Ironmaking and Steelmaking Processes. Efficient Technologies for Greenhouse Emissions Abatement, (n.d.). https://doi.org/https://doi.org/10.1007/978-3-030-21209-4.

[8] J. Perpiñán, M. Bailera, L.M. Romeo, B. Peña, V. Eveloy, CO2 Recycling in the Iron and Steel Industry via Power to Gas and Oxy-Fuel Combustion, Energies. 14 (2021) 7090. https://doi.org/10.3390/en14217090.

[9] A. Rist, N. Meysson, A dual graphic representation of the blast-furnace mass and heat balances, Jom. 19 (1967) 50–59. https://doi.org/10.1007/bf03378564.

[10] A. Rist, N. Meysson, Étude graphique de la marche du haut fourneau avec vent humide et injections aux tuyères, Rev. Metall. 62 (1965) 995–1040. https://doi.org/10.1051/metal/196562110995.

[11] A. Rist, N. Meysson, Recherche graphique de la mise au mille minimale du haut fourneau a faible température de vent, Rev. Métallurgie. 61 (1964) 121–146. https://doi.org/10.1051/metal/196461020121.

[12] N. Meysson, J. Weber, A. Rist, Représentation graphique de la décomposition des carbonates dans le haut fourneau, Rev. Métallurgie. 61 (1964) 623–633. https://doi.org/10.1051/metal/196461070623.

[13] D.M. Kundrat, T. Miwa, A. Rist, Injections in the Iron Blast Furnace: A Graphics Study by Means of the Rist Operating Diagram, Metall. Trans. B. 22B (1991) 363–383. https://doi.org/10.1007/BF02651235.

[14] J. Tang, M. Chu, F. Li, Z. Zhang, Y. Tang, Z. Liu, J. Yagi, Mathematical simulation and life cycle assessment of blast furnace operation with hydrogen injection under constant pulverized coal injection, J. Clean. Prod. 278 (2021) 123191. https://doi.org/10.1016/j.jclepro.2020.123191.

[15] W.L. Zhan, K. Wu, Z.J. He, Q.H. Liu, X.J. Wu, Estimation of Energy Consumption in COREX Process Using a Modified Rist Operating Diagram, J. Iron Steel Res. Int. 22 (2015) 1078–1084. https://doi.org/10.1016/S1006-706X(15)30115-1.

[16] A. Babich, D. Senk, H. Gudenau, K.T. Mavrommatis, Ironmaking Textbook, RWTH Aachen University, 2008.

[17] K. Suzuki, K. Hayashi, K. Kuribara, T. Nakagaki, S. Kasahara, Quantitative evaluation of CO2 emission reduction of active carbon recycling energy system for ironmaking by modeling with aspen plus, ISIJ Int. 55 (2015) 340–347. https://doi.org/10.2355/isijinternational.55.340.

[18] A. Babich, D. Senk, J. Solar, I. de Marco, Efficiency of biomass use for blast furnace injection, ISIJ Int. 59 (2019) 2212–2219. https://doi.org/10.2355/isijinternational.ISIJINT-2019-337.

[19] A.F. Prego, A.C. Sanchez, A. Babich, H.W. Gudenau, L.G. Sanchez, S.L. Yaroshevskii, J.L. Menendez, Operación de hornos altos con inyección de carbón pulverizado en diferentes condiciones tecnológicas, Rev. Metal. 37 (2001) 423–436. https://doi.org/10.3989/revmetalm.2001.v37.i3.50810.3989/revmetalm.2001.v37.i3.508.

[20] A.K. Biswas, Principles of blast furnace ironmaking. Theory and practice, Cootha Publishing house, 1981.

[21] K.T.M. A. Babich, D. Senk, H. W. Gudenau, IRONMAKING, (2008) 402.

[22] M. Geerdes, R. Chaigneau, O. Lingiardi, R. van O. Molenaar, S.Y. R., J. Warren, Modern Blast Furnace Ironmaking An Introduction, IOS Press, 2020.

[23] A. Spanlang, W. Wukovits, B. Weiss, Development of a Blast Furnace Model with Thermodynamic Process Depiction by Means of the Rist Operating Diagram, BHM Berg- Und Hüttenmännische Monatshefte. 165 (2020) 243–247. https://doi.org/10.1007/s00501-020-00963-6.

[24] D. Wagner, O. Devisme, F. Patisson, D. Ablitzer, A laboratory study of the reduction of iron oxides by hydrogen, Sohn Int. Symp. 2 (2006) 111–120.

[25] A. Babich, Methodical instruction for the flame temperature calculation, Donetsk. (1988) 24.

[26] R.K. Sahu, S.K. Roy, P.K. Sen Ã, Applicability of Top Gas Recycle Blast Furnace with Downstream Integration and Sequestration in an Integrated Steel Plant, 1 (2015) 502–516. https://doi.org/10.1002/srin.201400196.

[27] S. Kasahara, Y. Inagaki, M. Ogawa, Flow sheet model evaluation of nuclear hydrogen steelmaking processes with VHTR-IS (very high temperature reactor and iodine-sulfur process), ISIJ Int. 52 (2012) 1409–1419. https://doi.org/10.2355/isijinternational.52.1409.

[28] P. Jin, Z. Jiang, C. Bao, Y. Lu, J. Zhang, X. Zhang, Mathematical Modeling of the Energy Consumption and Carbon Emission for the Oxygen Blast Furnace with Top Gas Recycling, Steel Res. Int. 87 (2016) 320–329. https://doi.org/10.1002/srin.201500054.

[29] Development of Systems using Renewable Energy-derived Hydrogen Development of Power-to-gas System to Synthesize Methane from Renewable Hydrogen and Exhaust CO2 for Supplying via Conventiontional Gas Grid., 2019. https://www.nedo.go.jp/library/seika/shosai_201903/20180000000638.html.

[30] D.H.D. Rocha, D.S. Siqueira, R.J. Silva, Exergoenvironmental analysis for evaluating coal-fired power plants technologies, Energy. 233 (2021). https://doi.org/10.1016/j.energy.2021.121169.

[31] P. Lisbona, M. Bailera, B. Peña, L.M. Romeo, Integration of CO2 capture and conversion, in: M.R. Rahimpour, M. Farsi, M.A. Makarem (Eds.), Adv. Carbon Capture, Woodhead Publishing, 2020: pp. 503–522. https://doi.org/10.1016/B978-0-12-819657-1.00022-0.

[32] J. Gervasi, L. Dubois, D. Thomas, Simulation of the post-combustion CO2 capture with Aspen HysysTM software: Study of different configurations of an absorptionregeneration process for the application to cement flue gases, Energy Procedia. 63 (2014) 1018–1028. https://doi.org/10.1016/j.egypro.2014.11.109.

[33] M.A. Morales-Mora, C.F. Pretelìn-Vergara, S.A. Martínez-Delgadillo, C. Iuga, C. Nolasco-Hipolito, Environmental assessment of a combined heat and power plant configuration proposal with post-combustion CO2 capture for the Mexican oil and gas industry, Clean Technol. Environ. Policy. 21 (2019) 213–226. https://doi.org/10.1007/s10098-018-1630-3.

[34] K.C. Mills, S. Karagadde, P.D. Lee, L. Yuan, F. Shahbazian, Calculation of Physical Properties for Use in Models of Continuous Casting Process-Part 2: Steels, ISIJ Int. 56 (2016) 274–281. https://doi.org/10.2355/isijinternational.ISIJINT-2015-365.
[35] U. Saburo, On the Specific Heat of Iron-Carbon System at High Temperatures, and the Heat Changes Accompanying Those of Phase, in: 335th Rep. Res. Inst. Iron, Steel Other Met., Universitätsbibliothek Johann Christian Senckenberg., Sendai, 1935: pp. 665–795. http://publikationen.ub.uni-frankfurt.de/files/14043/E001892575.pdf.
[36] R.H. Perry, D.W. Green, Perry's Chemical Engineers' Handbook, 7th ed., McGraw-Hill Education, 1997.
[37] D.W. Green, M.Z. Southard, Perry's chemical engineers' handbook, 9th ed., McGraw-Hill Education, 2019.
[38] B. Leśniak, łukasz Słupik, G. Jakubina, The determination of the specific heat capacity of coal based on literature data, Chemik. 67 (2013) 560–571.